7-13-2022

Fabrication of Nonplanar Surfaces Via 5-Axis 3D Printing

Ajinkya S. Patil
ap4264@rit.edu

RIT

Fabrication of Nonplanar Surfaces Via 5-Axis 3D Printing

by

Ajinkya S. Patil

A Thesis Submitted in Partial Fulfilment of the Requirements for the

Degree of Master of Science in Mechanical Engineering

AMPrint Center

Department of Industrial Engineering

Kate Gleason College of Engineering

ROCHESTER INSTITUTE OF TECHNOLOGY

Rochester, New York

July 13th, 2022

By: Ajinkya S. Patil

A Thesis Submitted in Partial Fulfilment of the Requirements for the Degree of Master of Science in Mechanical Engineering

Department of Mechanical Engineering

Kate Gleason College of Engineering

Rochester Institute of Technology

Approved by:

Dr. Denis Cormier

Thesis Advisor *Date*

Department of Industrial and Systems Engineering

Dr. Rui Liu

Thesis Committee Member *Date*

Department of Mechanical Engineering

Dr. Yunbo Zhang

Thesis Committee Member *Date*

Department of Industrial and Systems Engineering

Dr. Jason Kolodziej

Department Representative, Thesis Committee Member *Date*

Department of Mechanical Engineering

ABSTRACT

The advancements in manufacturing have always played a vital role in human life. One of the most recent and growing manufacturing methods is additive manufacturing (AM). AM has been in focus for its ability to manufacture intricate parts with internal features which are not possible with traditional manufacturing processes. Making parts lighter and stronger has been the goal for most AM processes. The advancements in AM have made it possible to produce parts with high strength internal structures. The overall strength of the manufactured plastic parts depends on several variables. The part's strength is determined by the material, the build direction, the infill settings, and the printing parameters. Optimization of each of these variables is critical for obtaining the desired result for the intended application of the printed part. One of the major drawbacks of these parts is the weak interlayer bonding within parts which are susceptible to failure under high loads. Similarly, the stair stepping effect compromises the surface finish of a part. This is prominently seen when the angle of inclination is less than 30 degrees. Previous research shows that the mixture of non-planar and planar layers in a 3DP part can improve its surface finish. Non-Planar 3D printing done using a 3-axis machine is limited by the angle of the nozzle with respect to the previously printed layers. This study will focus on incorporating 5-axis 3D printer toolpath motions to print nonplanar surfaces. It will also shed some light on the enhanced mechanical properties of the parts which have non-planar layers as compared to conventionally 3D printed parts.

TABLE OF CONTENTS

LIST OF FIGURES

LIST OF TABLES

1.0 PROBLEM INTRODUCTION AND THESIS SCOPE

Additive Manufacturing (AM) is said to be the future of modern manufacturing. The amount of freedom and the ability to produce complex geometries has given designers an extra dimension to work in. While normal document printing prints on a flat surface in 2 dimensions (2D), 3D printing (3DP) uses the third axis to print an object with thickness. The basic idea of 3DP is printing 2-D layers on top of each other to produce a 3-dimensional object [1].

Today the main use of 3DP objects is prototypes. Very few companies have commercially integrated 3DP parts in the actual product. Various types of printing processes have their own benefits and disadvantages. This document specifically focuses on a process called Fused Deposition Modeling or FDM. FDM is a process in which a hot nozzle is used to melt the polymer filament, and an extruder lays out the molten plastic to create layers. This is one of the most common 3DP processes and is used widely [2].

3DP is a growing field, and the applications are enormous. However, there are some limitations that hinder adoption of the technology. This is due to various problems encountered with the 3DP parts, such as limited material choice, poor surface finish, slower production rates, and many more. Two of the major problems are large printing times and low surface finish. As 3DP is just printing 2D layers on top of other layers, there is a certain step-like feel to objects with sloped surface geometries. This causes poor surface finish and reduces the strength of the part [2].

Due to this discretized layer structure of printed objects, stair-stepping artifacts occur on the surfaces where the slope is close to horizontal. The stair stepping is considerably worse on surfaces with a low ramp angle than on those with a high ramp angle. Stair-stepping also adversely affects the part's aesthetics and influences the mechanical properties of the printed object. Friction, fluid-dynamics, and aerodynamics are different from the designed object. For example, on a printed wing, these stair-stepping artifacts can produce air turbulence and reduce lift. There are many was to achieve high surface finish. The use of smaller layer height can improve the surface finish, but will increase the print time drastically [3].

This thesis explores the process planning of 3D printed non-planar FDM surfaces using a 5-axis FDM 3D printer. These parts are tested using 3-point bend tests and Charpy impact toughness tests for improved mechanical strengths as compared to conventionally 3D printed parts. The parts are also tested for improvements in surface finish, to assess the effect that non-planar layering will have on decreasing the stair stepping effect. Lastly, as recent research shows the mechanically enhanced properties of woven layers on planar parts [4], a proof-of-concept demonstration of woven toolpaths for nonplanar surfaces will be presented.

2.0 LITERATURE REVIEW

Manufacturing is roughly defined as making goods by hand or by machine. At a high level, there are two types of manufacturing - subtractive manufacturing and additive manufacturing. Subtractive manufacturing is the process in which material removal takes place from solid objects like bars, plates, blocks, sheets, etc. To complete this process, methods like drilling, boring, and milling are used to get the desired shape and size [5].

3D printing is basically printing 2-D layers on top of each other to form a 3D object. AM and 3DP are two terms that are generally used to describe such layer wise manufacturing processes. It is called additive because it adds material to make an object as opposed to subtractive manufacturing which removes material to get a desired shape [6].

The process of 3D printing involves breaking up a 3D shape into 2D slices that are sequentially printed to make the object. Early on, AM was only used to create prototypes that would help creators and designers visualize the final product and make improvements if needed. It is generally known that models can be far more helpful in product development than simple sketches or Computer Aided Drawing (CAD) drawings. In today's product development processes, models are nearly unavoidable in order to validate the designs [7].

AM is one of the fastest developing fields in manufacturing, and there are many different methods for printing material. The most used production methods are Fused Filament Fabrication (FFF), Selective Laser Melting (SLM), Stereolithography (SLA), Selective Laser Sintering (SLS), Material Jetting (MJP), etc. In every technique, material is deposited in layers. Stacking of these layers creates an object, thus it is also called layer-based manufacturing. Early on, the printed models were used as prototypes [8]. As improvements have been made in the processes and materials, the parts which are manufactured are getting more and more accurate. AM is no longer a process just used to develop prototypes. It is now an accepted industrial process for production of functional parts in certain fields such as aerospace and medical devices.

2.1 AM Processes

Even though there are different methods used in AM, the high-level workflow followed is generic. There are certain steps to be followed to create a 3DP object. Those steps are as follows:

conceptual development of the idea, CAD design of the model, generation of an STL or other 3D printing file format (i.e. 3MF, AMF), slicing of the CAD model to generate the printing toolpath G-codes, preparing the machine, printing the part, cleaning the part, and lastly post processing done on the part before use. These steps are shown in Figure 1 and are further described in detail in the sections below [1].

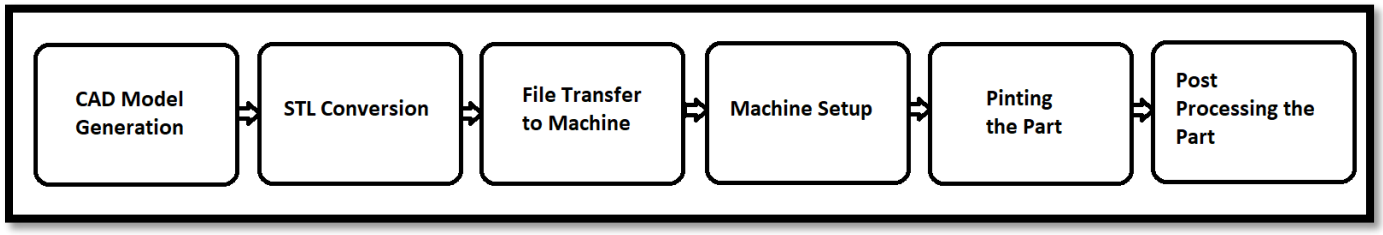

Figure 1 Process Flow for Generating a 3DP Part

2.1.1 CAD Model Generation

Every part created using AM is designed using CAD software. A software model is created to fully describe the internal and external features of the product in detail. There are various software packages used to draw a model, and each of them can create an output of a 3D solid. The other way to make a CAD model is reverse engineering. This uses the concept of laser or optical scanning. The object to be replicated is scanned from every possible side to get a full map of the topology. This is used when the part to be produced does not have a CAD file. The drawback of this method is that it is difficult to create internal features, as it is not possible to scan the insides of an object with lasers and optical sensors. This is the step where the design and product development team gives the input and decides the dimensions and features of the product [9].

2.1.2 Generating STL Files from CAD Models

The STL file format is usually generated by a CAD program. These files represent triangular meshes that describe the surfaces of 3D models. The process of dividing the surface of an object into triangles to cover each surface without overlaps or gaps is called tessellation. The color and texture of the surface are not represented in this format. The information of the triangular facets stored in the STL file format includes coordinates of each vertex and the components of the unit normal vector to the triangle pointing outwards from the object. This format is then sent to a slicer for further generation of toolpath G-codes. The STL file format is the dominant file format

used in 3DP, however, other file formats are used as well. OBJ is one of the most important, as it stores the color and texture information of the object. OBJ is mainly used when the object is scanned. The Polygon file format (PLY) is also used to represent 3D scanned files [1], [2].

2.1.3 G-code Generation (Slicing)

G-code is a common computer language used in computer numerical control (CNC) machines. As 3DP machines are also CNC machines, G-codes are also used with the majority of these machines to produce 3D models. The slicing software used in this study is in a developing stage. Controllable machine parameters are generated based on the STL model and the settings to operate the printer. The slicing software takes into account the desired layer thickness, infill percentage, support for down-facing surfaces, adhesion, bed temperature, and extrusion speeds when generating G-codes for the required part to print. Each of the following parameters can be controlled by G-codes [10].

2.1.4 Machine Setup

Before the build process, the AM machine must be properly set up. The processes are fairly automated, but things like material availability and power are to be setup prior to the printing process [9].

2.1.5 Printing the Part

After G-code is generated and the machine is set up, the printing process is to be executed on the printer. The G-code information is generally transferred to the machine through a pen drive or a micro SD card. In large manufacturing units, G-codes are transferred via network. The printer reads the G-code commands and executes them in the order they are given. There is usually no need to continuously monitor the machine, as it is an automated process. Before the print starts, the printer prepares itself by heating up the print head, and all axes are driven to a home position. Print bed leveling and priming of the print head is done if the printer supports the feature. After this starting check, the printer starts to produce the object. Usually the print time depends on many factors like layer height, infill density and size and shape of the object. After the part is printed, it can be removed from the print bed and can be taken for post processing [11].

2.1.6 Post Processing

After the part is removed from the built plate, it may require post processing. Before this, the part may be weak and have support material on it. If needed, the part is cured. Then the support material is removed. This is a time consuming process and needs experienced manual operation [2].

2.2 3-Axis Fused Deposition Modelling

There are many processes used in AM, and they can be broadly classified as follows:

- Vat polymerization (SLA).
- Material jetting.
- Binder jetting.
- Material extrusion (FFF/FDM).
- Sheet lamination (LOM).
- Powder bed fusion (SLM/SLS).
- Directed energy deposition (LENS).

One of the most commonly used processes is fused filament fabrication (FFF). FFF is a process in which a filament is fed to a heated nozzle by a motor where it is melted. This melted filament is pushed through the nozzle and is then deposited in the XY plane on the machine. The Z-axis is also controlled and moves by a single layer height every time the printing of the layer is finished [9].

The key elements of an FFF system are as follows [12]:

- Feed mechanism
- Liquefier and print head
- XYZ gantry
- Build plate
- Build chamber

2.2.1 Material Feed Mechanism

Granular or pelletized feedstock with a screw-type extruder may be used in FFF machines, however, there are very few FFF machines using this type of feed mechanism. The most

commonly used feedstock material in FFF is thermoplastic filament with diameter of either 1.75 mm or 2.85 mm. The feeding mechanism for these filaments is quite different from those used for granular materials. In a wire-feed mechanism, the filament is pushed through the system with the help of a pinch roller mechanism as shown in the Figure 2. These rollers have grooved or toothed surfaces to create sufficient friction to grab the filament and push it through the nozzle. One of the rollers is connected to an extruder motor which provides the energy to feed the filament through the system. The feed rate of the filament can be controlled by modifying the speed of the extruder motor [2].

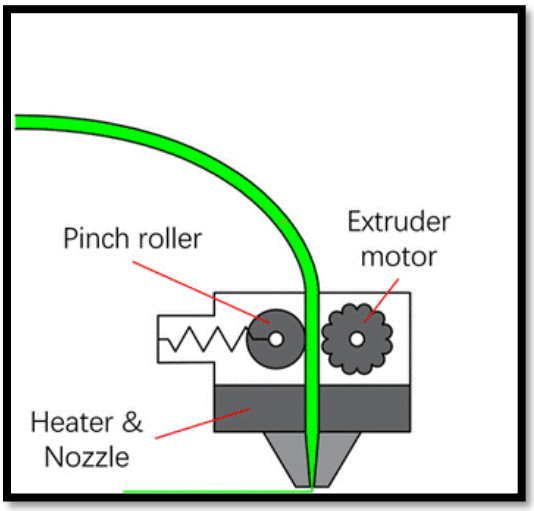

Figure 2 Pinch Roller and Extruder Motor Mechanism [13]

3.2.2 Liquefier and Print Head

After the feed mechanism, the filament reaches the liquefier. This is generally a block of metal with a hole that allows the flow of the filament which is being melted. This system is generally heated with resistive heating cartridges whose temperatures can be controlled by changing the current that passes through them. The reason behind this change is that different materials have different melting points. As a feedback mechanism, a thermistor or thermocouple is used to read the temperature, and a controller is used to maintain it. The temperature of the liquefier remains the same throughout the block. A print head is attached at the end of the liquefier block. This is a nozzle through which the liquid plastic flows. These nozzles are replaceable and can come in different diameters (e.g. 0.4 mm, 0.6 mm, 0.8 mm, etc.) [2].

2.2.3 Gantry

The liquefier and the print head are typically attached to a gantry type system which enables the system to move in the X Y and Z directions. The power to enable this motion comes from three different motors connected to each axis. The velocity of the print head, and ultimately the speed of part fabrication, is determined by the revolutions per minute (RPM) of these motors. There are end-stop limit switches for each of the X, Y and Z axes to prevent over travel. Figure 3 shows the schematic of a 3DP gantry [2].

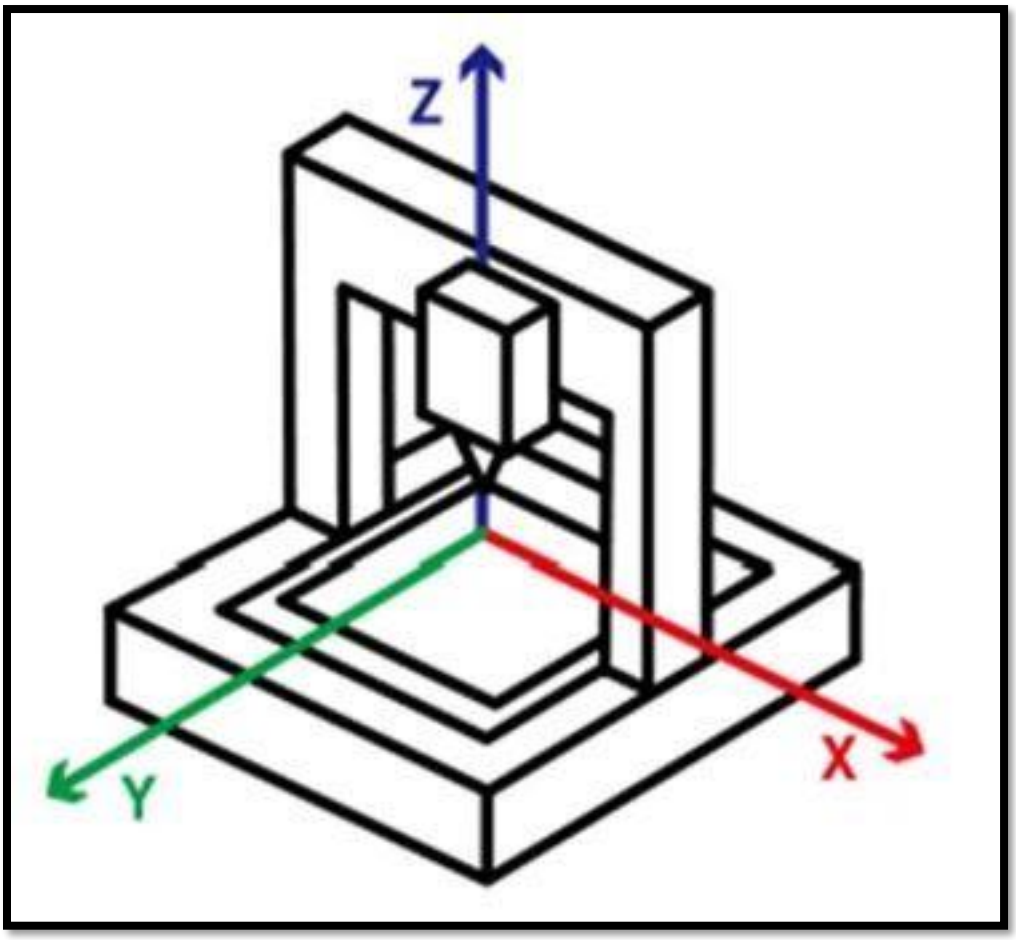

Figure 3 Schematic of 3D Printer Gantry With Axis

2.3 Potential Problems in FFF Parts

There are various problems in FFF printing, but two of the most important drawbacks in FFF printing are the stair stepping effect and low mechanical strength. These issues are discussed in further detail [14].

2.3.1 Mechanical Strength of Parts

There are many factors on which 3DP part quality is judged. Some of the major factors are part strength, print time, appearance of the parts, and cost of production [14].

In this section, ways to optimize 3DP parts for strength are presented. The three major factors affecting part strength are 3DP settings, 3DP material, and printing orientation [14].

3D Printer Settings

Two major 3DP setting that can be changed in order to get desired part strength are infill percentage and shell thickness [14].

Infill Percentage

The infill percentage of a part indicates how dense the part interior will be. The setting can range from 0% to 100%. A 0% percent infill part will have a hollow interior, and a 100% infill part be fully solid as shown in Figure 4. The infill setting will have a great impact on compressive strength of the part [15].

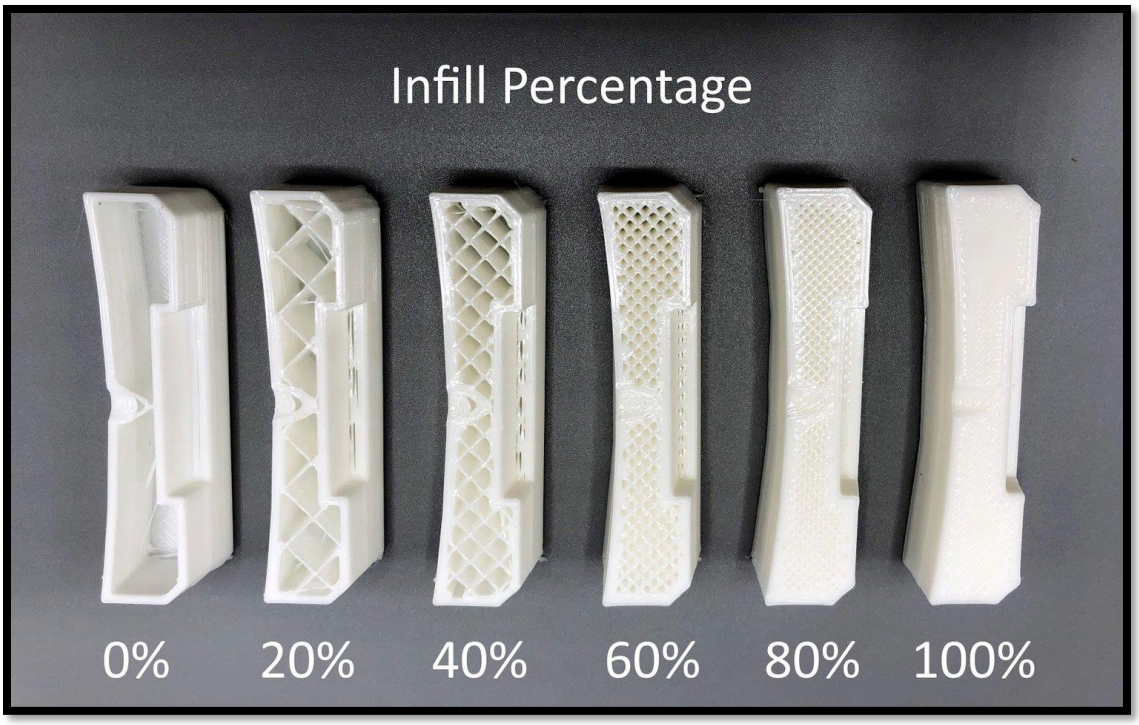

Figure 4 Different Infill Percentages [16]

A part with 60-70% of infill will have a reasonable balance between part strength and weight. Increasing the infill percentage above this will have relatively little impact on strength. When printing large parts, increasing the infill percentage can drastically increase the cost and print time [15].

Shell Thickness

Another setting that will affect part strength is shell thickness. Shell thickness is the thickness of the outer surface of the part. A thickness of 1.0 mm - 1.5 mm is often used to print parts, and increasing this can sometimes increase the tensile strength of the part. Increasing the solid shell thickness of the part while keeping the infill percentage constant can increase the part strength and/or stiffness. This fact is significant in light of the 5-axis surface printing process planning research presented later in this document [15].

3DP Material

The materials used in FFF printing will have a significant impact on the part quality. Some of the most commonly used FFF materials include PLA, ABS and PETG plastic. All the mentioned materials exhibit different strength characteristics which are to be considered while printing a part. If a part needs high tensile or flexural strength, one can use PETG or PLA. If a part is subjected to slightly elevated temperature and/or requires greater impact toughness, one can use ABS [17].

Part Orientation

Part orientation, which is illustrated in Figure 5, refers to how the part is positioned on the print bed while printing. Part orientation is one of the major factors in 3DP for strength considerations. This factor is unique to 3DP parts and has a significant impact on the strength of the part [15].

As we know, 3DP parts are manufactured by depositing layers on top of layers while gradually increasing the height of the part to form a 3-D part. Even though plastic on each layer bonds with the previous layer, these bonds between the layers are much weaker than the strength of the bulk plastic. 3DP parts therefore mostly break at the interfaces between layers [14], [17].

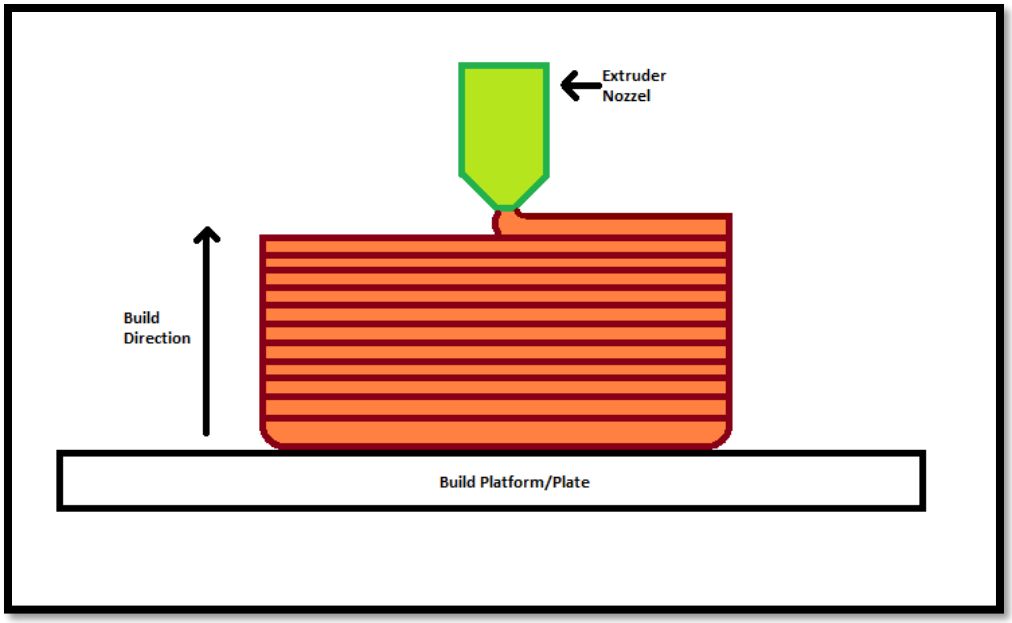

Figure 5 Print Orientation

Build orientation is a major consideration for parts that will be subjected to tensile forces parallel to the z-axis layer building direction as illustrated in Figure 6 [17].

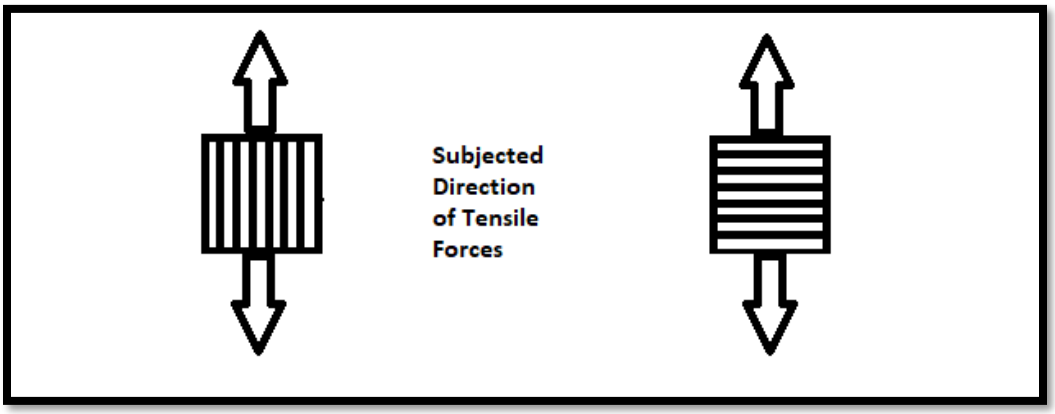

Figure 6 Tensile Force Acting On A 3DP Part

2.3.2 Stair Stepping Effect

The stair stepping effect is a limitation for all layer manufacturing processes. It depends on various factors, but this effect is prominently seen while printing inclined or curved surfaces. The effect is considered to increase with an increase in layer thickness. As seen in Figure 7, there can be a drastic difference between the nominal CAD surface of a part and the actual part surface manufactured using layered manufacturing [18] [19].

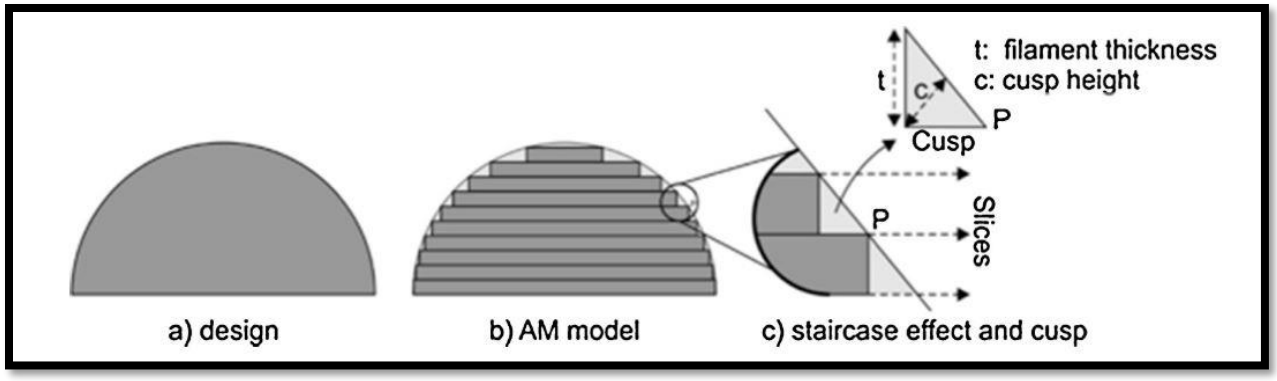

Figure 7 Difference Between CAD Surfaces and 3DP Part Surfaces [19]

In experiments conducted by Ahlers et al. [18], the authors concluded that the stair stepping effect for FFF printed surface increases for surface angles below 20 degrees. As shown in Figure 8, for a given layer thickness, the surfaces whose slopes are nearly vertical will have less roughness, while surfaces with more shallow slopes will have more prominent stair steps and larger error [18], [20].

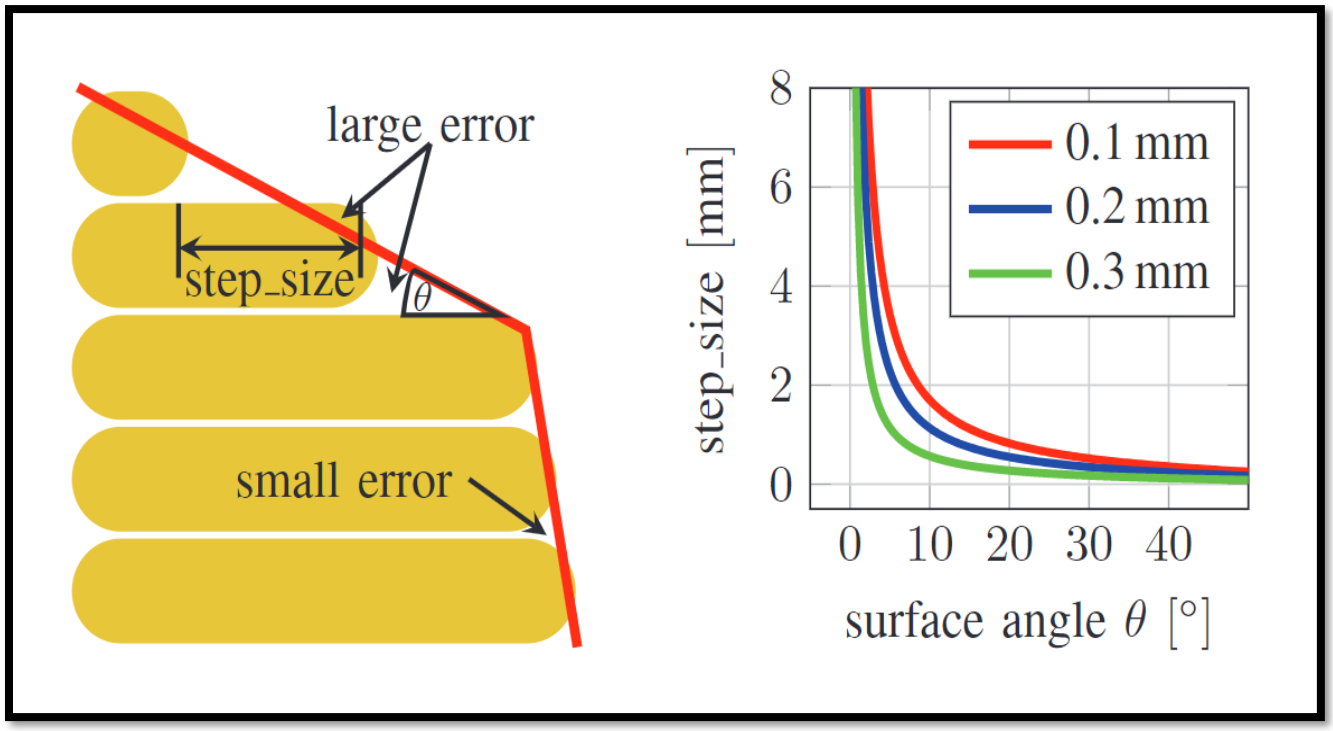

Figure 8 Stair Stepping at Different Surface Angles (θ) [18]

2.4 Non-Planar FFF Surface Printing

Problems such as low mechanical strength and stair stepping effects discussed in the previous section are being addressed by researchers in an emerging area called nonplanar FFF printing [21].

In non-planar surface printing, the exterior surfaces of parts are not produced via the conventional layer-by-layer approach. Instead the exterior surfaces of the part are produced by sweeping the FFF extrusion head along the model's non-planar surface geometry thus resulting in smoother surfaces and potentially stronger parts [22].

This type of printing can further be divided in two sections-

- Non-planar printing using a 3-axis machine.
- Non-planar printing using a 5-axis machine.

2.4.1 Non-Planar Printing Using A 3-Axis Machine

In non-planar with 3 axis machines, an active Z axis approach is taken to print the surfaces. The active Z axis FFF technique uses simultaneous motion in the X, Y and Z axes to produce 3D surfaces and cross sectional areas [23].

Curved Layer Fused Filament Fabrication (CLFFF) was introduced by Chakraborty et al. to tackle the problems in conventional 3DP. They worked on generating the active Z axis toolpath by offsetting part surfaces using Bezier surfaces to create 3D layers. However no parts were manufactured and tested [24].

To generate an active Z axis part, Singamneni et al. generated toolpaths by offsetting surface point data from the STL file in the Z-axis direction. They then printed parts using CLFFF with ABS filament. 3-point bent test were conducted, and flexural properties were compared with those of conventionally printed parts. The authors concluded that parts manufactured using the CLFFF technique exhibited a 40% increase in load before fracture [25].

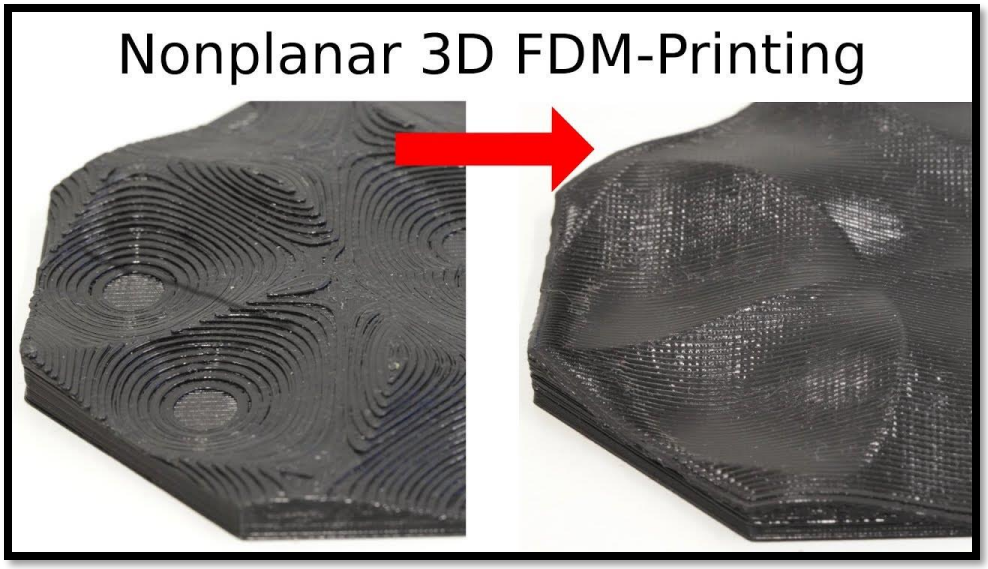

Figure 9 Comparison of Planar and Non-Planar 3D FFF Part.[16], [17]

2.4.1 Challenges In Non-Planer Printing Using 3-Axis FFF Printers

Ahlers et al. 2019 demonstrated active Z-axis printing using an Ultimaker 2 printer, which is a 3-axis gantry type FFF printer. The authors observed that when printing nonplanar surfaces with an active Z axis approach, the 3D printer and the printed part are prone to self-collision. Specifically, self-collision between the nozzle extruder body or cooling fans of the print head and the part can occur with surfaces below the current printing layers where material has already been deposited. This is illustrated in Figure 10 [18].

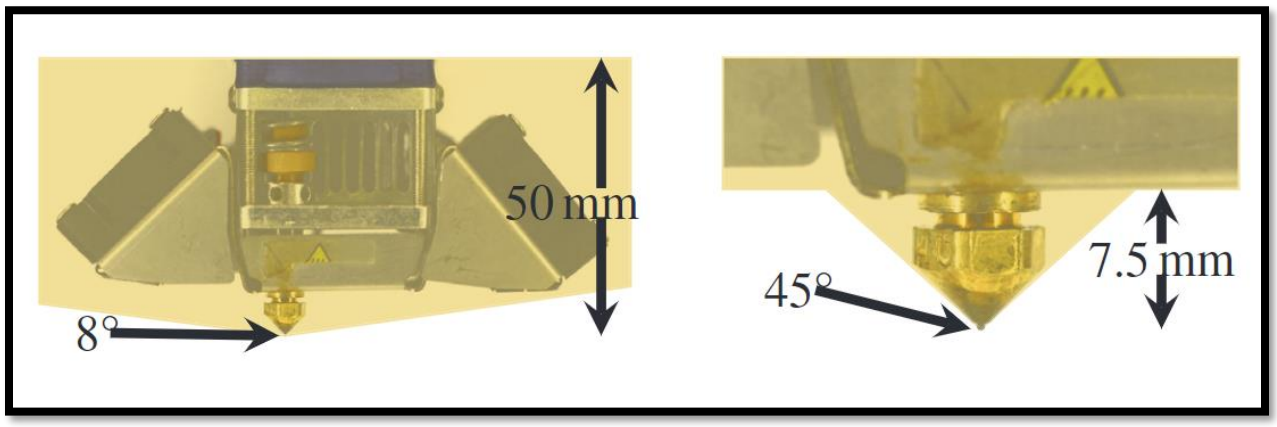

Figure 10 Non Printable Geometries Due to Ultimaker 2 printer Nozzle Collision [18].

Figure 11 illustrates how the geometry of the filament extrusion head limits the ability of some printers to follow non-planar conformal surfaces. As the head moves up and down along a non-planar surface, the fans, heat brakes, and nozzle are prone to collide with previously deposited material for surfaces having anything other than very shallow surface angles [18]. Figure 11 further illustrates the acute bend angle that the extruded thermoplastic must take when printing in the downhill direction.

This limitation of printing either large surfaces with small non planar angles or small surfaces with large non planar angles can be reduced by using long slender nozzles together with a 5-axis deposition tool. This approach generates toolpaths in which the nozzle of the printer is able to tilt and rotate during deposition to avoid self-collisions [23] [18].

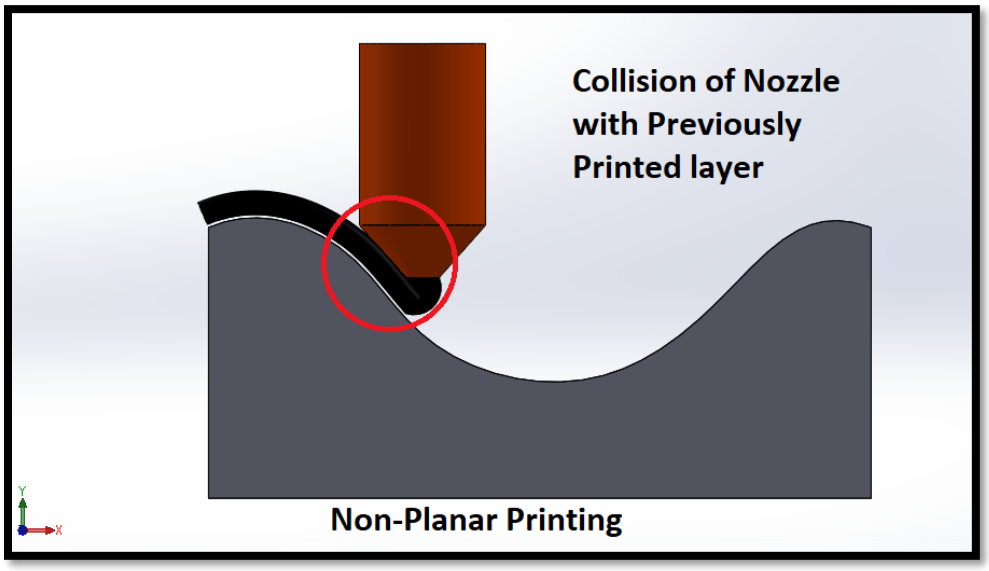

Figure 11 Nozzle Collision While Printing Non Planar Layers On A 3-Axis Machine

2.5 5-Axis FFF Printing

Using a 5-axis FFF machine to print non-planar surfaces is a novel field that is being explored by a growing number of additive manufacturing researchers. As discussed in the previous chapter, this can address multiple challenges that are observed in conventional 3D printing as well as non-planar printing with 3 axis FFF. The basic operations in 5 axis printing are similar to

conventional additive manufacturing methods. A 5-axis machine configuration gets a bit more complex with the addition of two rotary axes, which are the B and C axes. Axis C introduces rotary motion of the extrusion head about the Z axis, while the B axis introduces rotary motion of the extrusion head about the X axis. This configuration helps in many ways. By adding these two axes, the extruder nozzle can be held perpendicular, or relatively close to perpendicular, to the non-planar printing surface during deposition as illustrated in Figures 12 and 13. This helps in solving some of the aforementioned problems related to 3-axis FFF printing.

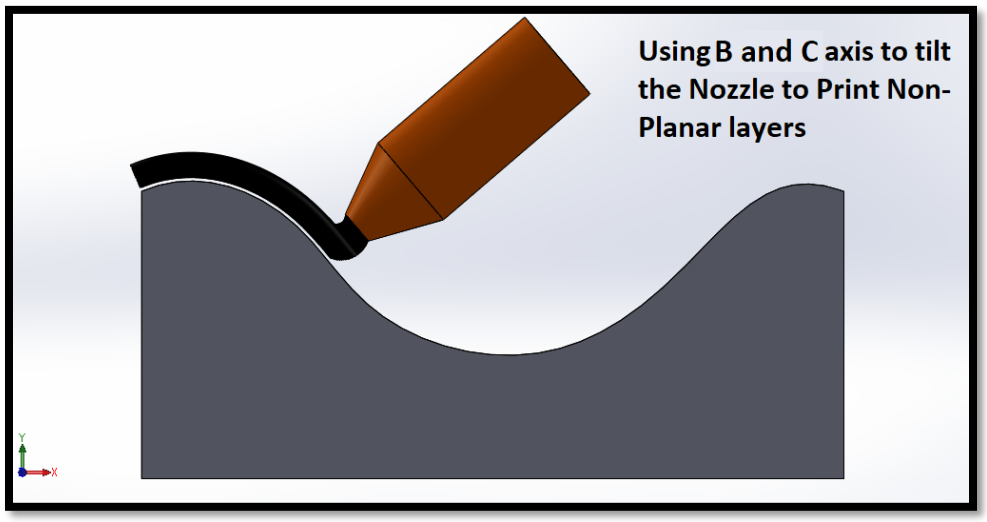

Figure 12 Rotation of Axis In Order to Keep the Nozzle Perpendicular to the Printing Surface

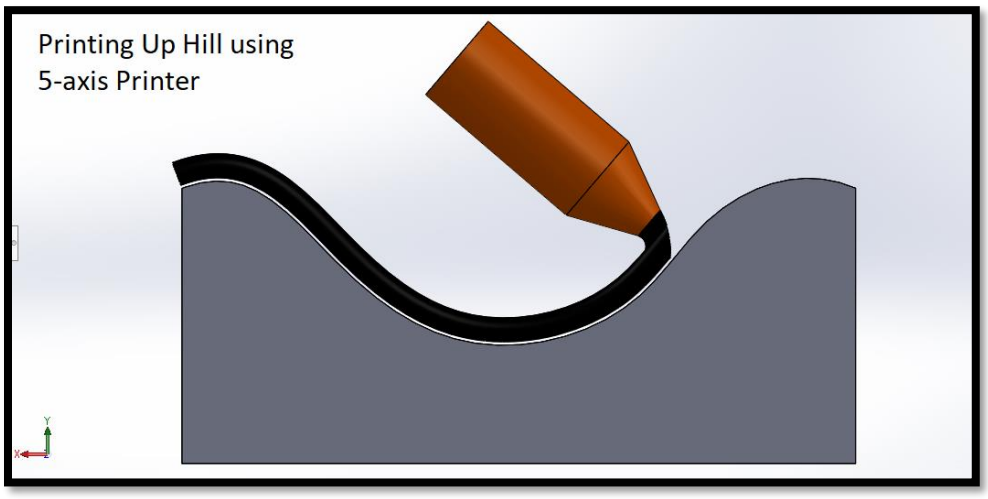

Figure 13 Printing up Hill without Nozzle Collision

In recent years, a small number of research teams have worked on developing and testing systems that can print non-planar surfaces. Kaill et al. [26] used a 5-axis FFF printer to print nonplanar FFF surfaces which were then tested under compressive loading. Toolpaths for a dome shape were manually generated due to the absence of non-planar FFF slicers. The researchers

printed this part with a conventional 3D FFF technique as well as a nonplanar 5-axis FFF printer. The authors concluded that printing a part with 5-axis deposition of material along the principle stress vector of the part reduced the anisotropic nature of the FFF part and increased the load-bearing capability of the part by a factor of 3.5 [26]

Another team of researchers lead by Muhammad Asif from Auckland University of Technology developed a 5 axis photopolymer extrusion 3D printer. The non-planar parts were made by moving the nozzle in free space while curing the deposited resin using UV diode lasers. A proof of concept was demonstrated by manufacturing free form parts. As automated software comparable to a conventional 3D printer slicing software was not available, parts with complex geometries were not produced [27].

Luo et al. from National Taiwan University worked on surface coating of a pre manufactured hemispherical part using a 5 axis FFF printer. They first manufactured a hemisphere using a conventional FDM 3D printer. A conventional three-axis G-code slicer was used to develop the five-axis printing trajectory. The researchers generated their own non-planar toolpath generation algorithm which analyzed the top layer of the geometry to determine the rotational axis' tilt angles to keep the nozzle normal to the surface. They concluded that using this method of printing non-planar surfaces has a limitation, as the nozzle geometry prohibits printing of complex surfaces. They also noted that the printing distance between the model and the nozzle will become greater when the model is tilted in surface coatings and hence will create a non-uniform surface [28].

A recent paper by Hong et al. from Imperial College London demonstrated nonplanar FFF printing. They used a Graphical User Interface (GUI) based conformal slicer that the researchers developed as an alternative to using computer numerical computing (CNC) toolpath generation to generate conformal toolpaths. The machine that they used was Prusa i3 MK3s which was modified by replacing the print bed with controllable 2-axis rotating stage. They demonstrated their approach by manufacturing conformal surfaces on top of preexisting non planar surfaces [29].

In a paper published by Dai C et al. the researcher has shown the capability of using robotic arms to produce support free structures. The non-planar layers were manufactured by rotating the bed and the extruder to avoid any support requirement [30].

Teibrich et al. used the 5-axis FFF technique to patch physical objects by printing structures on top of existing surfaces. They used a dual axis rotating bed type FFF printer. A Creative Senz3D depth camera was used to scan the existing model and create a 3D model. The 5 axis maneuverability was used to then align the part to print the filament on the desired area [31].

5-axis nonplanar AM is also being used in Wire Arc Additive Manufacturing (WAAM). As WAAM melts wire with large diameters and lays it along a toolpath, its stair stepping effect is more prominent. The amount of material deposited is several kilograms per hour. This strategy of manufacturing parts also needs more control over the deposition height. To achieve that, Diourté et al. worked on a Continuous Three-Dimensional Path Planning (CTPP) technique in which they manufactured a part with conventional 3 axis WAAM and used the normal surface vectors to generate CTPP toolpaths by keeping the tool axis normal to the surface vector [32].

2.6 3D Printed Woven Structures

In an attempt to increase the mechanical strength of parts by aligning carbon fibers, new methods of layer depositions are being researched. One such approach 3D prints continuous fiber with woven structures [4]. In 2018, Dickson et al. explained the method of generating a planar woven pattern by a FFF technique [33]. This concept is illustrated in Figures 14 and 15.

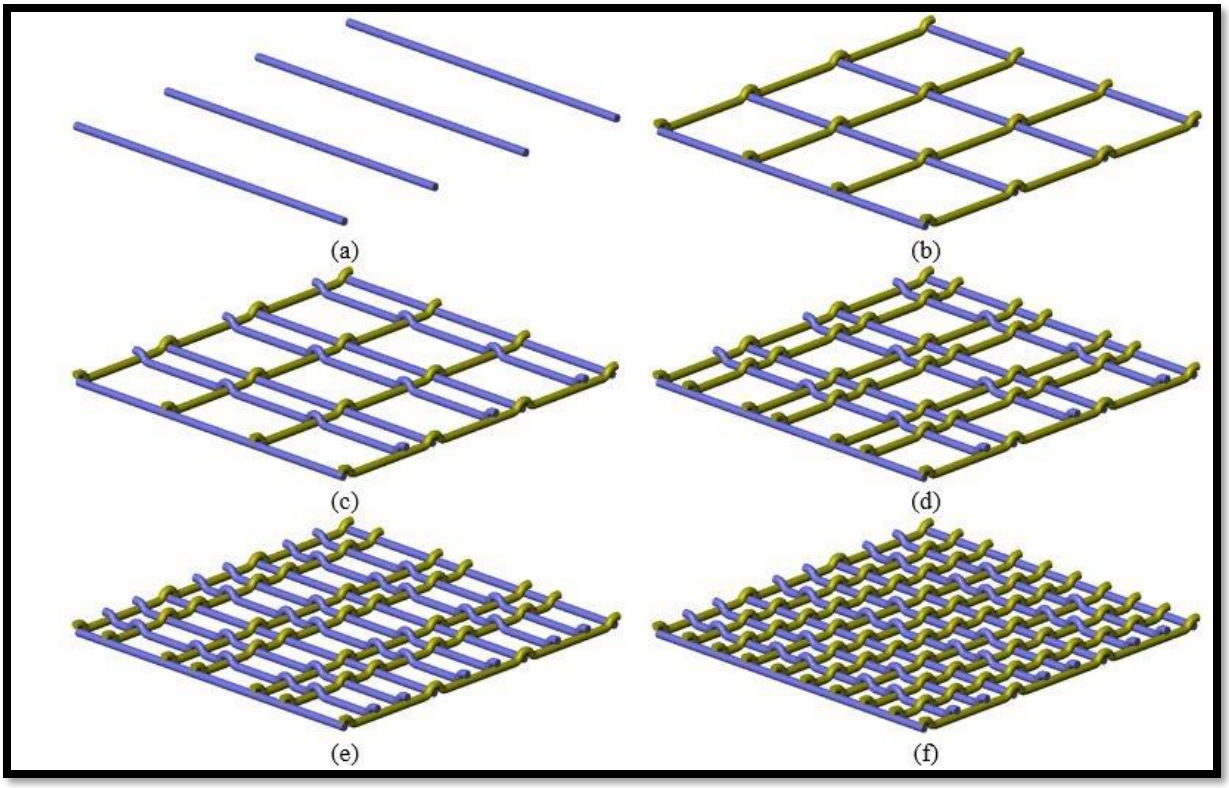

Figure 14 This Illustration Shows the Sequence (From Step A to F) And Position of Consecutive Layer Deposition on a Planar Surface to form Interlocking between Layers.

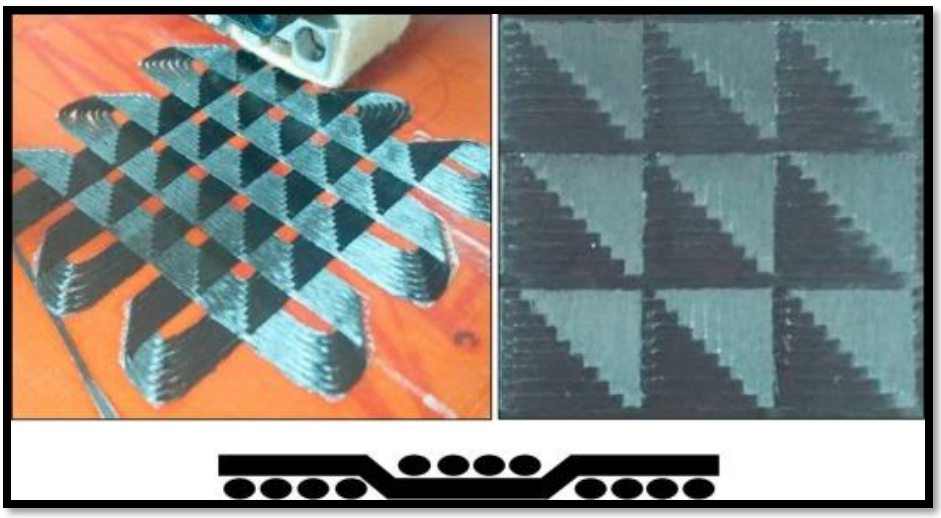

Figure 15 Planar Printing of Woven Carbon Fiber [33].

Woven sheets are produced by laying multiple sheets of material on top of each other with some degree of interlocking between them. The parts produced by these interlocking fibers were tested

by Ekoi et al. against the parts produced by non-woven fibers. They conducted tensile, flexural and fatigue testes on these parts and concluded that in fatigue testing, the woven composite were superior to the nonwoven composite when tested at 70% of their ultimate strength for 200000 cycles [4].

2.7 Problem Statement

This literature review has described several approaches to 3D printing of non-planar surfaces, and several limitations have been described. This thesis seeks to work on addressing some of these issues. As seen, most published research uses custom made 5-axis 3D printers with manually generated g-code. In the remainder of this thesis, a commercially available software package (Autodesk PowerMill Ultimate with an additive manufacturing plug-in) and machine (5Axis Maker) package are studied. To the best of the author's knowledge, PowerMill has not been used to generate 5-axis FFF toolpaths with a 5Axis Maker machine. Chapter 3 therefore documents the machine setup and software process planning steps. A custom Powermill post-processor for the 5Axis Maker machine was jointly developed by RIT and Autodesk, and that plug-in will be openly available for other researchers to use for future research.

In the coming chapters, three different types of parts with non-planar surfaces are considered. Process planning of these parts is described, sample parts are printed, and mechanical properties are assessed using standard 3 point bent testing and Charpy impact testing. These results will be compared to properties of conventional FFF parts.

Finally, as discussed in the literature review, producing FFF parts with a woven pattern has mechanical benefits. Hence for the first time, we have demonstrated an approach to generate toolpaths to produce woven non-planar surfaces. This can be used as a proof of concept for further research.

3.0 PROCESS PLANNING FOR 5-AXIS ADDITIVE MANUFACTURING

As shown in the literature review, 5-axis additive manufacturing is different in certain ways from 3-dimensional additive manufacturing. Process planning techniques with optimal printing parameters for non-planar surfaces therefore do not exist right now. In this chapter, we will be going through the steps needed to generate toolpaths to print different types of non-planar surfaces.

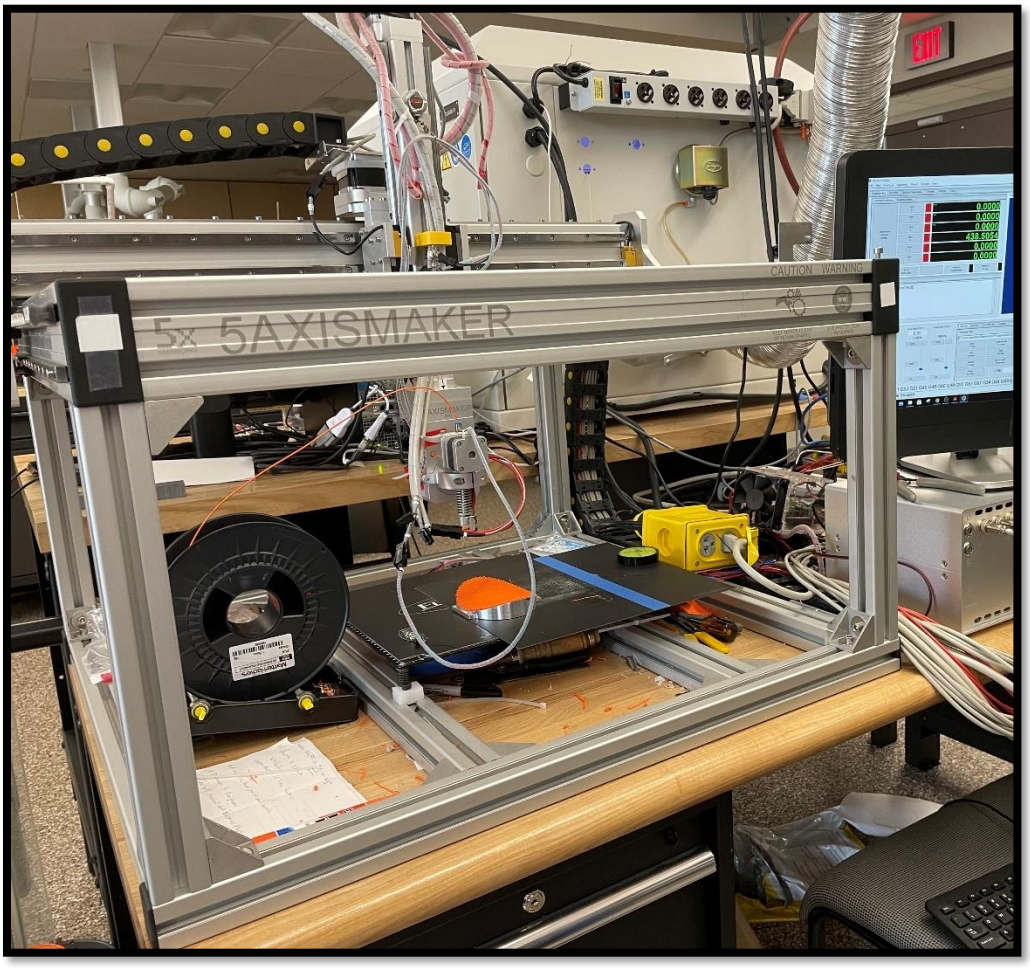

Figure 16 5 Axis Maker Machine

The hardware used here is a 5Axis Maker machine which is shown in Figure 16. This is a commercially available desktop machine which has a gantry system to move in the X, Y and Z

directions. At the tool end, it has an FFF heater and extruder assembly. The extruder assembly has the ability to rotate in 2 axes. As shown in Figure 17 the B-axis introduces extruder rotation about the X axis of the machine's coordinate system. The C-axis introduces extruder rotation about the Z axis of the machine's coordinate system. Combining the three linear axes of motion with the two rotary axes of motion, one gets 5 axis printing capability. Due to this being such a new technique, there have historically been no commercial 3D printer slicers that will generate a toolpath for the 5Axis Maker FFF printer.

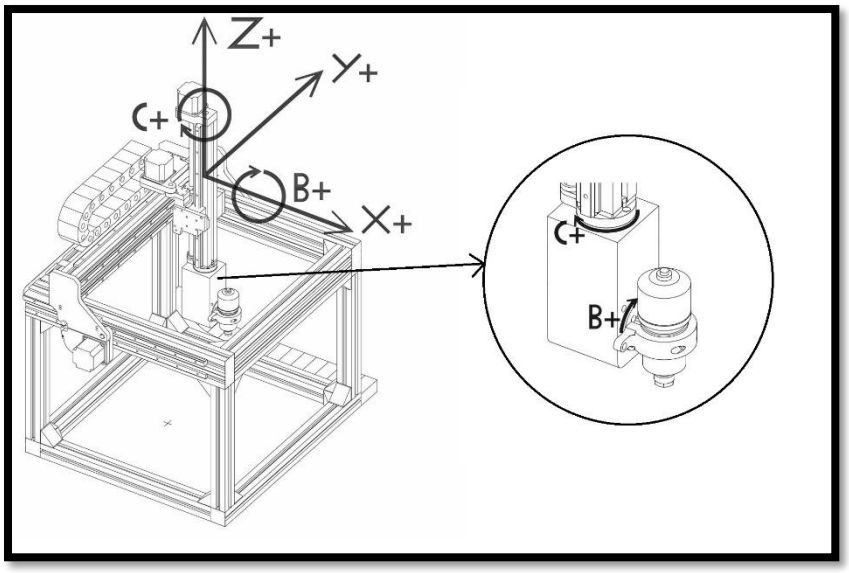

Figure 17 All Axis Of 5 Axis Maker Machine[34]

In this work, the Powermill Ultimate CNC CAM software from Autodesk was used to develop non-planar additive toolpaths. A postprocessor was developed in collaboration with Autodesk for the 5Axis Maker machine. This post processor was based on a generic gantry milling machine post processor, and the spindle axis was turned into the extruder axis of the FFF printer.

The entire process of preparing the G-code and executing it on the printer is divided into three different sections, and every section uses a different software to operate. Figure18 shows the

process flow. Subsequent tabs will explain each step in further detail.

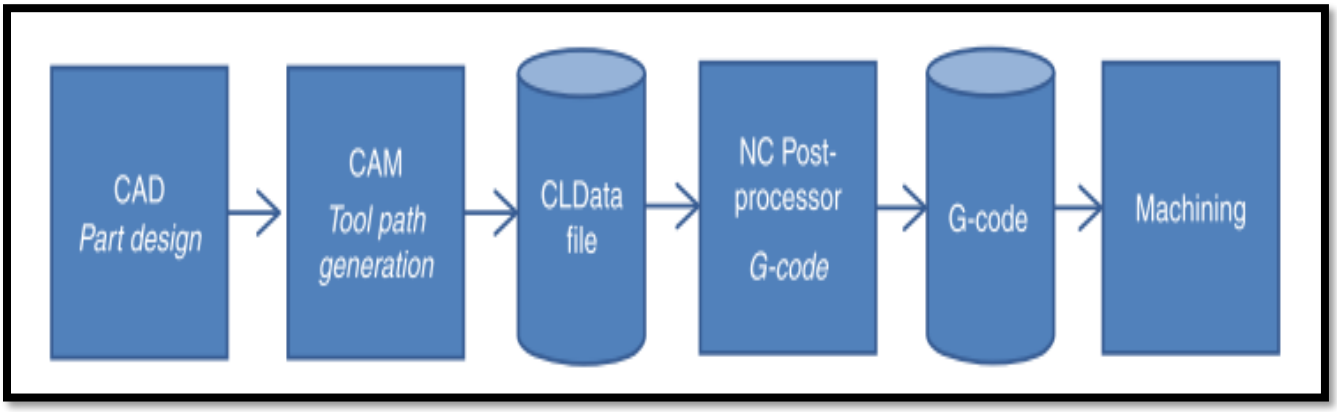

Figure 18 Process Flow For Printing Non-Planar Surfaces With 5 Axis Maker.

3.1 CAD File Generation

As opposed to the work of Hong [29], who needs to use a specific CAD packages to prepare the model, this method can use CAD files generated in any software. The CAD file should be a part file and have a planar base. Autodesk Powermill Ultimate is used as our CAM software. In this particular example, Solidworks has been used to design the part. The file type is .SLDPRT. Powermill is able to accept other file types though.

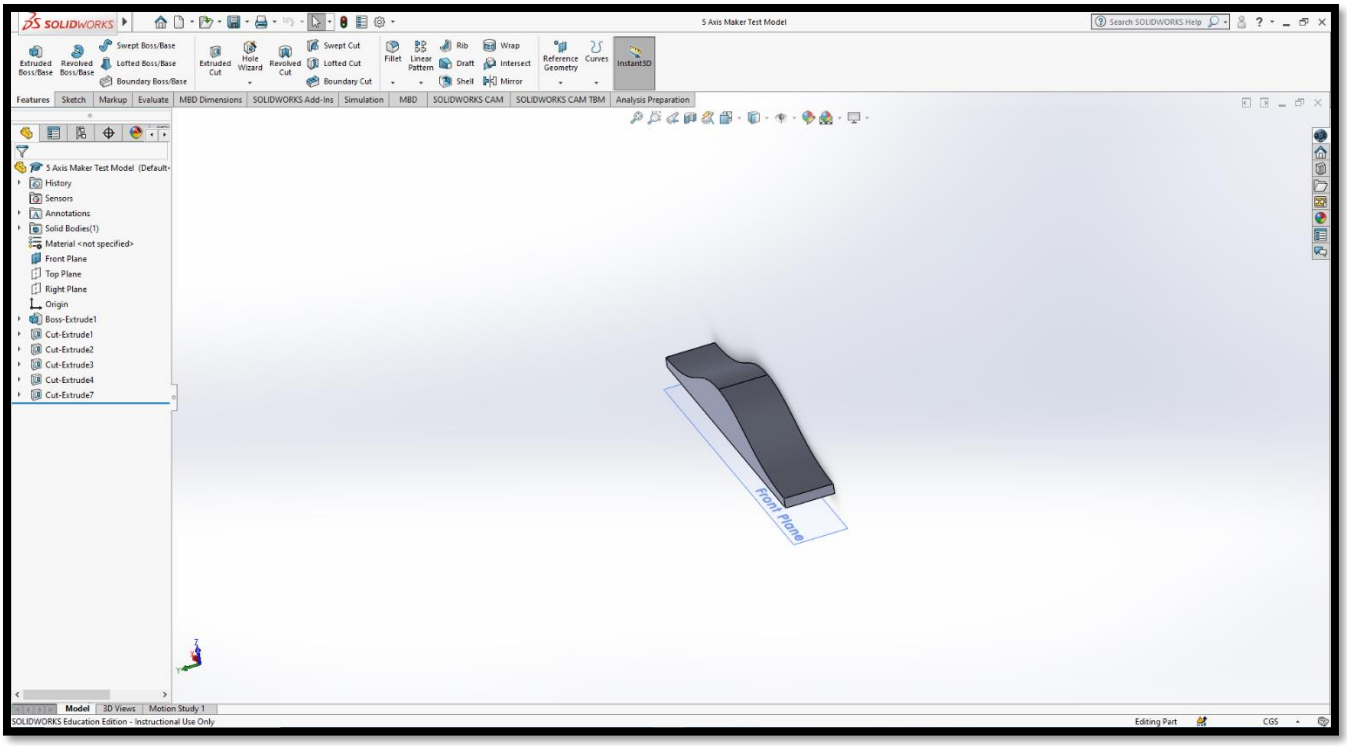

Figure 19 Solidworks Part File

3.2 Setting up Autodesk Powermill 2022.

This part is specifically designed to have a non-planar surface on top to demonstrate the 5-axis capabilities of our machine to print the top surface. Now that the CAD file of the part is ready, the next step is to generate a toolpath for that part. There are very few software packages available at this time which can generate 5-axis additive toolpaths, and all of them are in relatively early stages of development. The only commercially software available at this time to generate a 5-axis additive toolpath for the 5Axis Maker is Autodesk Powermill Ultimate 2022 with the Additive Manufacturing plug-in.

RIT's AMPrint Center collaborated with Autodesk to generate a Post Processor for the 5Axis Maker machine. The post processer was developed with the Autodesk Manufacturing Post Processor Utility (AMPPU). This software is licensed and is downloaded from Autodesk website.

Once the software is installed and running, the first thing one needs to do is to enable the AM plugin. To do that we need to go to **File>Options>Manage Installed Plugins>Enable all**.

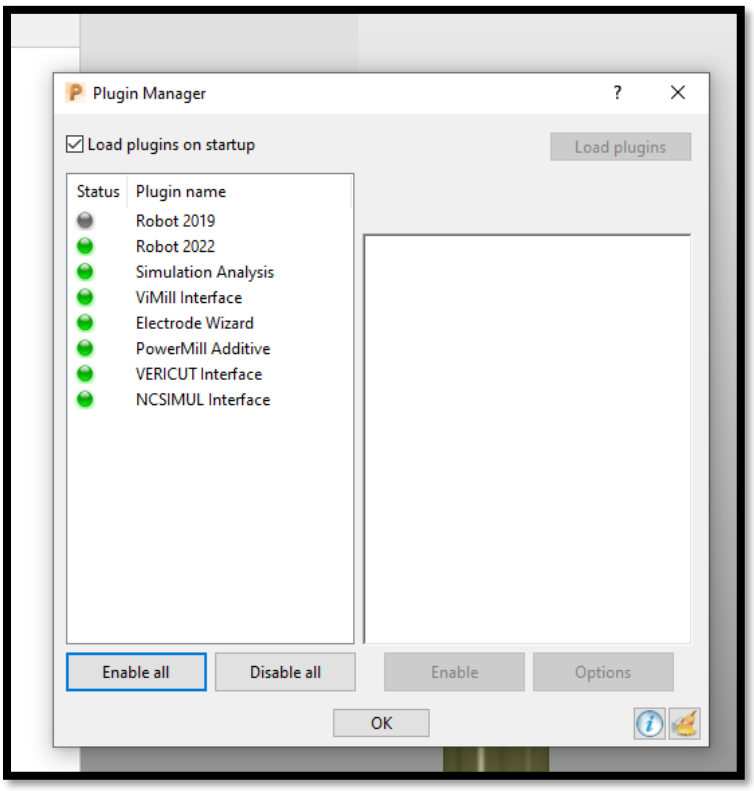

Figure 20 Additive Plugin Turning on Window

Following this step, the green indicator in front of "Powermill Additive" should turn on. The Home tab then displays an additional tab named "Additive".

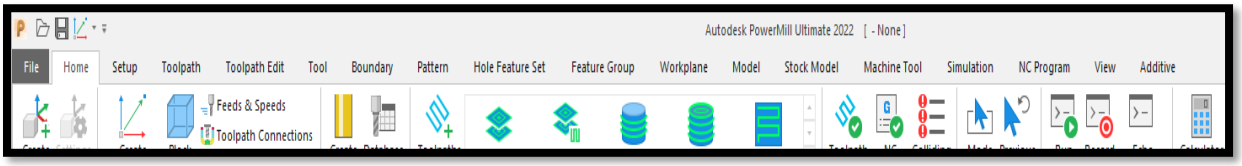

Figure 21 Toolbar with Additive Tab

The next step is to set up the Machine and import CAD models in Powermill.

3.3 Steps to Generate 5-axis Toolpaths

3.3.1 Importing the Machine Model

In this step, the Machine Tool menu is used to import the machine model (.mtd file) into the project. This file specifies details of the geometry of the machine and its dimensional limits.

There is a large library of machine models, including robotic arms, available in the software. The RIT-Autodesk collaboration resulted in a new configuration file for the 5Axis Maker machine. With the help of the manufacturer, we were able to get the machine model in a .mtd file format.

To import the machine model file, one right clicks on the Machine Tool tab in the Explorer window on the left hand side of the screen. From the dropdown menu, one then selects “Import Machine Tool…” which opens a browser window.

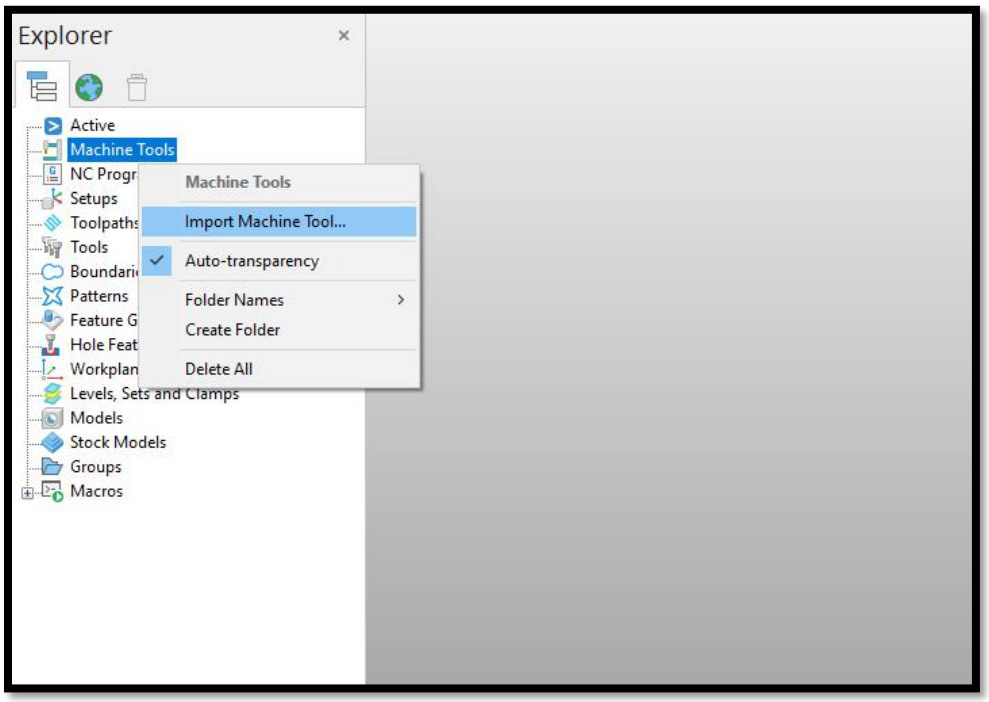

Figure 22 Importing A Machine Tool

The .mtd file is located, and one then presses **Open**. The .mtd file for 5-axis Maker machine is stored in **Downloads>5axismaker additive machine model>5axismaker 5X 600X600 additive.mtd.**

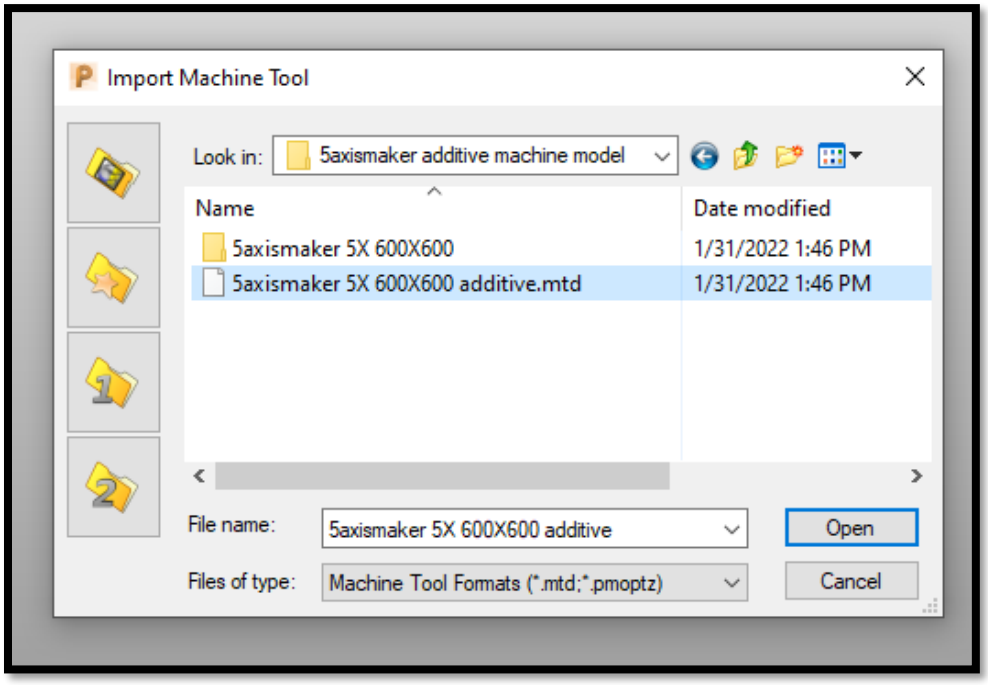

Figure 23 Machine Tool File Import

This will bring the 5Axis Maker model on the screen, and all the limits of printing/machining will be set according the machine's geometrical limits.

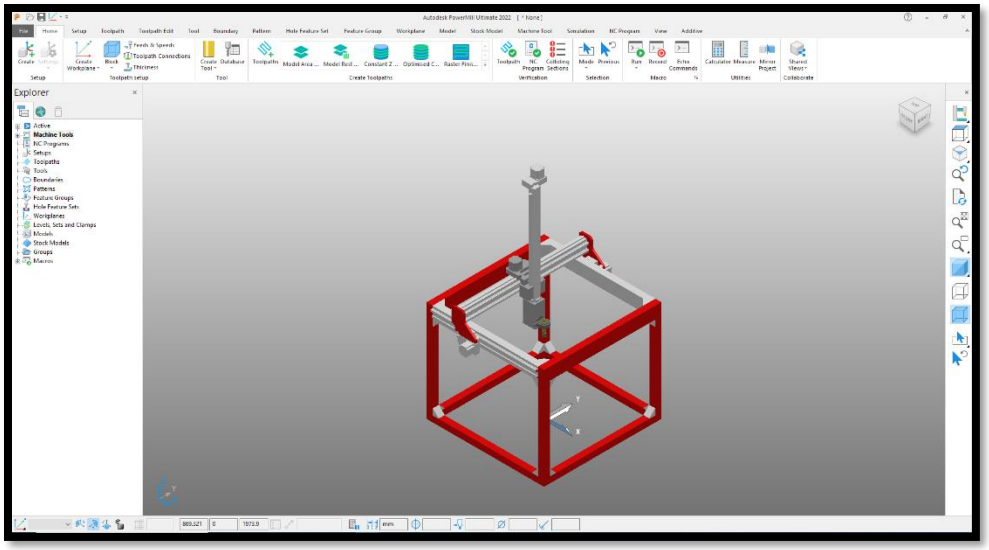

Figure 24 5Axis Maker Machine Tool

3.3.2 Importing a CAD Model

This step brings the CAD model into the Powermill project. To import the model, one right clicks on the Model tab in the Explorer window. The Import Model tab is then selected from the drop-down menu.

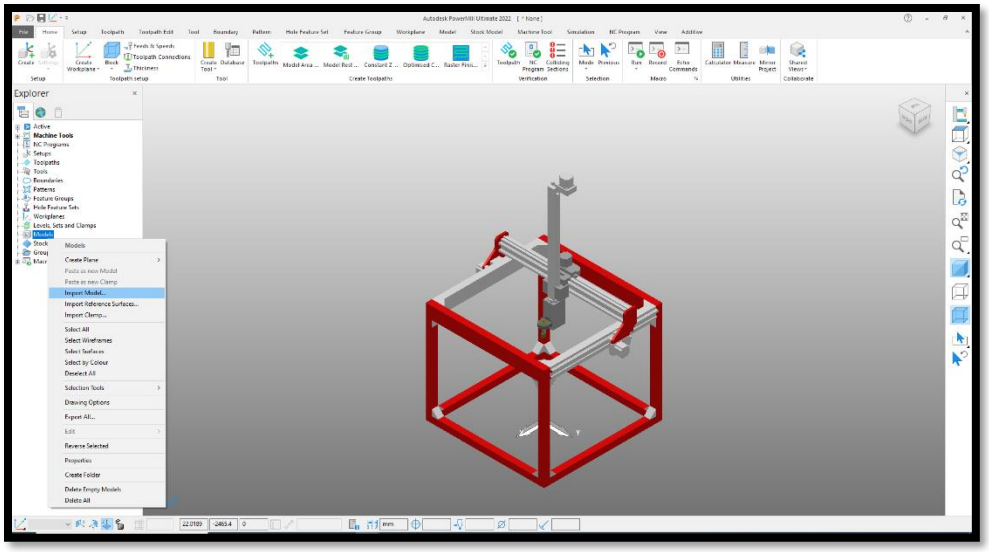

Figure 25 CAD Model Import

One navigates to the CAD file location in the browser window and then selects **Open** to import the file into the project.

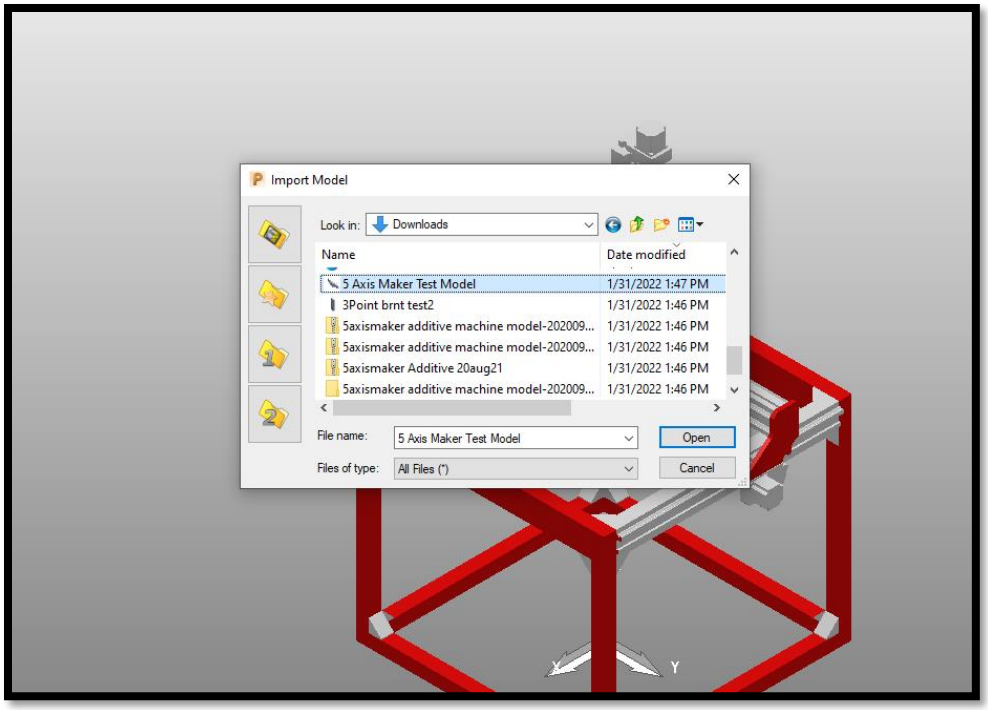

Figure 26 CAD Model Import Window

Once the desired CAD Model is imported ("5 Axis Maker Test Model" in this example) one will see a message box along with graphics showing the CAD model relative to the machine.

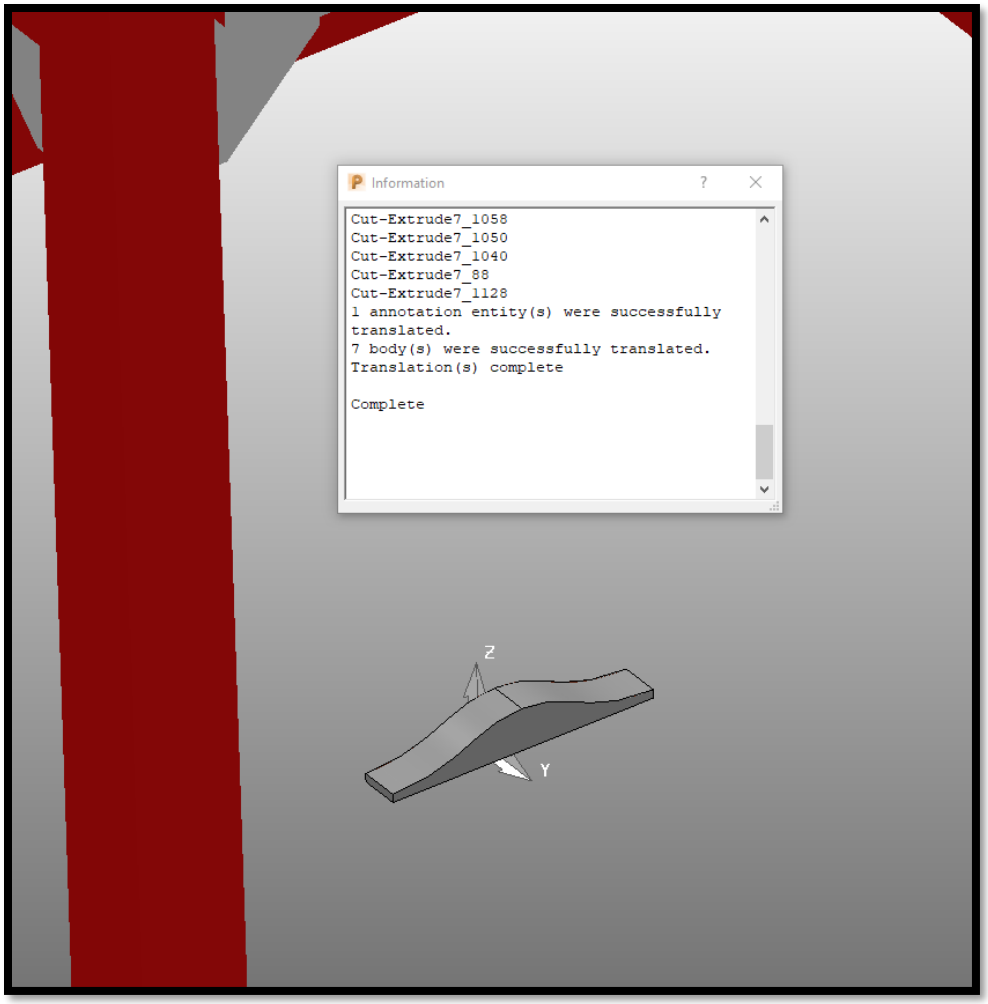

Figure 27 CAD Model Import Complete Message

3.3.3 Translating the CAD model

The imported CAD model will have the same orientation as it had when it was designed. The model may therefore need to be oriented in such a way that the flat surfaces are parallel to the print bed of the FFF machine. The reason for this is because Powermill is not yet capable of generating supports for overhang part surfaces (as of this writing). When the part has its flat surface facing downward, that bottom surface needs to be translated to a height of 100 mm in the positive Z-axis of the machine's coordinate system. This will place the bottom surface of the part on the machine's print bed.

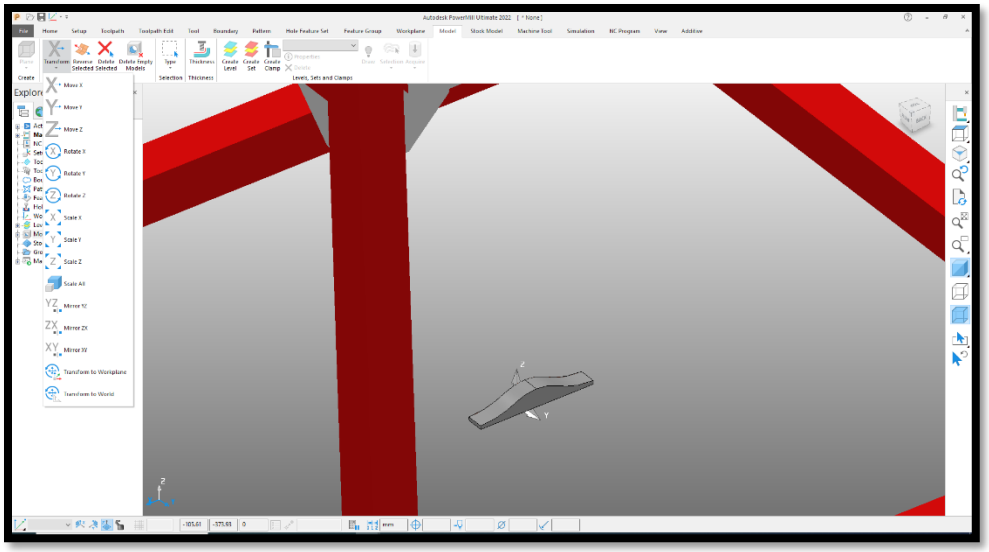

Figure 28 CAD Model Translation

3.3.4 Adding Workplanes

With the machine being set up, the part geometry imported, and the part positioned and oriented correctly, the next step is to add Workplanes to the machine model and the CAD model. These Workplanes will define the location of the model and machine in 3-dimensional space.

To add Workplanes, one clicks the **Home** tab and selects the **Create Workplanes** option. This generates a free floating XYZ origin point. This point is placed on one of the bottom corners of the CAD model by left clicking on the desired corner of the part. This generates Workplanes for the model. This step is repeated to place a second set of Workplanes corresponding to the preexisting origin at the center of the machine.

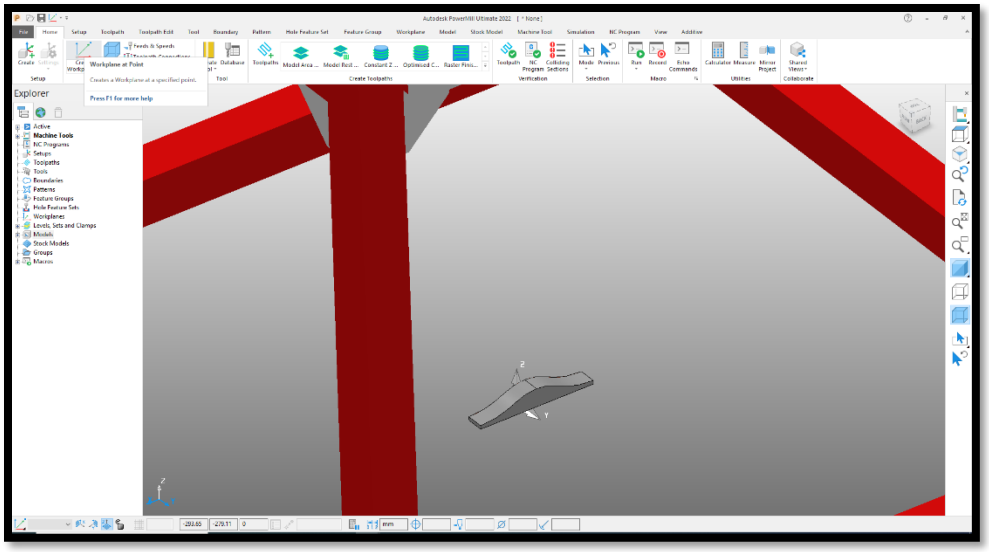

Figure 29 Adding Work Plane

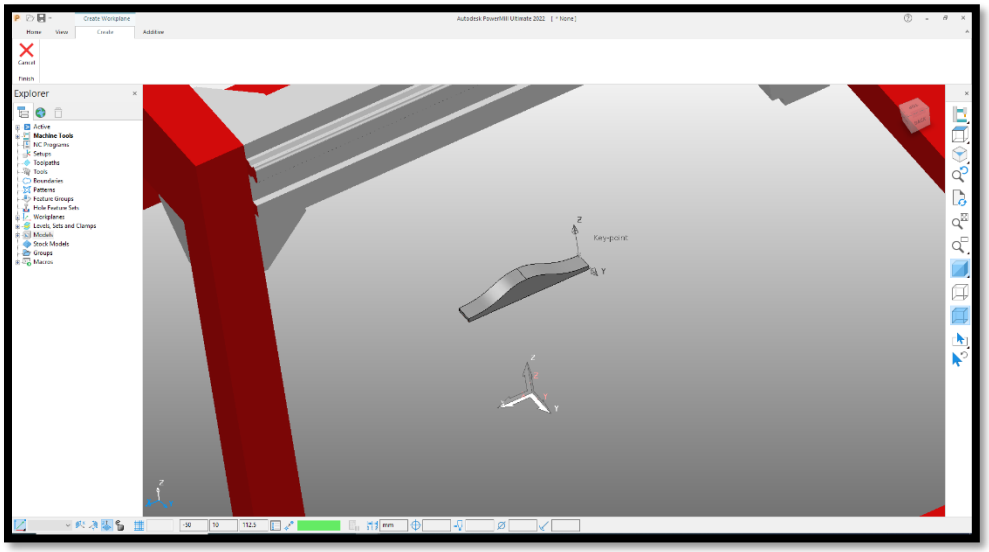

Figure 30 Adding Model and Machine Work Plane

This will produce two Workplanes that appear in the **Explorer** tab under the **Workplanes** branch of the tree. The Workplanes can be named "Model Workplanes" and "Machine Work Plane" respectively by right clicking and renaming them.

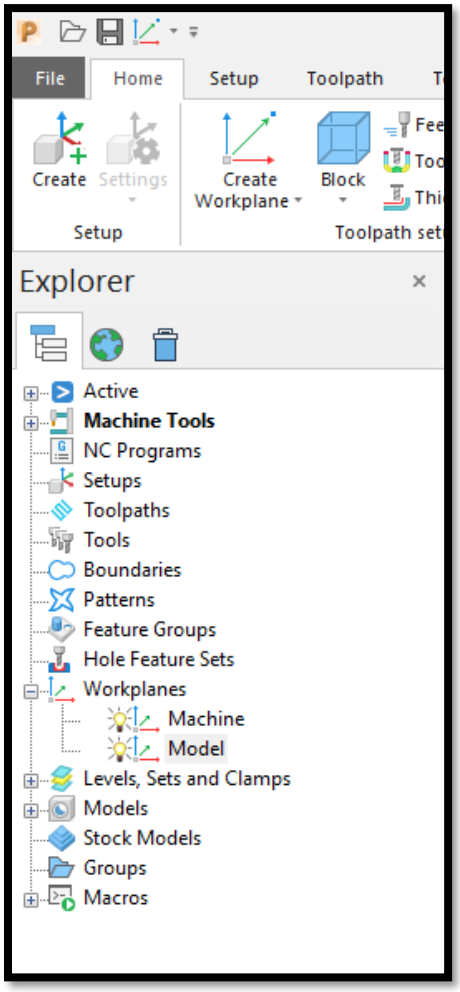

Figure 31 Active Work Planes

3.3.5 Creating Levels and Sets

Every project has one level and one or more sets. Generally speaking, a level is the base of the model on which the construction will start. A set is the collection of all the features on the model.

To create a Level and Set, one clicks on the **Model** tab, then clicks **Create Level**, and then clicks **Create Set**.

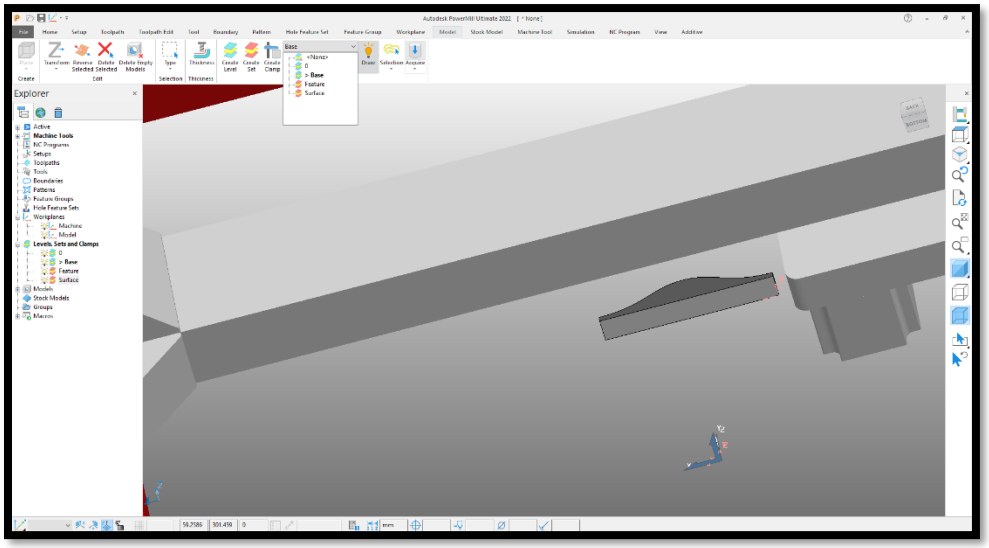

Figure 32 Levels and Sets Tab

There can only be one Level, however, there can be multiple Sets. From the drop down menu, one can select the newly created **Level**. On the model, select only the base surface of the model. The selected surface will turn dark. Clicking **Acquire** will set the bottom surface of the CAD model as the Level. This level can then be named "Base".

The next step is to identify the Set. While constructing a new 3D part, there will be one set which will include the Feature Construction which is used to build the feature via the normal 3DP process. A second set will be added for purposes of 5-axis 3DP of surface skins on the parts. To create the first set, select one Set, then select the entire CAD model and press **Acquire**. This will create a set which includes the CAD model geometry to be 3D printed. One can name this set as "**Feature**".

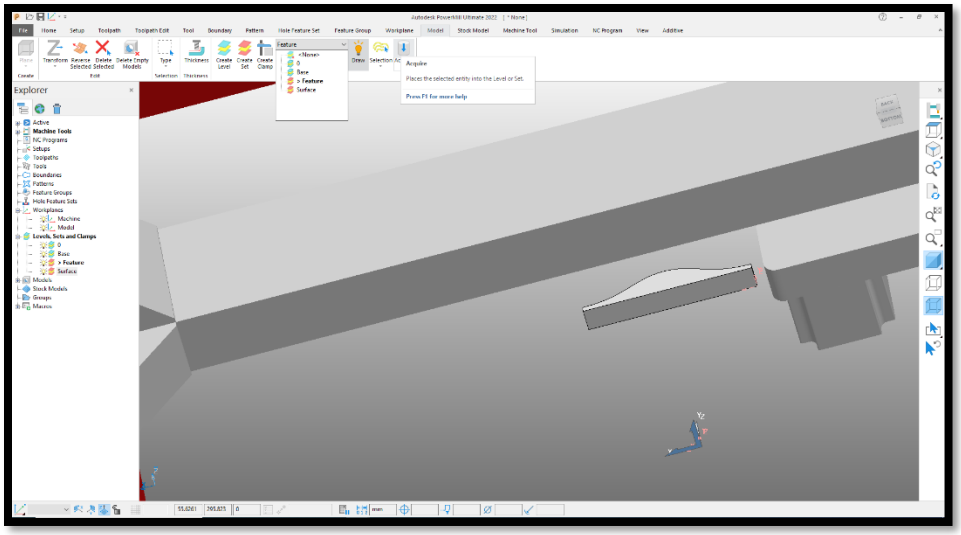

Figure 33 Adding Levels and Sets

Next, a similar process is followed to create another set which only includes the non-planar top surface of the part rather than the entire part. After pressing **Acquire**, one can name this set as "**Surface**".

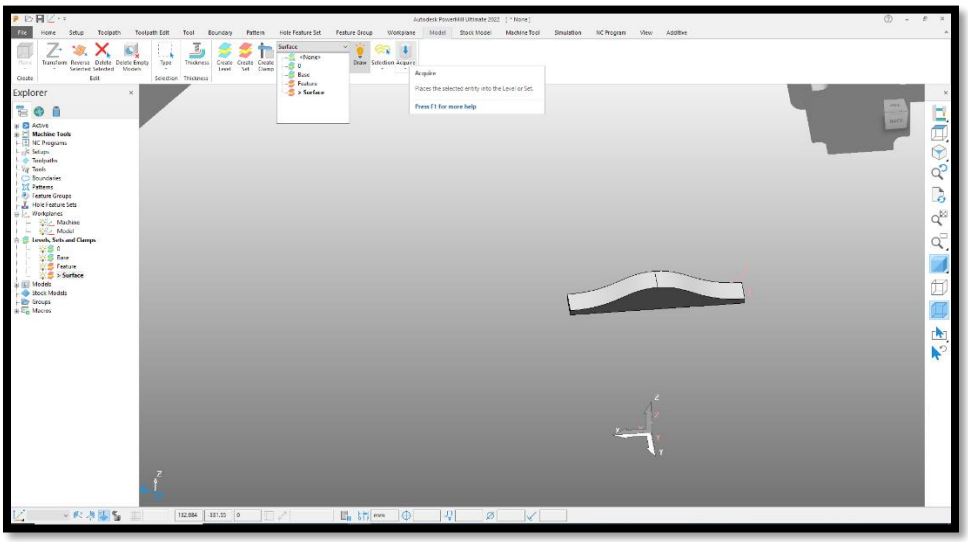

Figure 34 Renaming Level and Sets

After following the above steps, one is ready to start constructing the model toolpath.

3.3.6 Feature Construction

The first step to create a non-planar part is to print a base on which the non-planar skin will be printed. This process is started by clicking on the **Additive Tab** on the top left of the tool bar and then selecting **Feature Construction**. A new window opens in which the printing parameters are specified to create the additive toolpath.

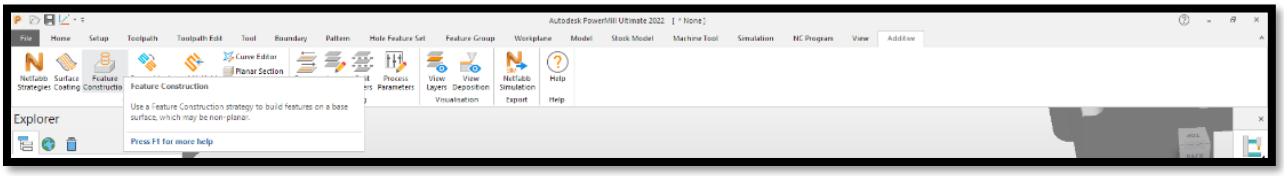

Figure 35 Feature Construction

The following sections briefly explain how to set the basic parameters in order to print a Feature.

Workplanes

This is where one selects the model Workplanes that tell the software where the model is located. Specifically, the Workplane that was named Model in the previous steps is selected from the drop down menu.

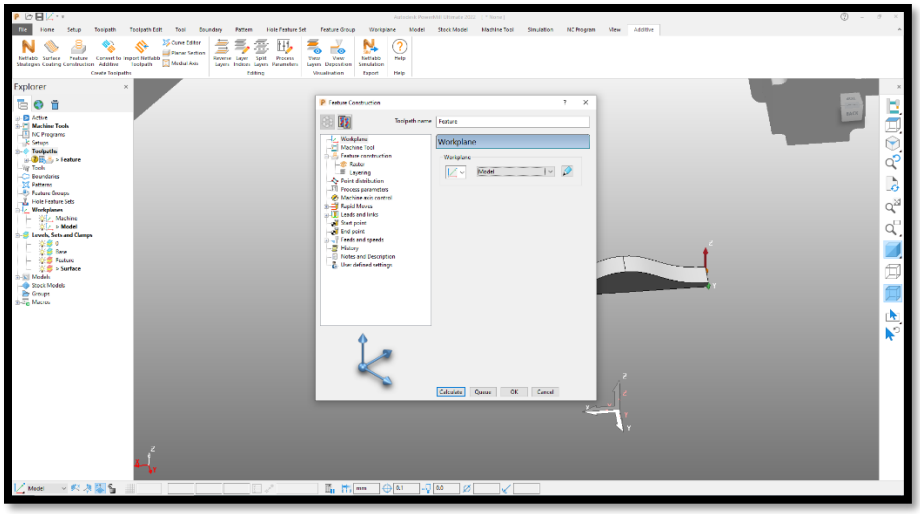

Figure 36 Model Workplanes selection in Feature Construction

Machine Tool

This is where machine tool used to generate the tool path is defined. Here, the 5Axis Maker machine that was imported in the first step is selected from the drop down menu. The next drop down menu is where the machine tool Workplane is selected. Select the "Machine" Workplanes that are located at the origin. The only box to be checked in this window is **Use Machine Tool When Possible**, This will use the rotary axis of the machine tool (B and C axis) when it is necessary.

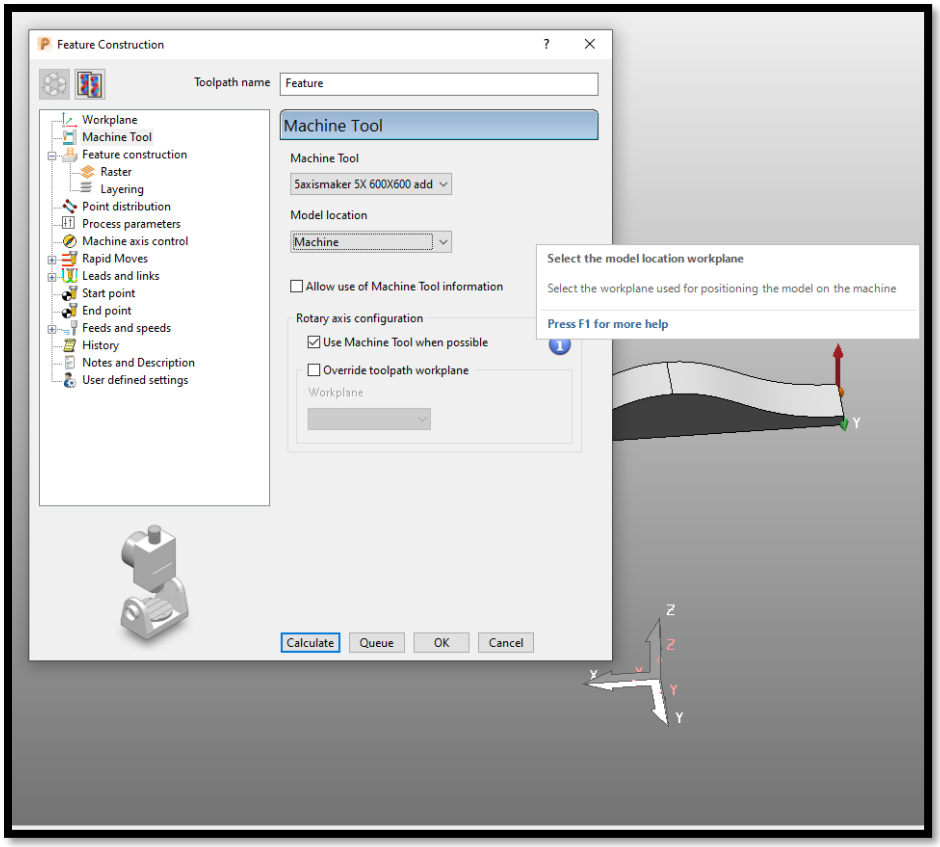

Figure 37 Machine Tool Feature Construction

Feature Construction

Several major printing parameters are set in this step. The first block in this window is named **Base**. In the Base section, the Plane level is selected. This is done by selecting **Type** as **Plane** and selecting the level that we have created. The level in our example is named "Base".

The third option is to select the style of printing. The differences in these styles are given below. The **Profile Passes** are used to create a shell (or "skin") on the selected outside surface(s) of our printed feature. In this example, the **Raster** style will be used, and **Profile Passes** will be set to **None**.

The next step is to select the Set containing the feature to be printed. From the drop down menu, select the set that had the entire feature and which was named "**Feature**".

At this point, the Base, the printing style, and the Feature have been selected. The next step is to select the tool geometry and the nozzle geometry. The first section allows one to set the

Tolerance, which determines how accurately the toolpath must follows the model contours. A selection of 0.1 is typically an acceptable part tolerance.

The **Focal Length** is the length of the tool, and is a very important input. The distance between the central C axis to the tip of the extrusion nozzle is the focal length of the tool. The focal length for the nozzle and printing head used in this research and shown in the photo is 83.3 mm. Note that this will change every time the extrusion nozzle or build platform is changed. If the input for focal length is smaller than the actual length, the nozzle will collide with the bed. If it is larger than the actual value, the nozzle will print in air, and material will not adhere to the print bed.

Bead Width is the width of the extruded bead laid down by the machine. This will depend on four major factors - Nozzle Diameter, Feed Rate, Filament Diameter and Layer Height. In this example, the bead width is set to 0.5 mm.

The **Stepover Distance** is the distance between two adjacent extrusion passes. This will have a significant influence on the density of the final part. The higher the stepover distance, the lower will be the density and vice versa. The **Allowance** is the amount by which one is willing to deviate from the ideal toolpath. This is expressed in expected percent deviation from ideal. The step over for used in this example part is 2 mm, and usually a 10% allowance is good to work with.

The Tool Axis Angles are the angles at which the tool will approach the part surface during printing. When possible, the best way to print is to set the **Lead** and **Lean** angles to zero.

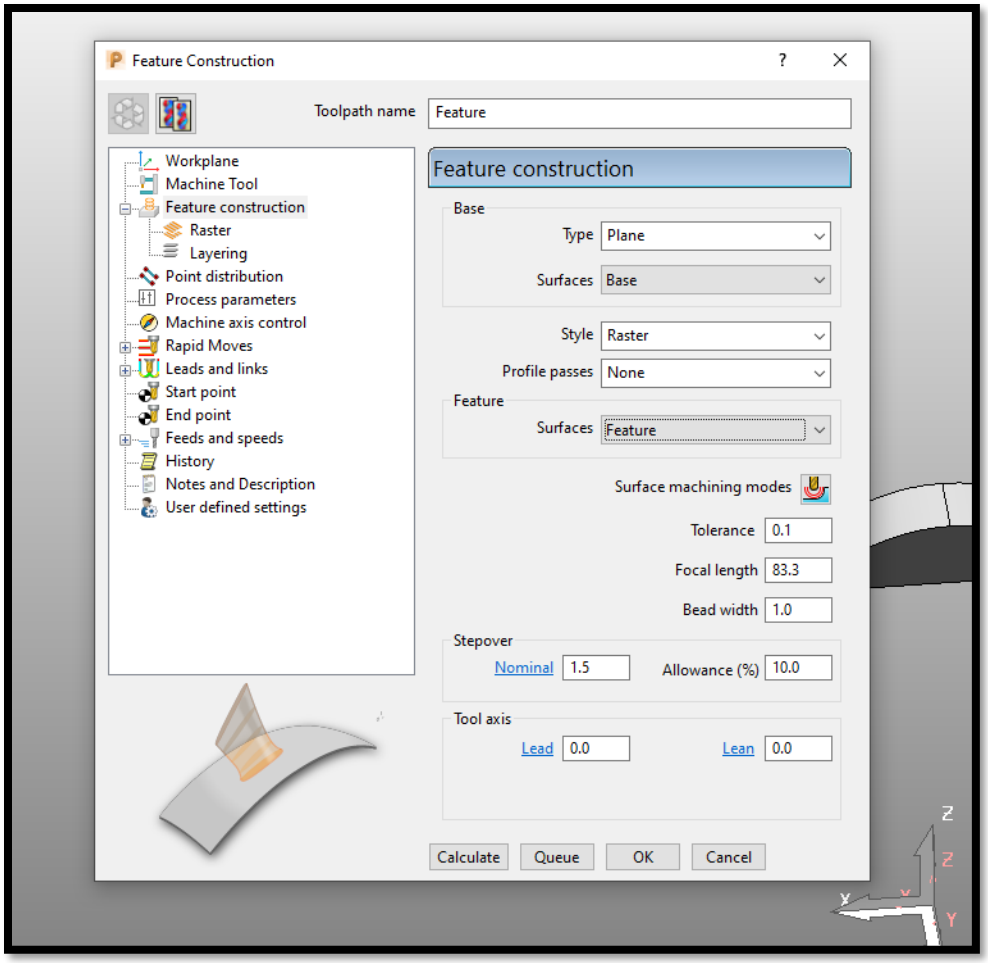

Figure 38 Feature Construction Settings

Raster

The next sub part in feature construction defines the parameters for the print style. For **Raster,** the first section is **Ordering**. This is where one specifies whether the printing will be done bi-directionally (e.g. left-right-left-right) or in just one direction (e.g. all traces printed only from left-to-right OR from right-to-left). To decrease the print time, **Two Way** printing is chosen from the drop down menu in this research. The **Start** corner that is selected will determine the starting point of printing and where the raster passes will begin.

The **Angle** selection will decide the angle of the raster passes relative to the X axis. One can specify a crossed mesh-like structure by entering different raster angles in this section.

The **Bottom** block is what defines the layering type and angle. The **Type** defines the arrangement of consecutive layers, and the angle determines the angle between the raster passes of each layer.

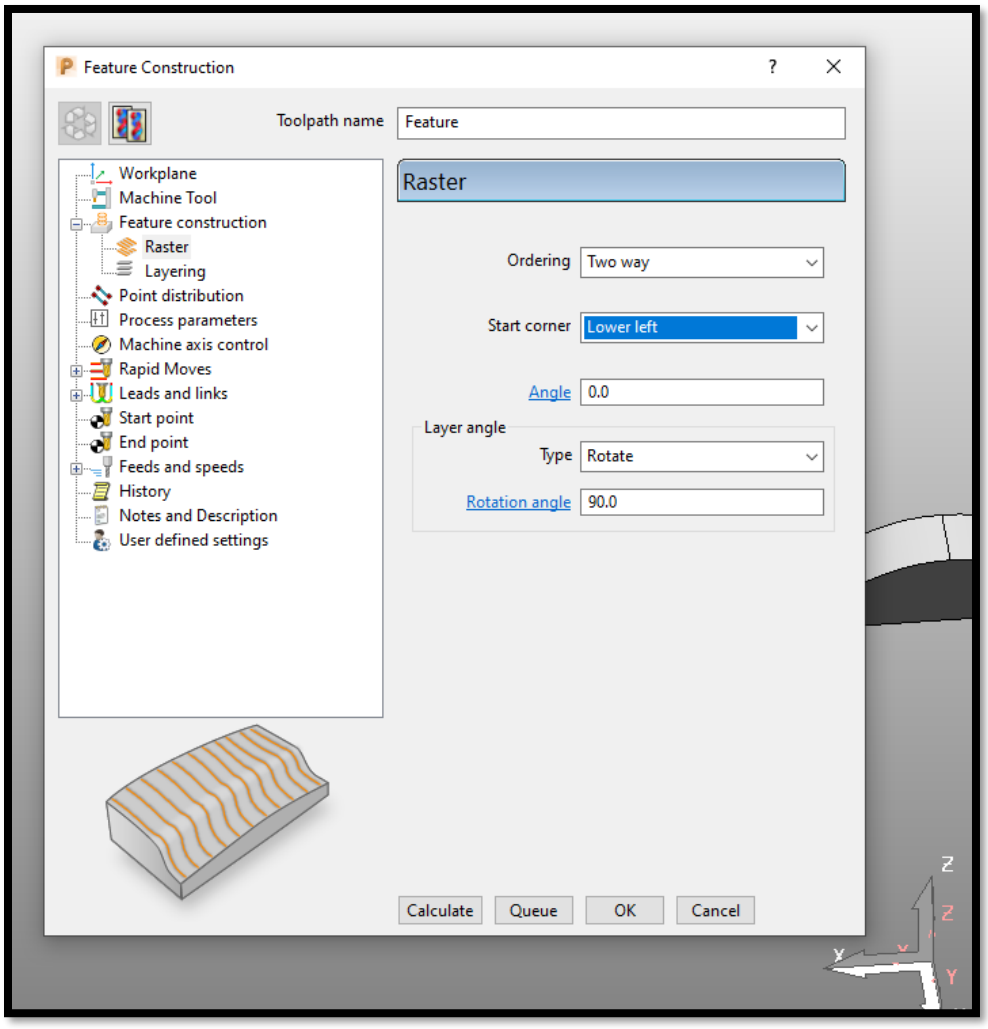

Figure 39 Raster Settings

Layering

The first section in **Layering** is **Offset from Base**. As the name suggests, this input field specifies the distance of the first layer from the build platform. For this example, this value is kept at zero. The extent of the part is defined in the next section. As the entire part is being printed in this step, one selects **Feature Extent**.

Layer Thickness is the height of each printed layer. The proper layer thickness is influenced by the nozzle diameter. The value being used in this research is 0.55 mm for a 0.4 mm diameter extrusion nozzle opening. Although the layer thickness need not be constant for all layers, a constant value is used in this research.

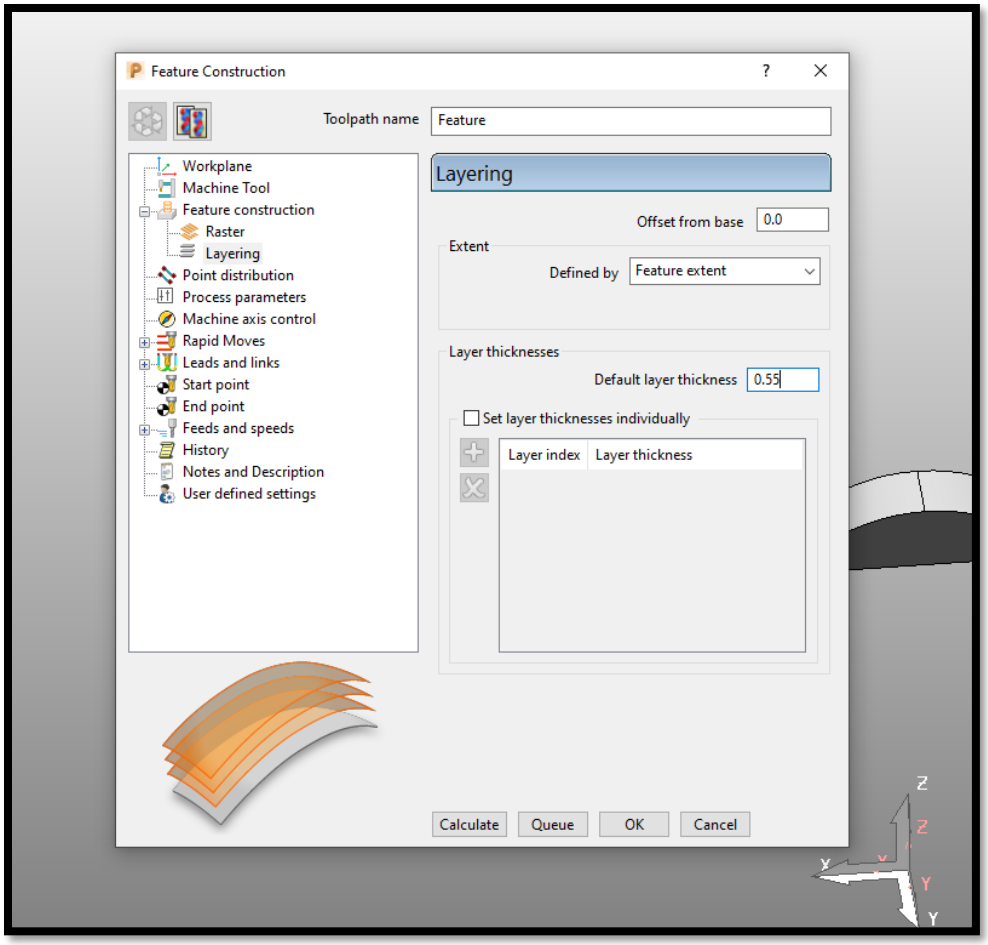

Figure 40 Layering Settings

Point Distribution

For the Point Distribution section, all default values are used in this research. **Output** type gives the option to control the point distribution of cutting tools. For additive manufacturing, it should always be set to **Tolerance and Keep Arcs** with a **Tolerance Factor** of 0.5. The point separation distance is not needed, so this box is unchecked. With **Rotary Axis Configuration**, the coordinate system (Machine Work plane) described in Machine tool is used to measure the azimuth and elevation of our rotating axes. The **Mesh Factor** gives the model preparation tolerance and is always kept at 0.5. It is not necessary to define the **Limit Maximum Triangle Length**.

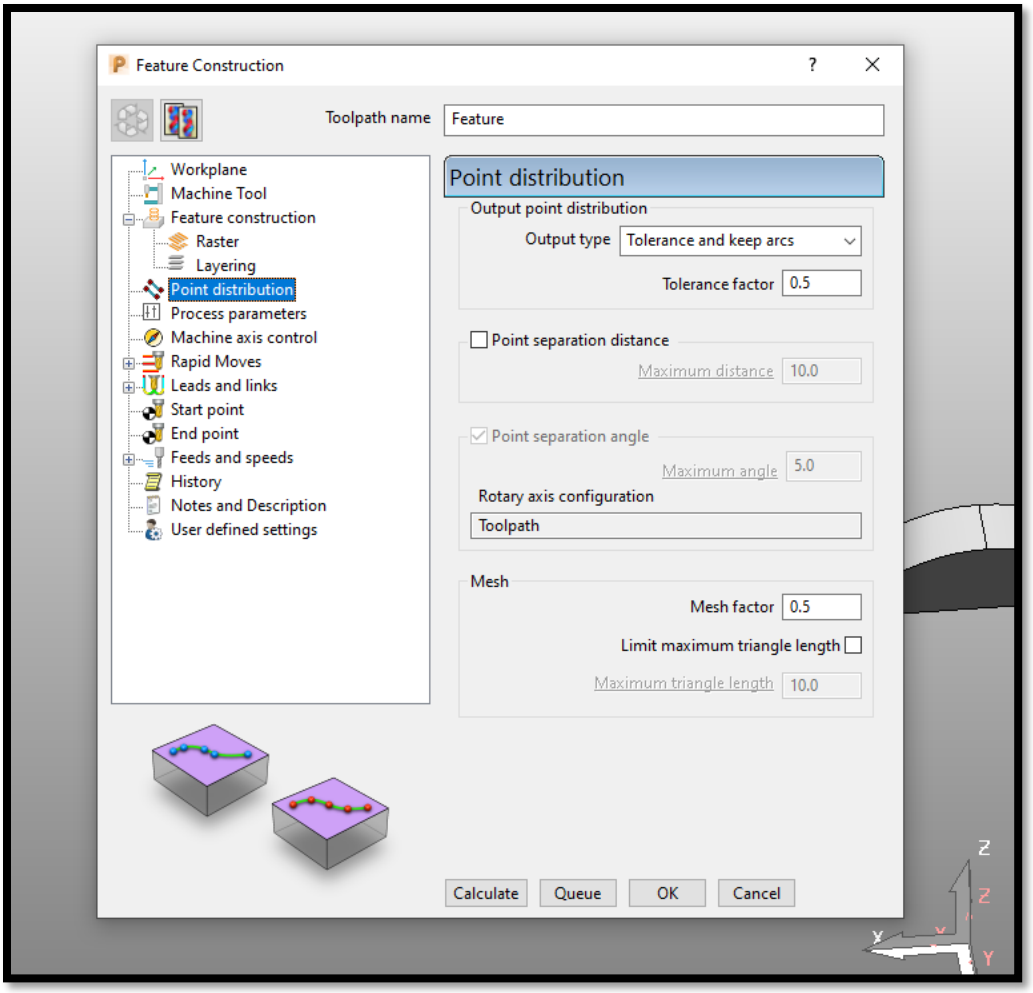

Figure 41 Point Distribution

Process Parameters

All of the process parameters have already been defined, hence it is not necessary to enter anything in this section.

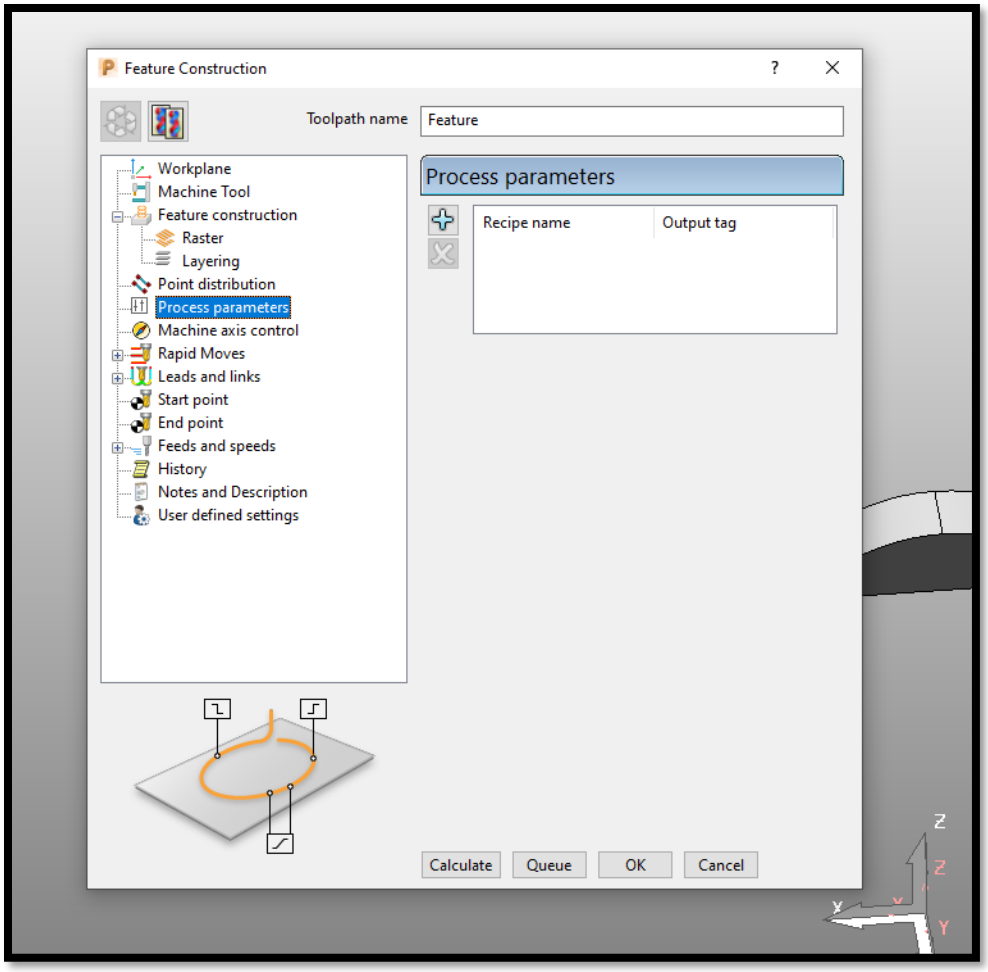

Figure 42 Process Parameters

Machine Axis Control

Selecting the **Use orientation vectors calculated during simulation** option allows Powermill to overwrite orientation vectors with those calculated during simulation. This happens only when the proposed orientation vectors cannot be achieved. The **Proposed orientation** should be set to **Free**, and it defines the type of machine axis control.

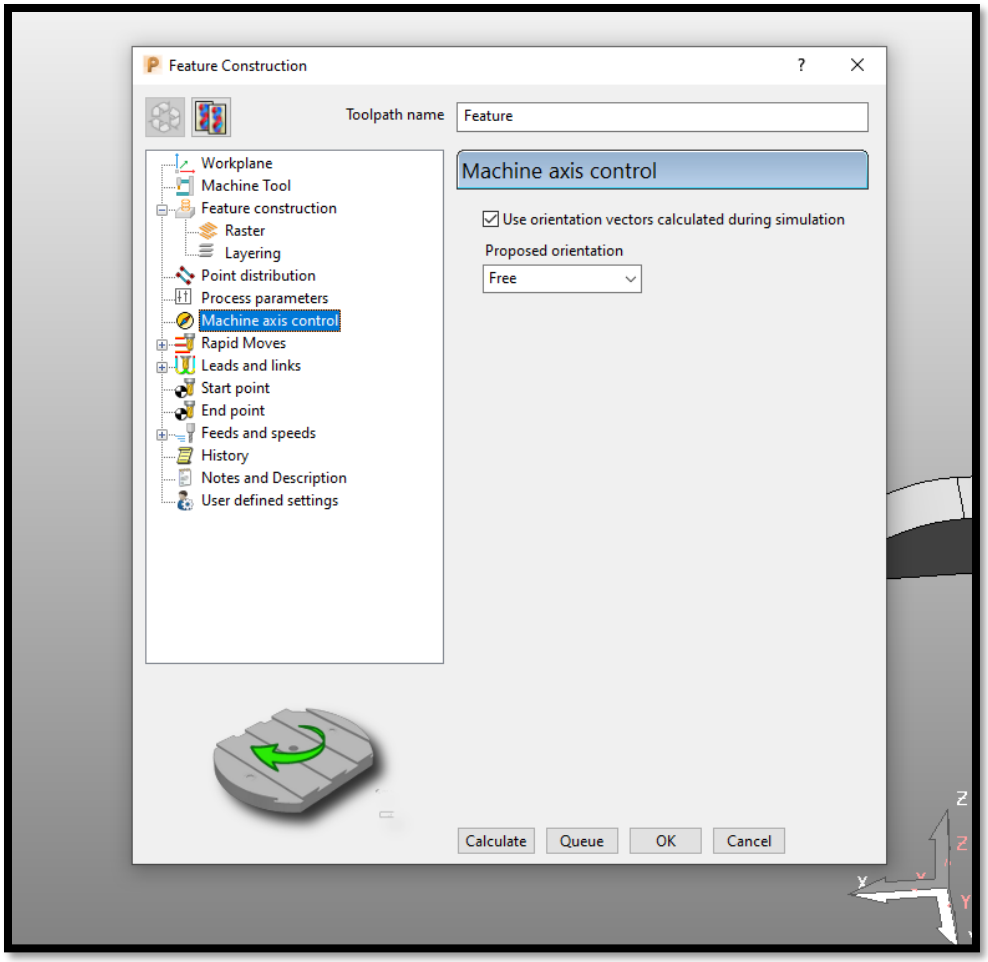

Figure 43 Machine Control Axis

Rapid Moves

This is where the **Safe Area**, **Rapid Height** and **Plunge Height** values are set. All the default settings are arranged according to the model and need not be changed.

Moves and Clearances values pertain to the lengths of retracts and approaches. All default values in this window can be accepted, as they consider the most conservative distances.

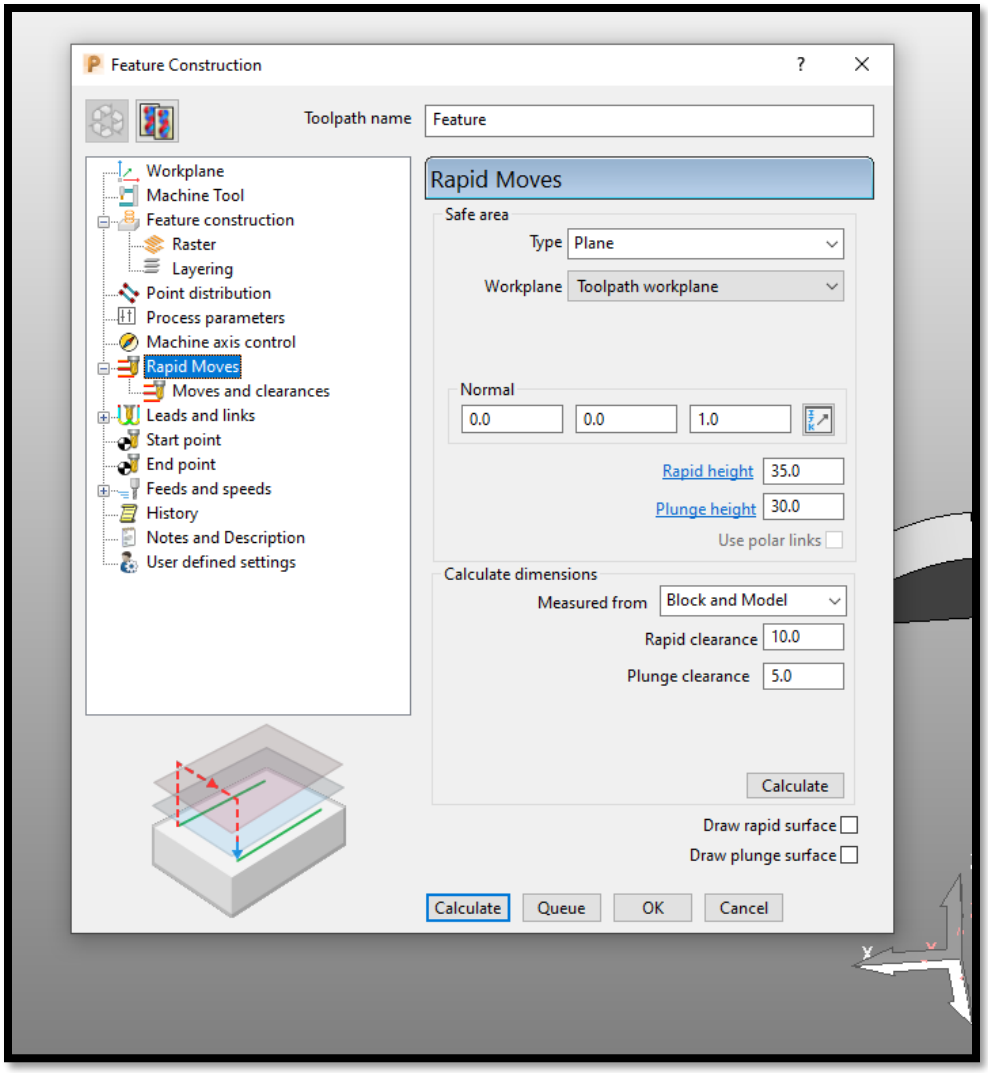

Figure 44 Rapid Moves

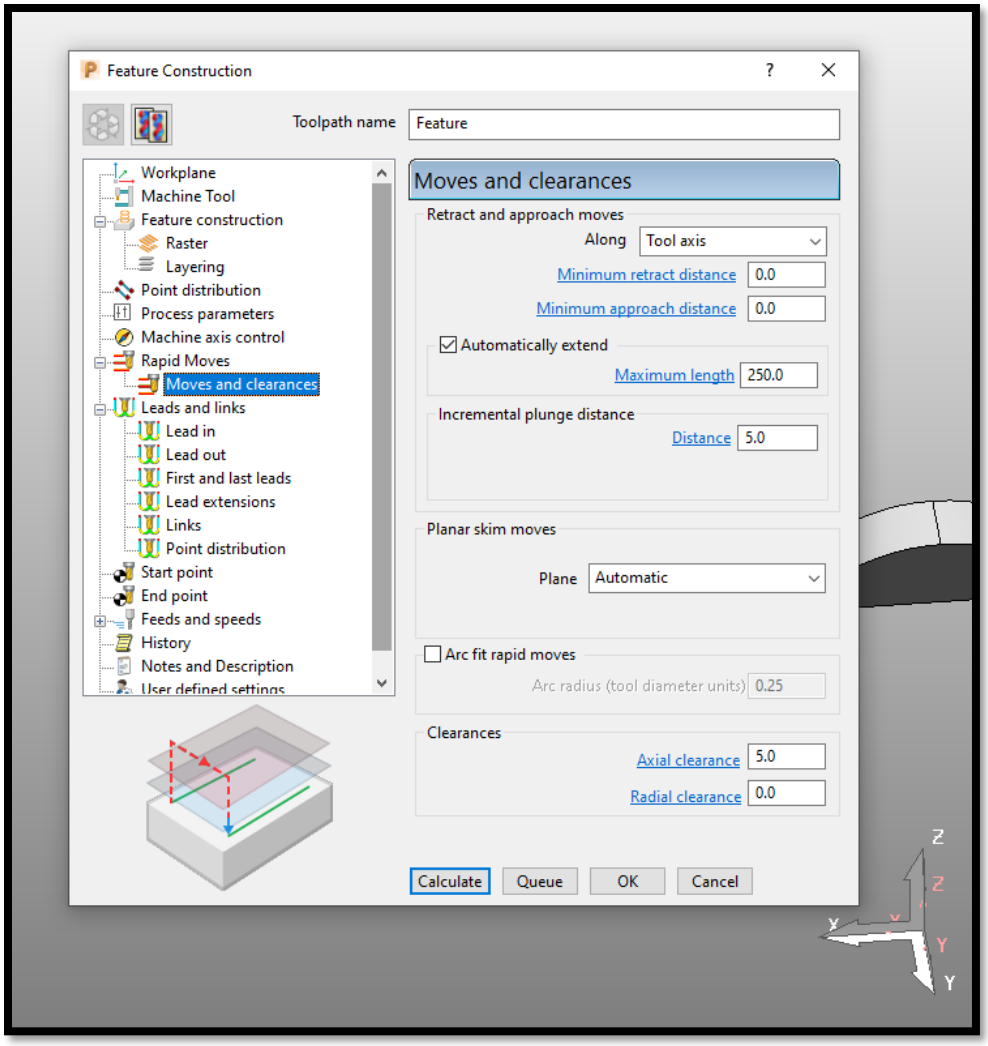

Figure 45 Moves and Clearances

Leads and Links

The only section that need non-default inputs is **Links**. Links are the motions of the tool head while doing non-printing moves from the end of one printed path to the start of the next printed path. To optimize the time of printing, the 1st and 2nd choice of link path is **Straight With No Constraints Applied**. When the 1st and 2nd choice of link fail, the machine will use the Default type. Again, to make printing less time consuming, the **Skim** value is chosen. There is no need for **Gough Check,** hence it is turned off.

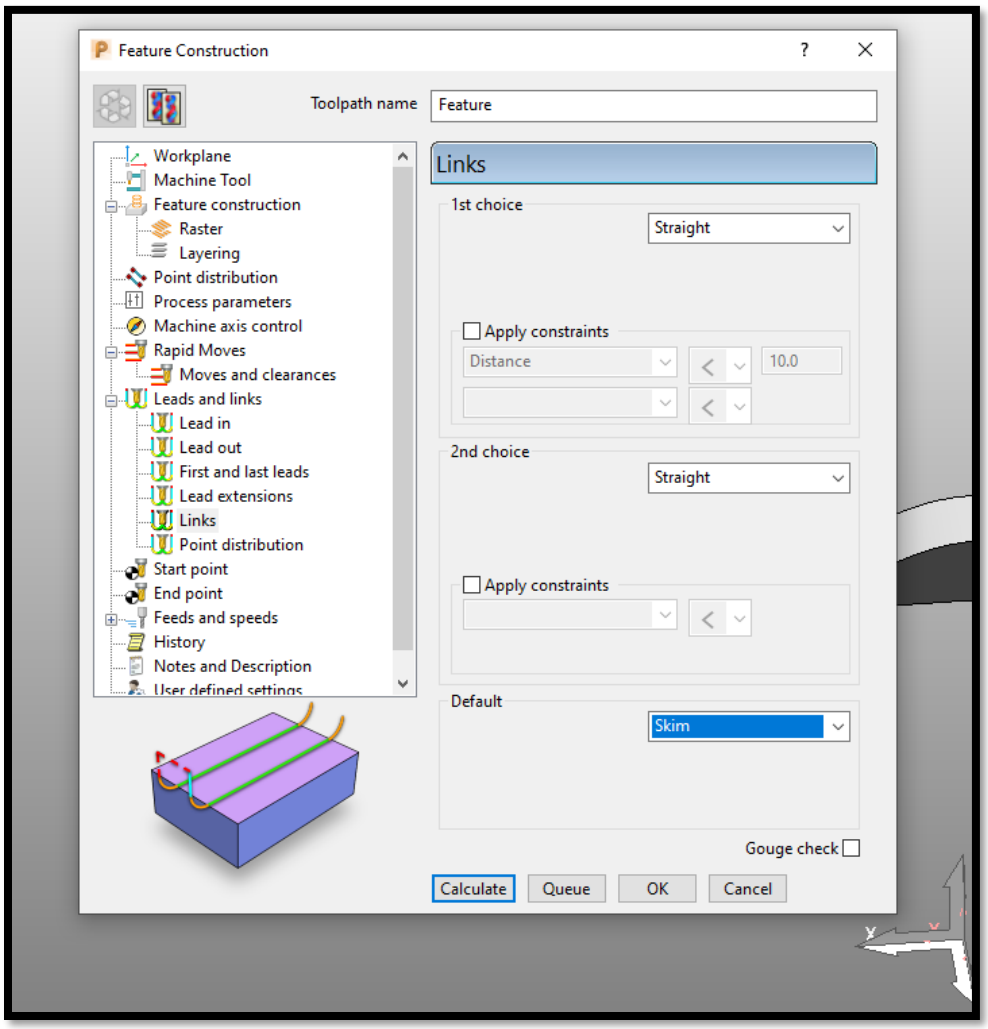

Figure 46 Links Settings

Start Point

In this research, the start point for printing is set to **Block Centre Safe** with the **Incremental Plunge** option selected.

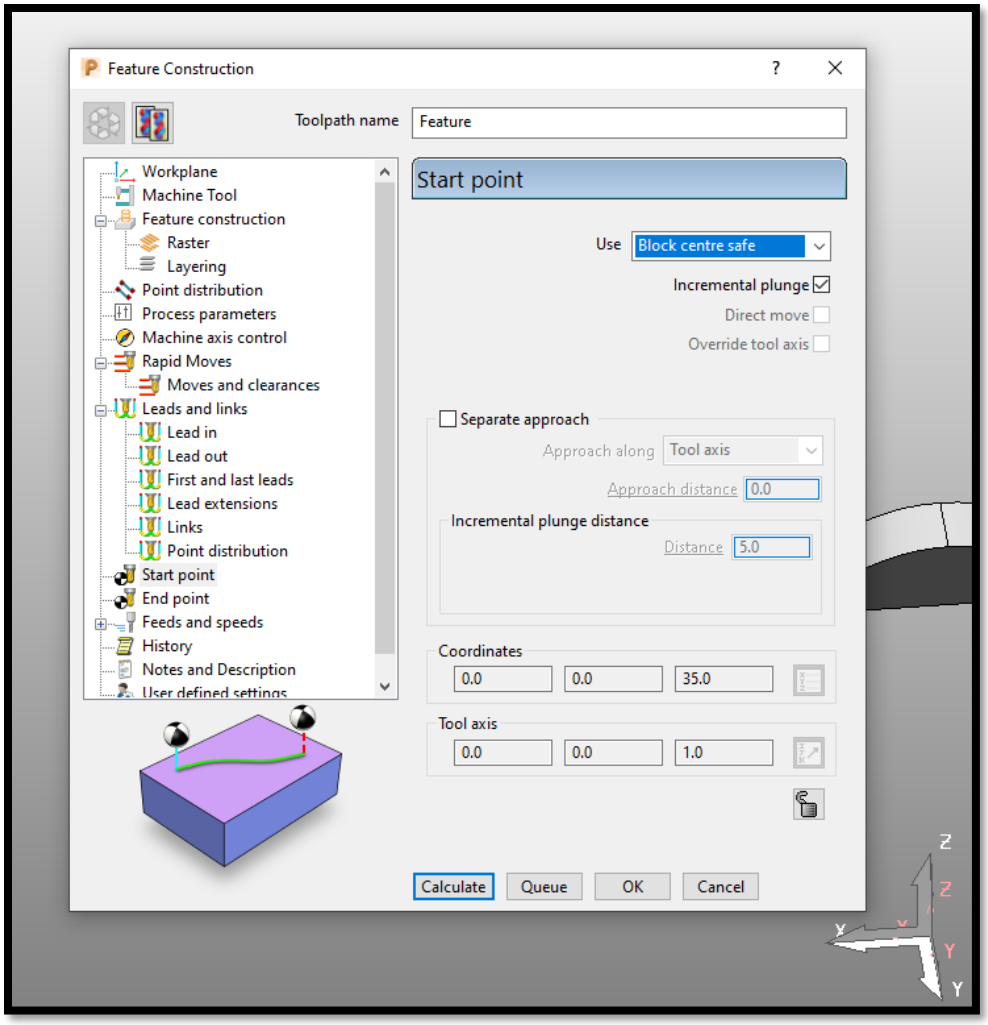

Figure 47 Start Point

End Point

A value of **Last Point Safe** is selected as the end point of the tool path.

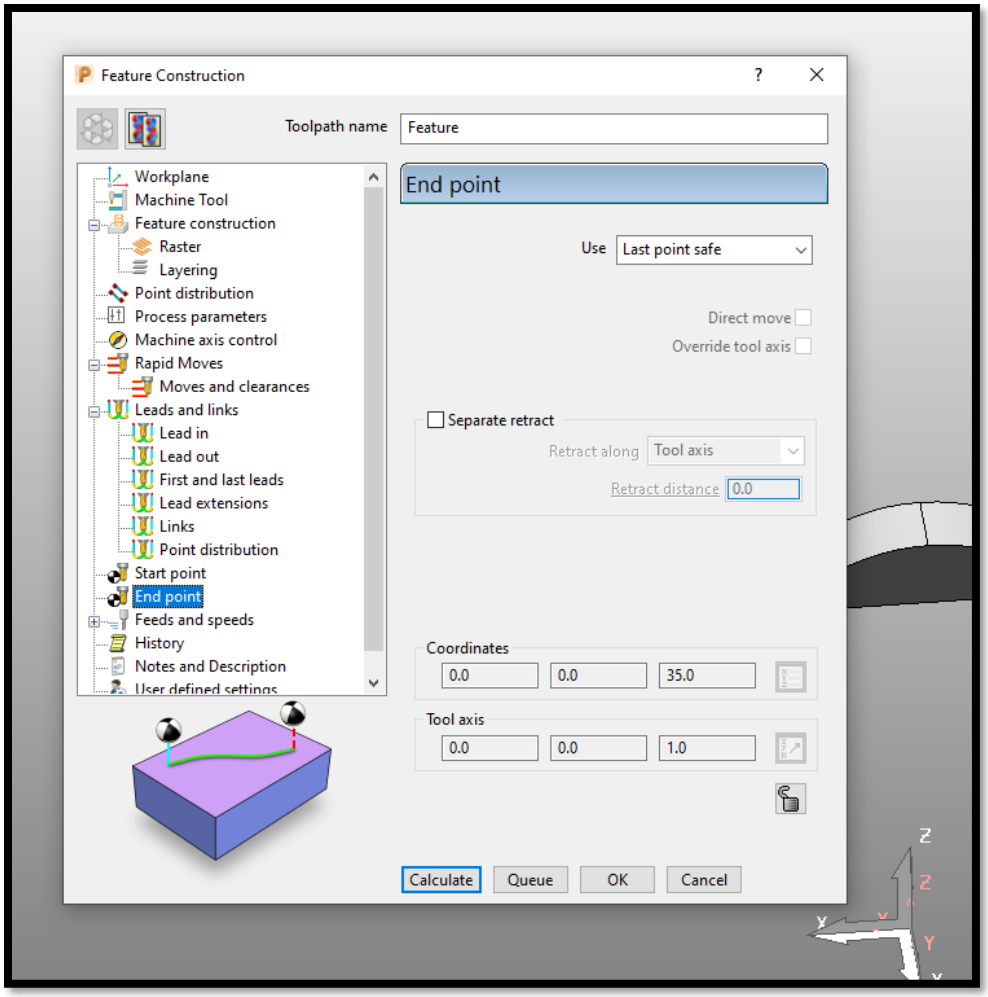

Figure 48 End Point

Feeds and Speed

The only speed that needs to be set in this section is the **Cutting Feed Rate**. As this is a printing operation (rather than cutting), the value here determines the speed at which the extrusion head moves while depositing material. For this research, a value of 1000 mm/min was used.

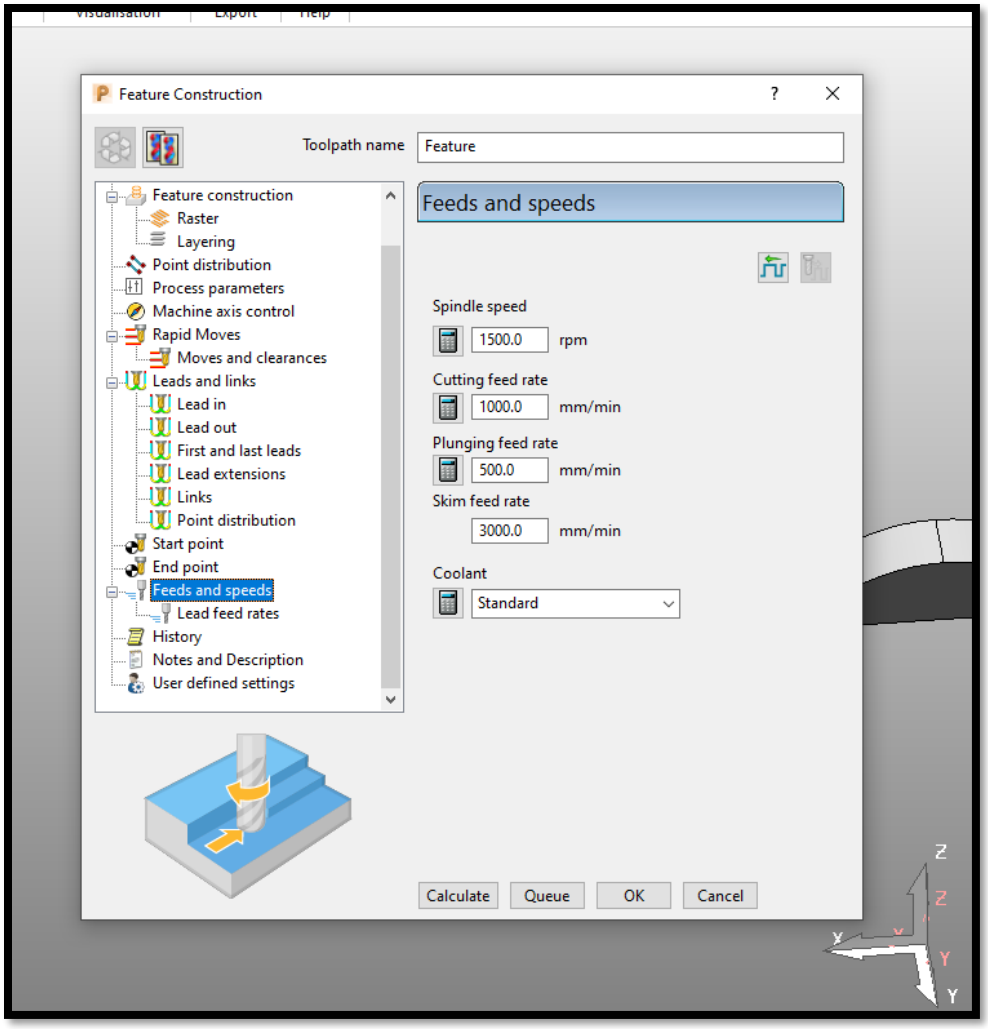

Figure 49 Feed Rates

Calculate

Now that all of the inputs are in place, it is time to click the **Calculate** button to generate the toolpaths that will produce the base feature geometry of the part in a layer wise fashion. The non-planar surface printing is done in the next step. Once the toolpath is calculated, it appears on the model.

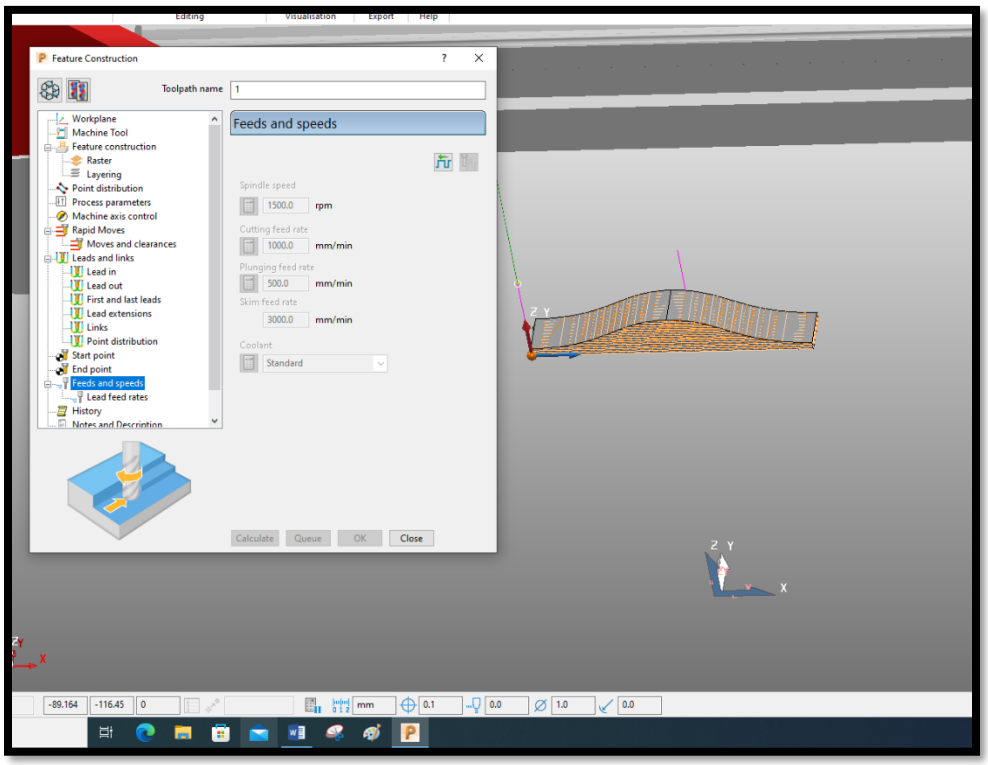

Figure 50 Calculating Feature Construction

3.3.7 Surface Coating

The main purpose for using a 5-axis machine is to print non-planar surfaces (or skins). The **Surface Coating** feature is used to design toolpaths for nonplanar layers. This option is found in the **Additive** tab.

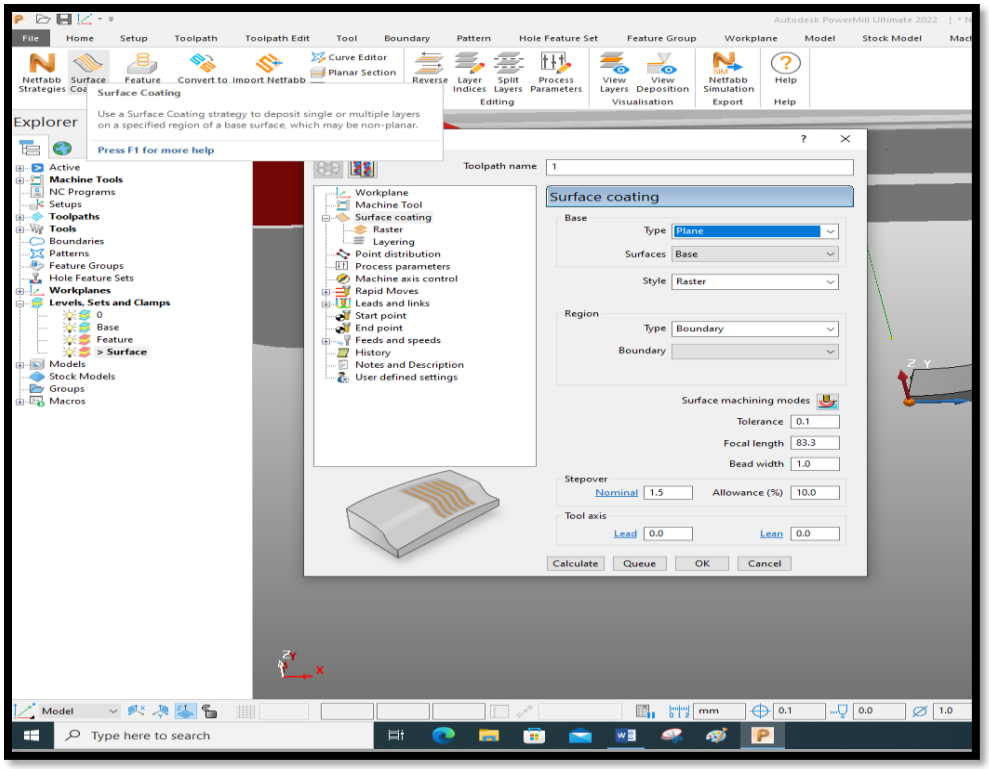

Figure 51 Non-Planar Surface Coating Feature

Duplicate Settings

Much of the surface coating toolpath generation mirros that of the feature construction that was just completed. Settings that are identical for both types of toolpath generation include:

- Workplanes
- Machine Tool
- Point Distribution
- Process Parameters
- Machine Axis Control
- Rapid Moves
- Start Point
- End Point

- Feeds and speeds
- History
- Notes and description
- User defined settings

Surface Coating

This is the first setting that will have changes. Under the **Base** options, setting the **Type** to **Arbitrary Surface** and **Surfaces** value to **Surfaces** will allow the user to print just surfaces on top of the previously printed solid. The Set that contains this non-planar surface is selected in the **Surface** section. In our case our set is named as "**Surface**".

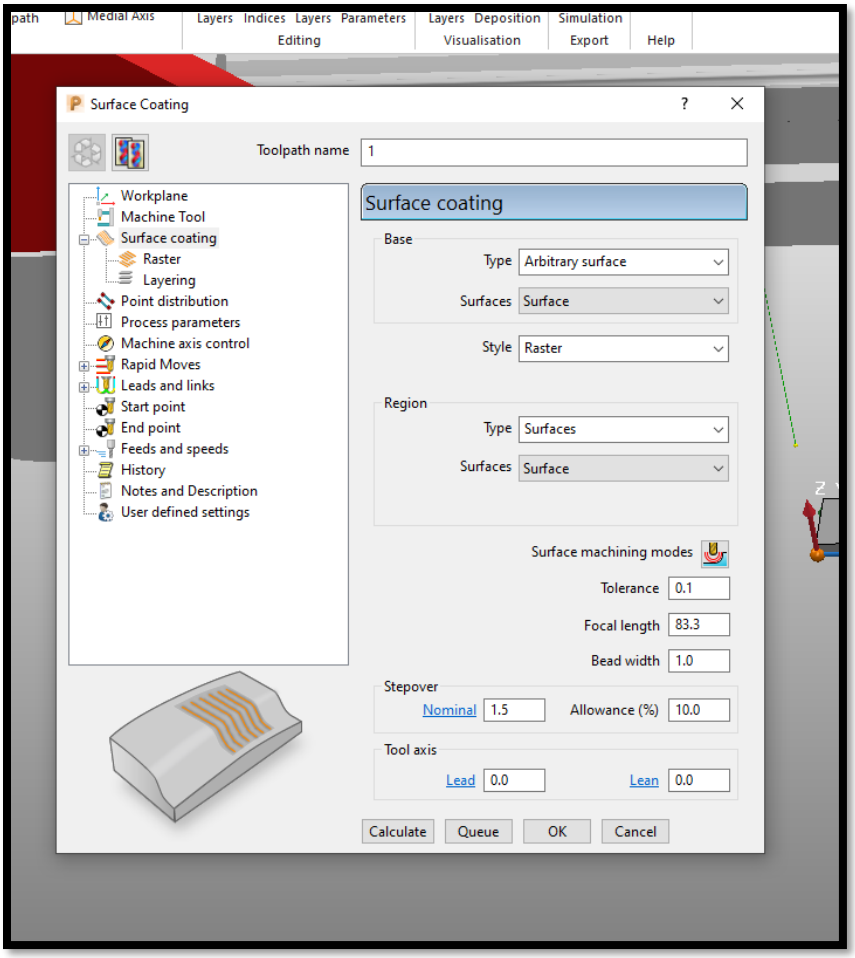

Figure 52 Surface Coating Region Selection

In this research, the **Style** of printing is set to **Raster,** which is the same as the style of printing used for the feature construction. The Region is where one selects the surface which is to be coated. The **Type** here is **Surface,** and the set to be selected is again the set which contains the non-planar surface. All other settings on this page are the same as those used in the feature construction section. They can, of course, be changed in order to print different types of parts.

Raster

This is again similar to the rastering used in feature construction, although to use the full potential of the 5-axis printing capabilities, one can use different raster and rotational angles.

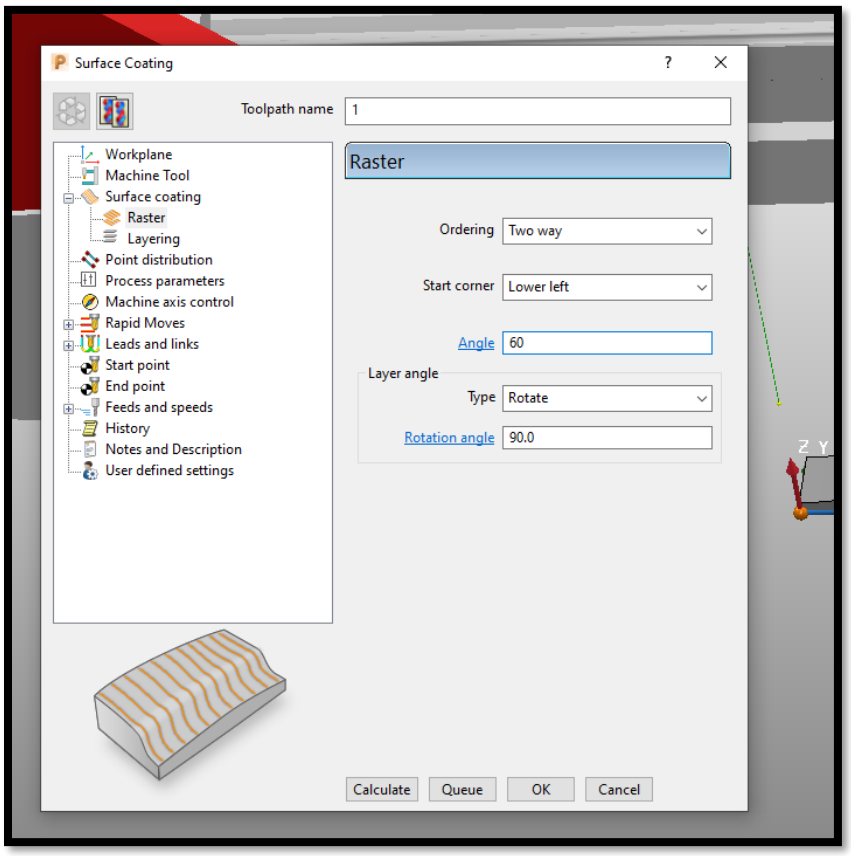

Figure 53 Surface Coating Raster

Layering

As this is a surface coating feature, one can choose to add multiple layers on top of the 3D printed base feature. To do that, one just selects **Number of Layers** and types how many layers are to be coated in the box below. The **Layer Thickness** can be the same as the layer thickness from the feature construction.

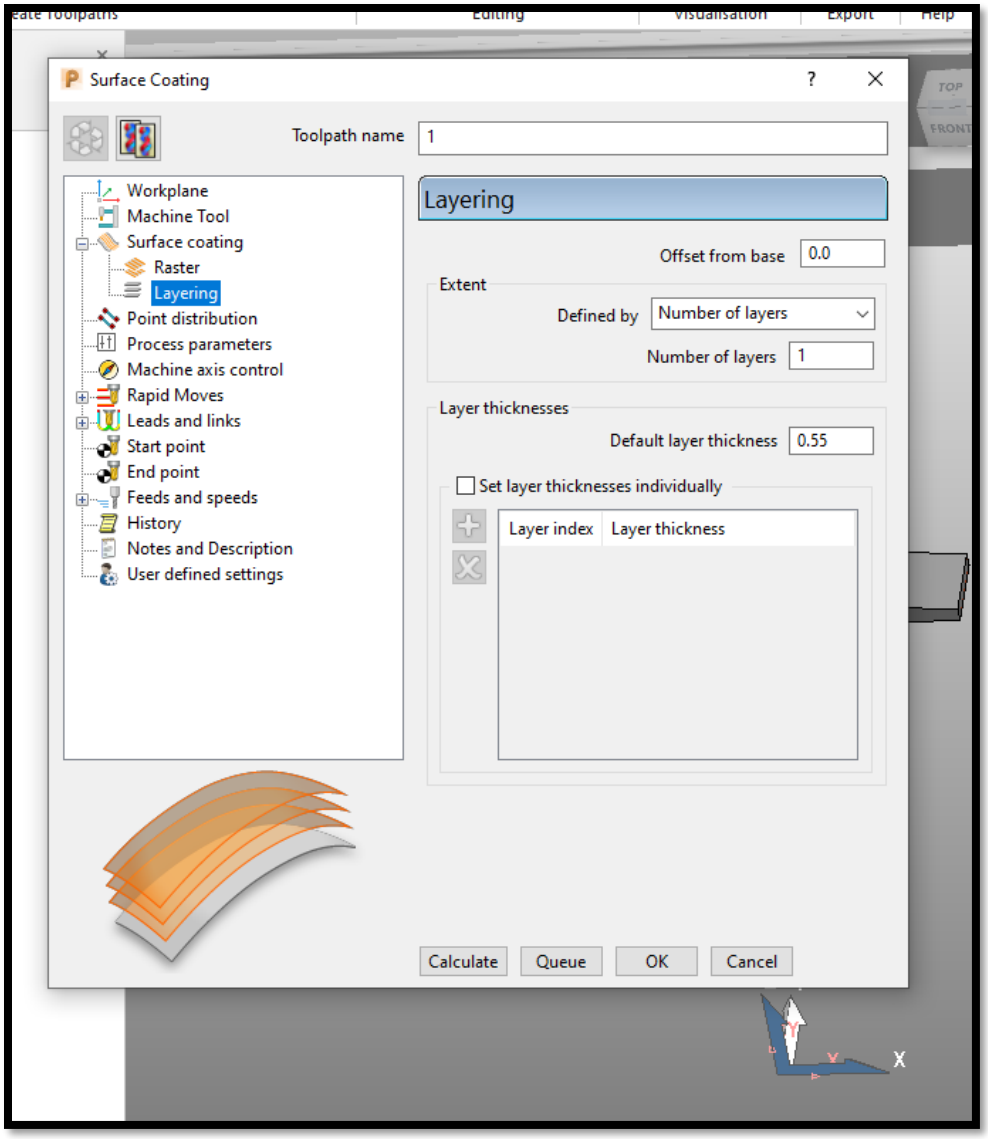

Figure 54 Surface Coating Layering

Leads and Links

The last input needed before non-planar toolpaths are generated is the Links. As the top layers are non-planar, the machine cannot move between layers in a straight motion. Therefore, the 1st and 2nd choice of **Links** for non-planar surfaces should be **On Surface,** and the default type should be **Skim**. The **Gouge Check** does not need to be selected.

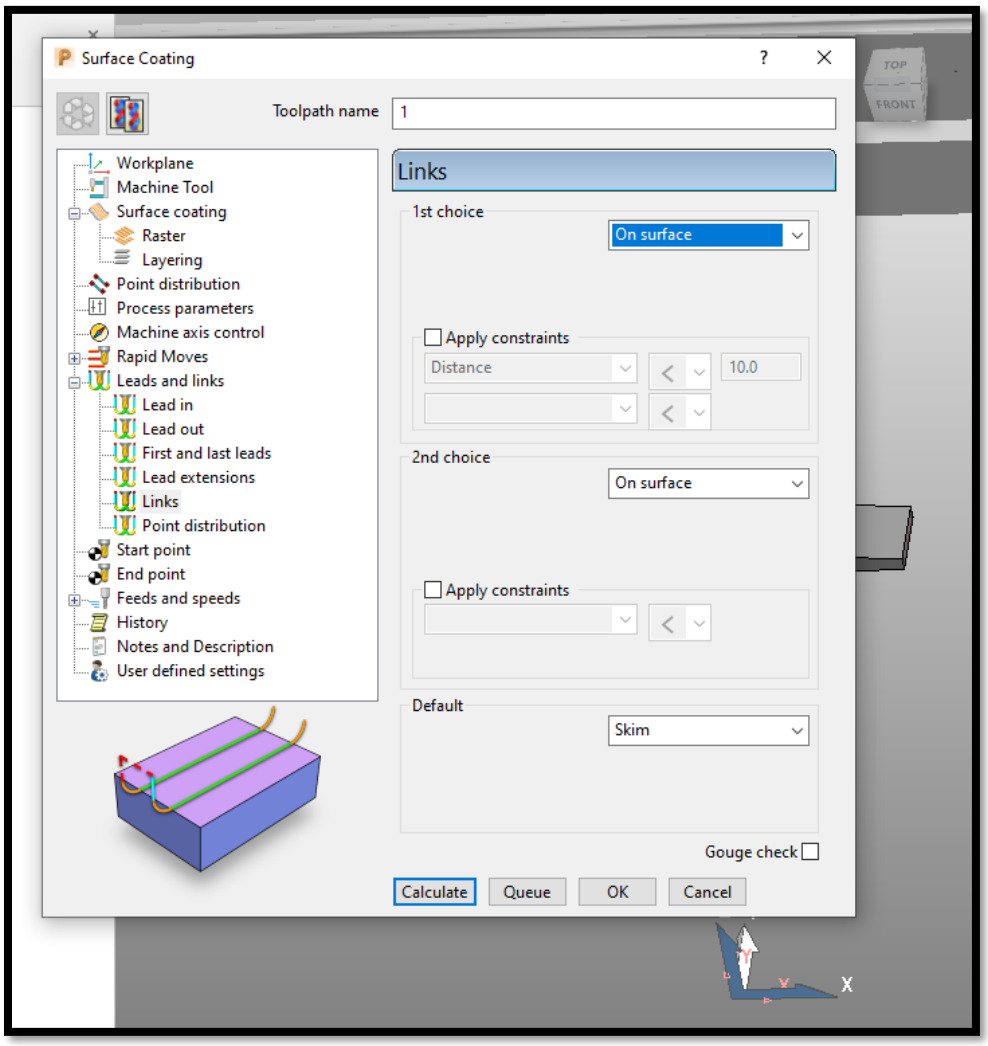

Figure 55 Surface Coating Leads and Links

Calculate

With all of the surface coating inputs specified, it is possible to calculate the toolpath of the nonplanar printing by pressing the **Calculate** button and then pressing **OK**.

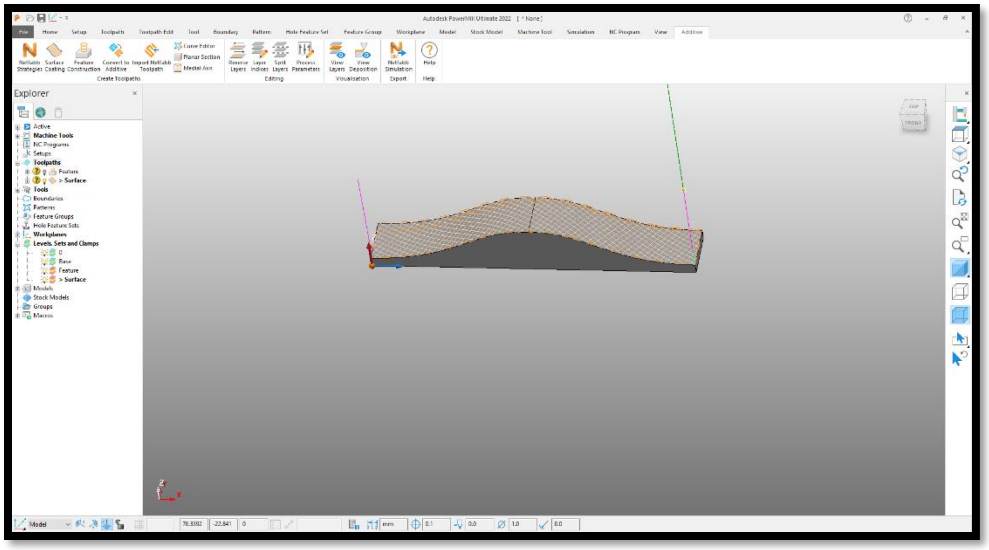

Figure 56 Surface Coated Toolpath Projected on the Part

3.3.8 Toolpaths

Under **Toolpaths** in the Explorer window, there will now be two toolpaths. They can be named "Feature Construction" and "Surface Coating" respectively. Now the next step is to generate an NC program that the machine can read and execute.

3.3.9 NC Program Generation

Right clicking on the **NC Programs** tab in the explorer window and then selecting **Create NC Program** will generate the G-code that is executed by the 5Axis Maker to print the base feature and conformal skin.

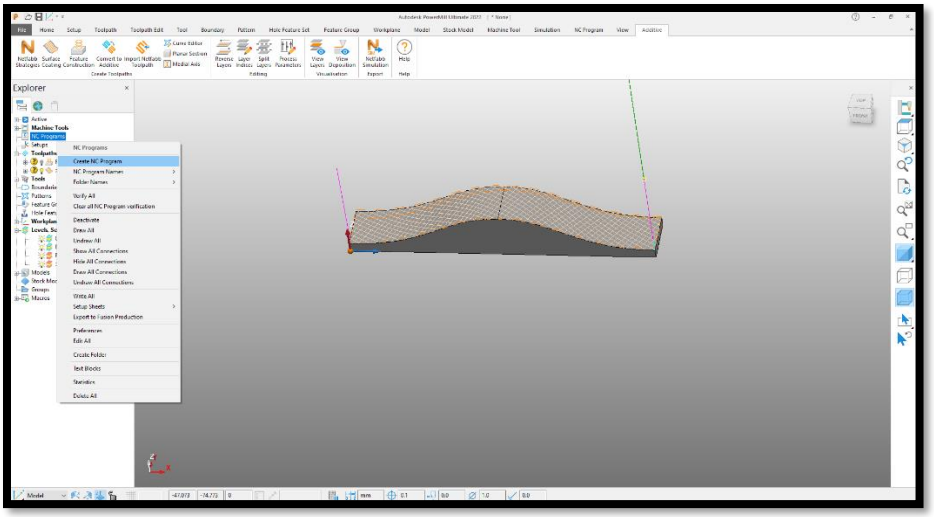

Figure 57 Creating NC Program

A new window will open. The first thing is to name the NC Program. Next, the location where the NC program should be saved is entered.

- In the machine tool section, the **5axismaker 5X 600X600 additive machine model** is selected. The **Model Location** is the plane where our machine is located (i.e Machine Workplanes).

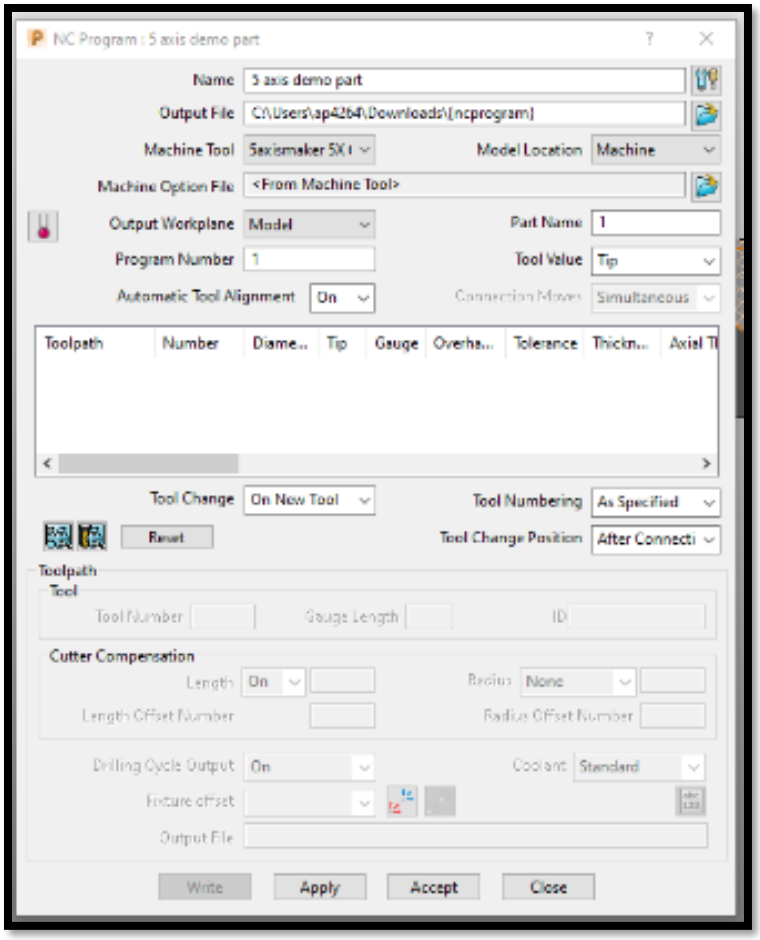

Figure 58 NC Program Setting

- **Machine Option** file - This is where the machine post processor is selected. The latest post processor created by Autodesk for the machine used in this research is **5axismaker Additive 20Aug 21**. One can browse to locate it from the computer, and then click **Accept**.

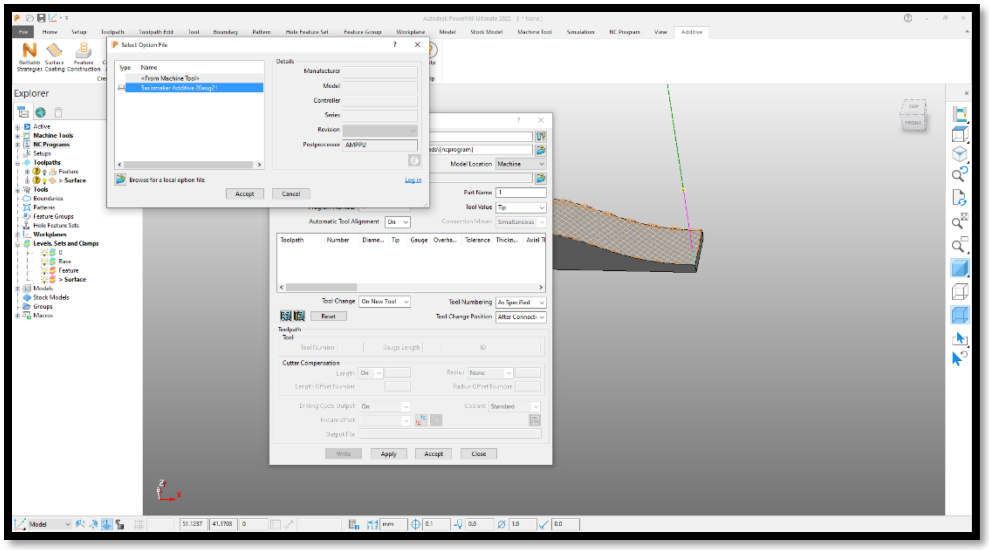

Figure 59 Importing 5-Axis Post Processor

- All other entries will be auto filled and do not need to be changed.
- The final step is to click **Apply** and then **Accept**.

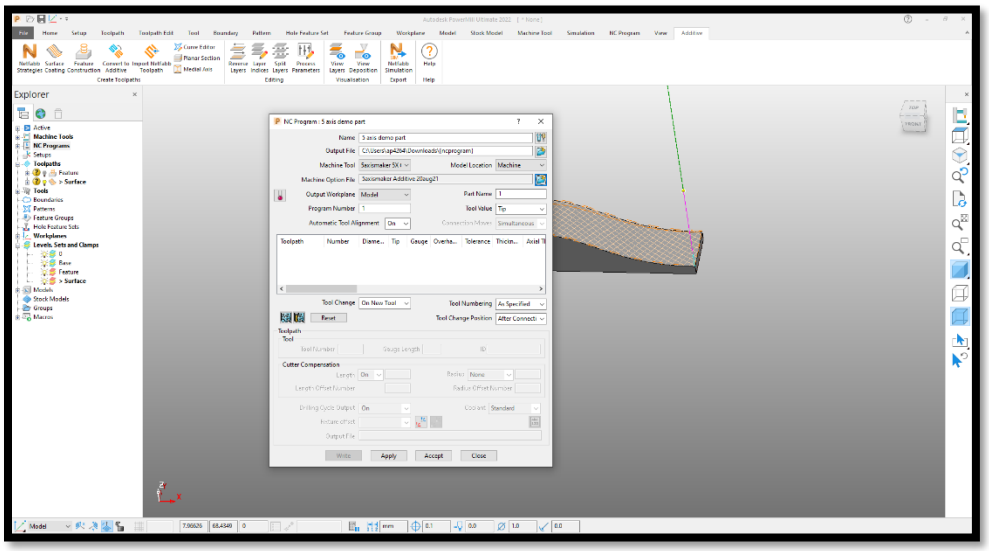

Figure 60 Final NC Program Setting

- Under the NC program section, an empty NC program is now created. The toolpath must be added to this NC program.

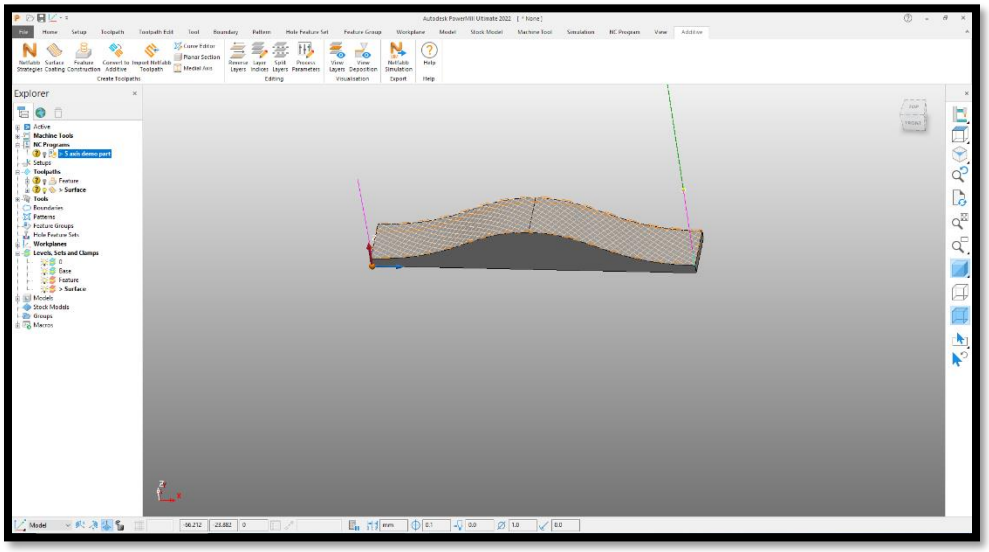

Figure 61 Importing Tool Paths to NC Program

- To add the toolpaths, one simply drags and drops both toolpaths that were created (Feature and Surface Coating) on the NC Program that was just created.

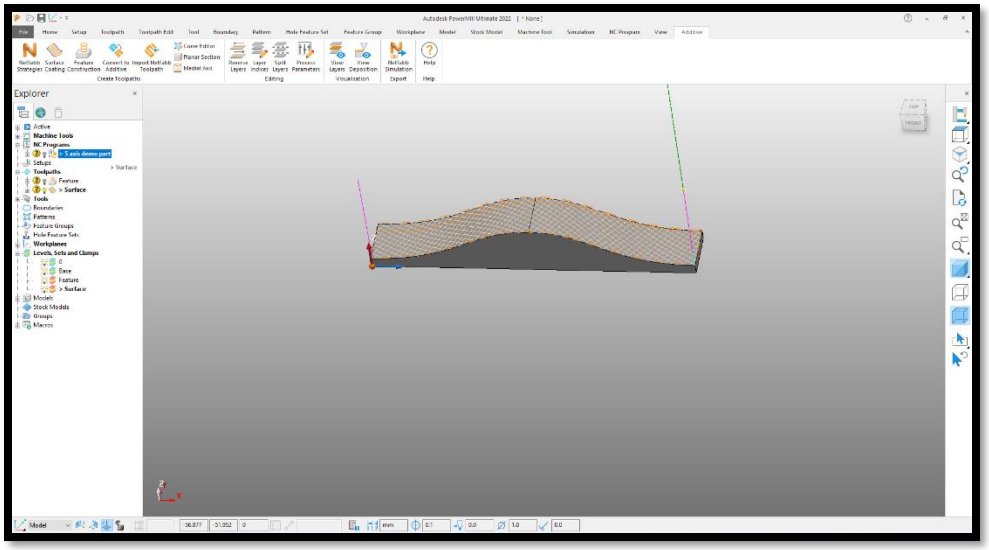

Figure 62 Tool Paths Imported

- The NC Program with the two toolpaths is now defined.
- To write the NC Program to the hard drive, right click on the program and then click on **Write**.

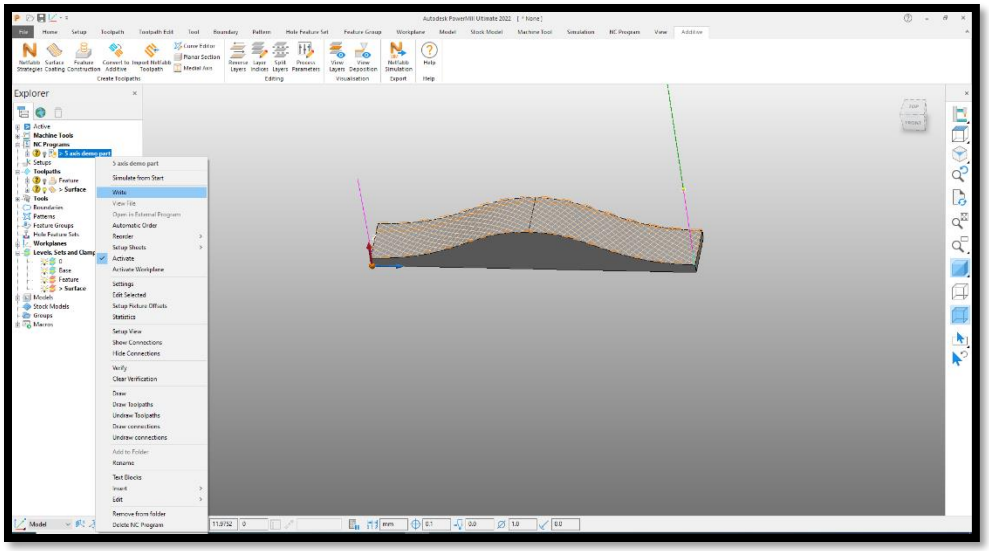

Figure 63 Writing NC Program

- The NC Program is written and is stored in the specified location as a .Tap file.

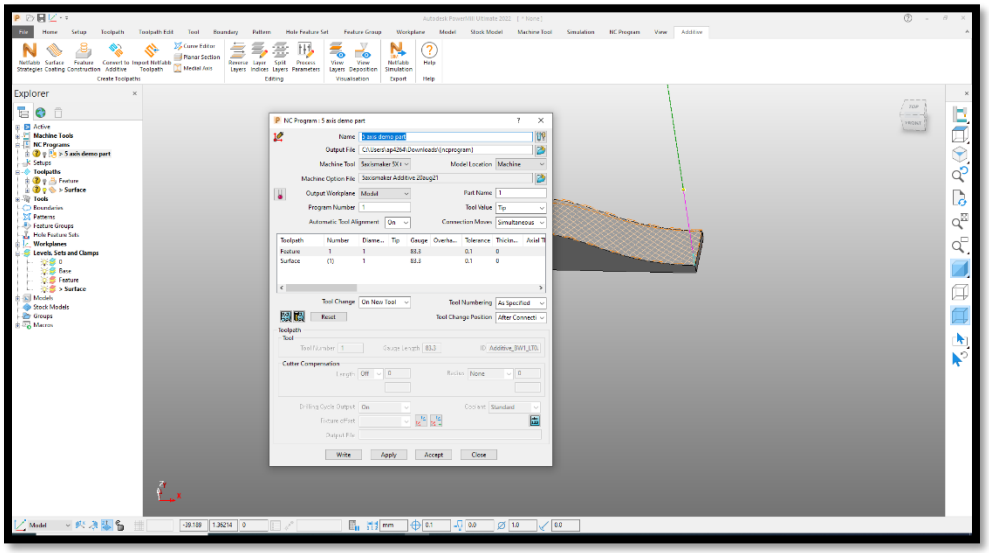

Figure 64 Final NC Program Window

This NC program is now ready to be imported to the 5Axis Maker's Mach-4 machine controller so that printing can commence.

3.4 Mach 4 and Machine Calibration

Now that the NC program has been created, it is necessary to prepare the machine to print the parts. The obvious first step is to start the machine. There are two switches on the controller. Pressing both switches and releasing the emergency stop button will start the machine. The top button on the controller starts all of the motors, and the bottom button turns on the heater. The temperature for the heater can be set on the right hand side panel.

Next, it is necessary to calibrate the machine and define the origin points for the X, Y, Z, B and C axes. Mach 4 is CNC motion control software used to control the 5Axis Maker machine. The Powermill post-processer written for the 5Axis Maker machine outputs G-code that can be read and executed by Mach 4. This software is also used to jog the motors and calibrate them by fixing datum positions.

In order to calibrate the machine and run the G-code, the Mach 4 software is launched from the PC attached to the controller. The 5 Axis Mach4 Profile is selected, and the OK button is pressed.

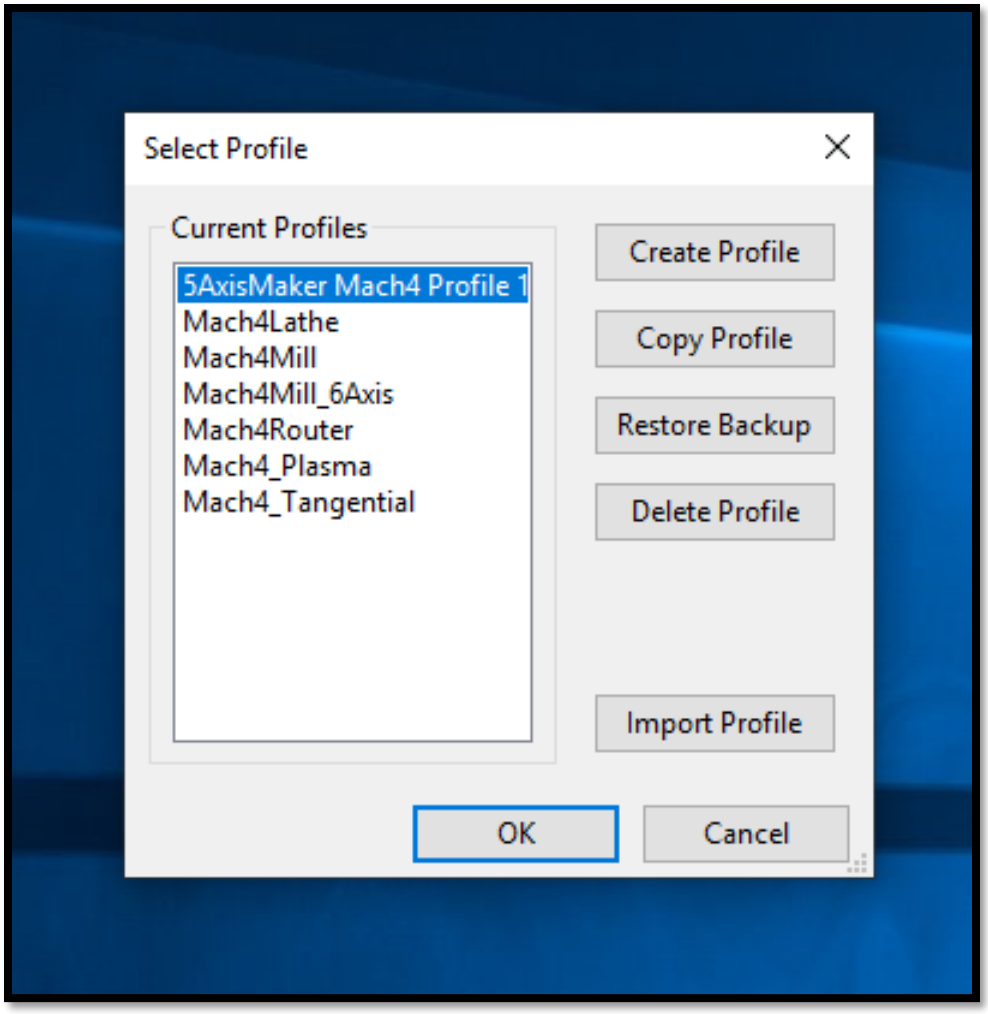

Figure 65 Starting up Mach 4 5-Axis Maker Profile

This takes the user to the home screen of the Mach 4 software. To start calibrating the machine, the blinking green **Enable** button on the bottom right of the screen is pressed. This enables the connection between Mach 4 and the machine's controller.

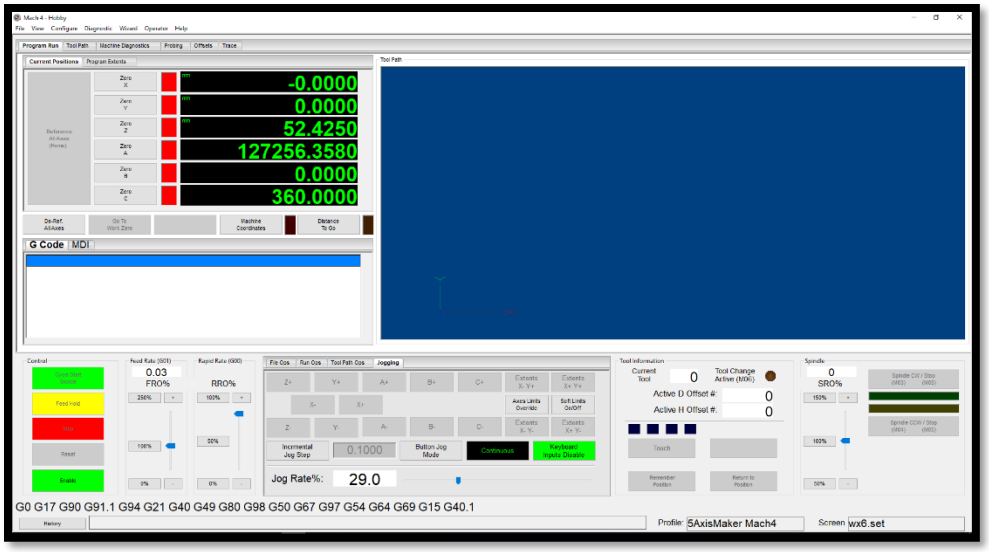

Figure 66 Mach 4 Home Page

Calibrating All Axes- To move all axes, the **Jogging** option is selected. Each axis can then be moved from this window. Pressing on the + or – buttons of any corresponding axis will result in physical motion of the corresponding axis on the machine.

A typical procedure is to bring the print head to the approximate center of the workspace by moving it in X and Y direction. With the print head at the center of the bed, one can then press the **Zero X** and **Zero Y** buttons in the software.

For the B and C axes, there are arrows on the machine (Figure 67) that indicate the home positons of those axes. Jogging those two axes in software until the corresponding arrows line up will set the zero position for both the C and B axes.

Figure 67 B and C axis Calibration Arrow Marks

At this point, the print head can be lowered very slowly towards the print bed in Z axis. The jog speed can be changed on the bottom of the screen. A piece of paper is placed between the nozzle tip and the bed. The nozzle is lowered towards the bed while the piece of paper is slide back and

forth. Just at the point where the paper is lightly pinched between the nozzle and the bed, the zero point for the Z axis can be set.

Assuming the nozzle was heating up during the machine calibration process, the filament can be fed into the print head. The PLA filament used for trials in this research is fed into the extruder motor. The extruder motor is designated as the A-axis in the Mach 4 software. When the filament is inserted into the inlet of the extruder, the A axis can be jogged in the positive direction in Mach 4 to feed the filament towards the heated nozzle. Feeding is continued until molten filament begins to come out of the nozzle. At this point, the A-axis can be zeroed in Mach 4.

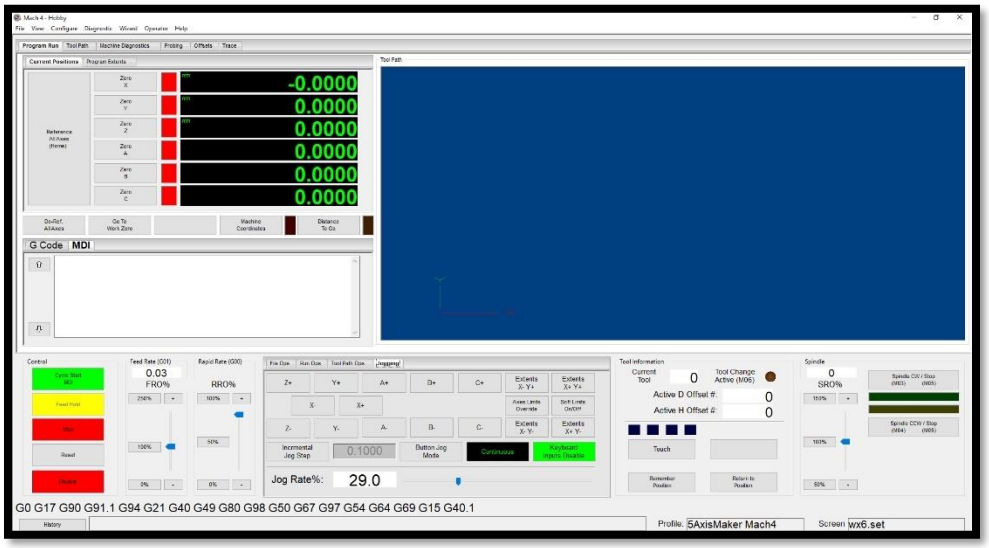

Figure 68 Mach 4 Jogging and Machine Calibration

At this point, all axes should be zeroed, and the machine axis calibration is complete.

Importing NC Code

Now that the machine is calibrated and the desired heater temperature has been reached, printing can commence. To import the NC file, click on **FileOps> Load G Code> Browse our file in the window> Click Open**.

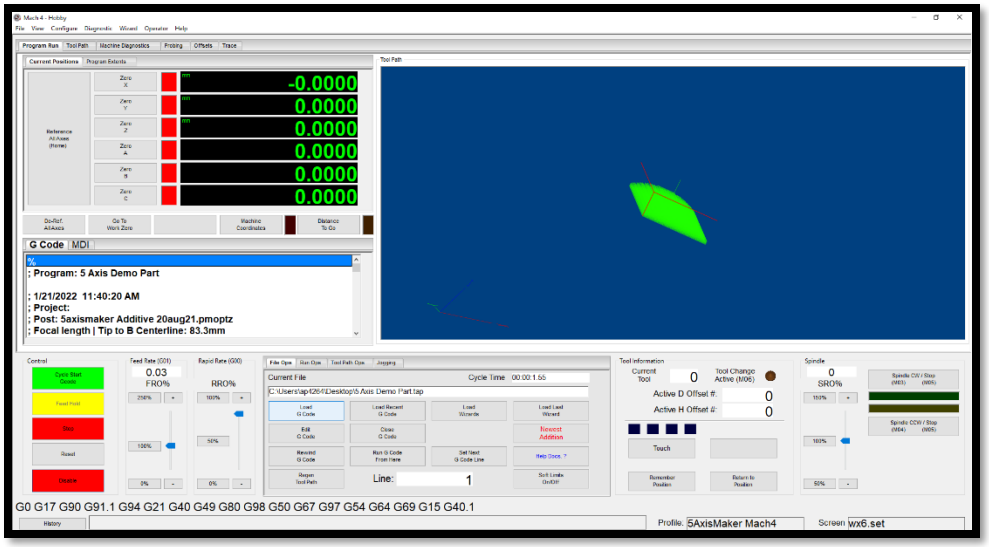

Figure 69 NC Program Imported

This will import the NC Program to Mach-4. After clicking **Start Cycle G-code**, printing will start.

3.5 Methods of Printing Different Non-Planar Parts

Using the above process planning approach for generating non-planar 5-axis toolpaths, three different printing scenarios are presented here.

3.5.1 Solid Parts With Non-Planar Top Surfaces

For maximum part strength regardless of part weight, a completely solid part with conformally printed up-facing skins can be printed. Toolpath generation for these types of parts will have the same basic structure as discussed above. The Feature Construction in this part will be dense and will have small step-over distances. The top layer of this feature will be coated with a non-planar surface using the Surface coating feature. This part will have a planar base and non-planar top layers. The end product will include both the feature and surface coating together as a part. The top layer can be introduced to make the part stronger or to improve the surface finish. All test parts presented in this research were produced with this method.

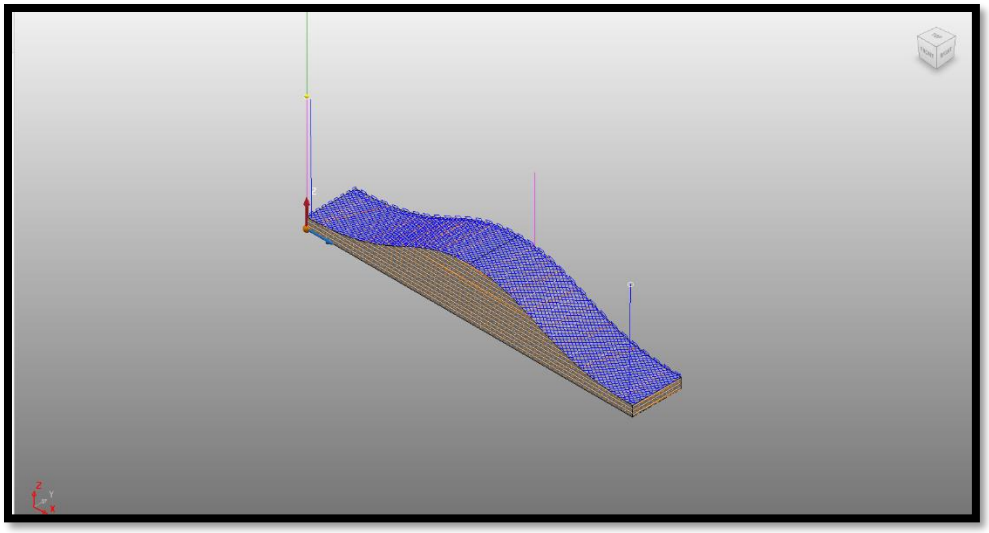

Figure 70 Solid Feature Construction With Solid Non-Planar Layers

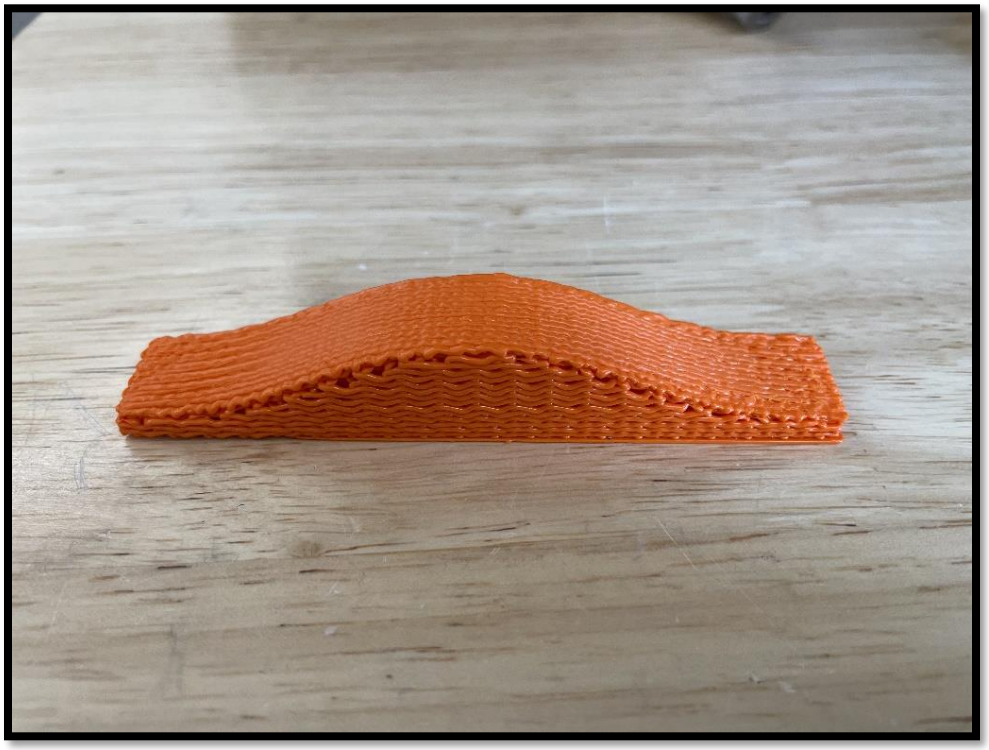

Figure 71 Solid Part Printed With 3-axis Feature Construction and Top Non-Planar Layers

3.5.2 Shell Parts with Support Structures

As previously mentioned, there is no provision in Powermill to generate support structures as of this writing. A work-around for this is to print a Shell Part with low density under the feature construction by specifying large step-over distances. This printed feature will act as a removable support structure. After the support is printed, the surface coating feature can be used to print non-planar layers on the structure. These non-planar layers correspond to Shell parts. In order to have a solid part, a dense top layer is produced with a minimum step-over distance that eliminates any gap between adjacent printed traces.

After each segment is printed, the support structure can be peeled away from the non-planar part.

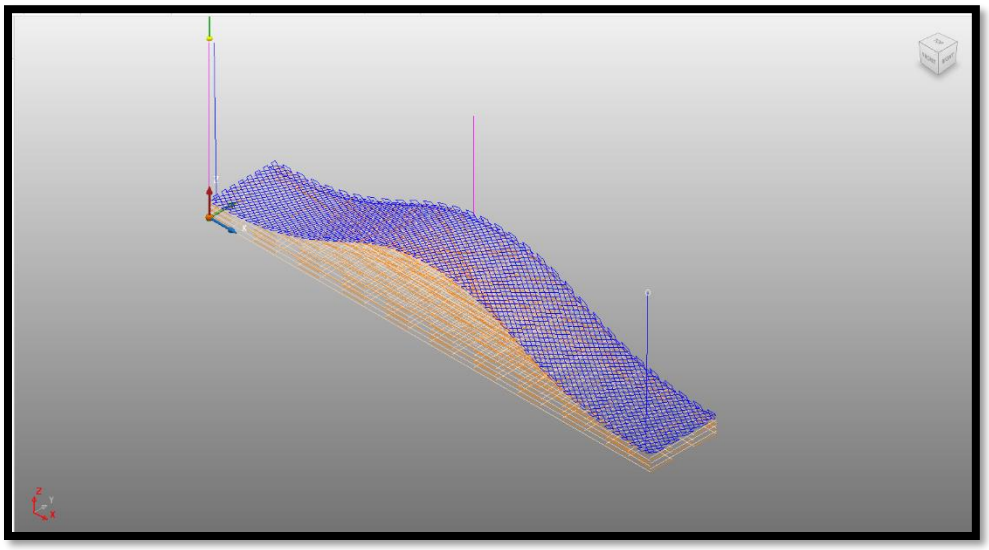

Figure 72 Feature Construction Used As A Support Structure To Print A Shell Part

Figure 73 Non-Planar Part Printed On A Support Structure

Figure 74 Removing Support from Non-Planar Part

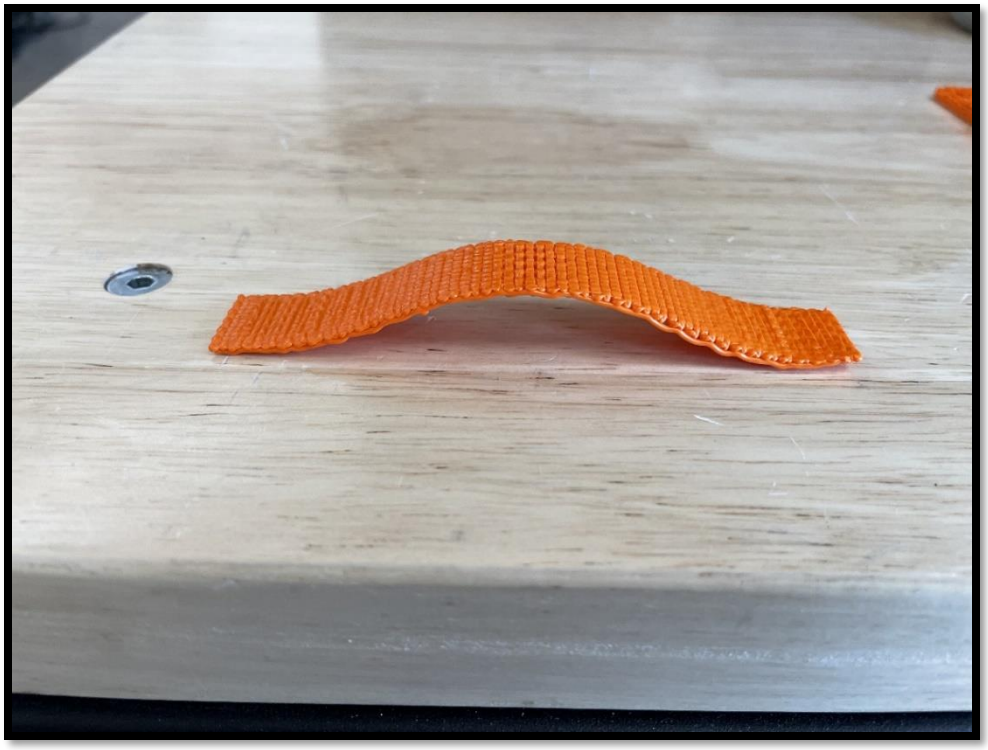

Figure 75 Non-Planar Part On A 3DP Support Structure

3.5.3 Non-Planar Surface Coating of Shell Parts

The third scenario for printing is surface printing. In this type of non-planar printing, parts are printed on top of pre-manufactured non-planar surfaces (e.g. mandrels, mold surfaces, etc.). In the example presented here, a skin is printed on a machined aluminum hyperbolic paraboloid shape.

Software

To create a shell part on top of a pre-manufactured surface, the Surface Finish command from Powermill is used. All previously described steps for importing the machine model and the part geometry are the same. As a feature construction is not being created (i.e. printing is done on a pre-existing part), the Level is not needed. It is only necessary to create a Set which will consist of the top non-planar layer. As the feature is already constructed (i.e. a machined aluminum non-planar base in this example), the surface coating feature alone is used to print the part. The only difference in the workflow is to select the Workplanes on the non-planar surface and not at the base of the feature. This step is very important, as one needs to select a point for the Workplanes creation that can be easily identified on the physical object while placing it on the machine bed.

One option is to machine a fiducial locating feature into the part for this purpose. This setting up of the Workplanes will set the zero points for the X, Y, Z, B and C axes.

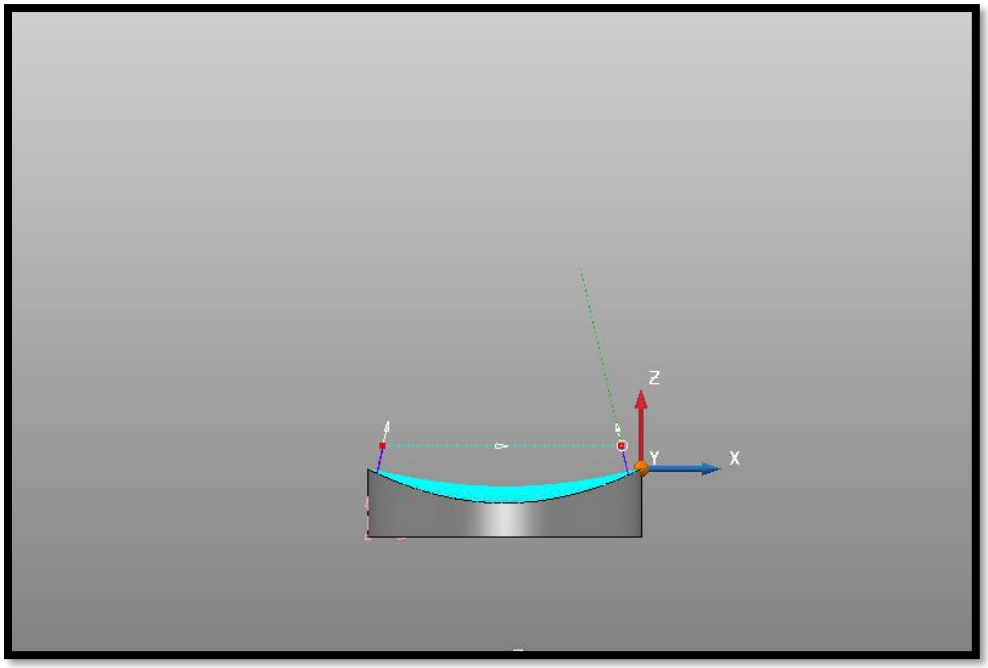

Figure 76 Work Plane Created On the Centerline and On One Edge of the Geometry for Easy Identification

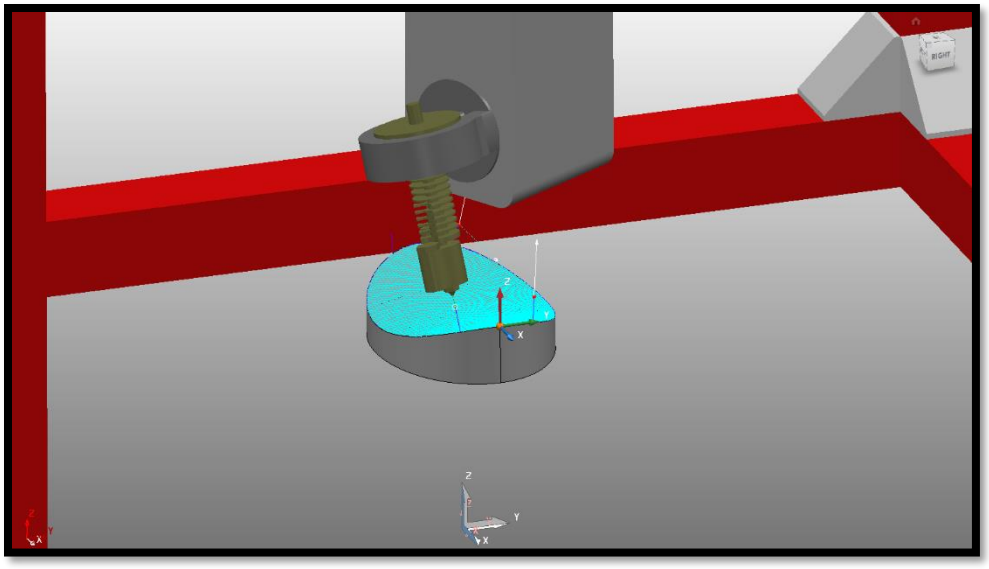

Figure 77 Surface Coating On the Top of the Part

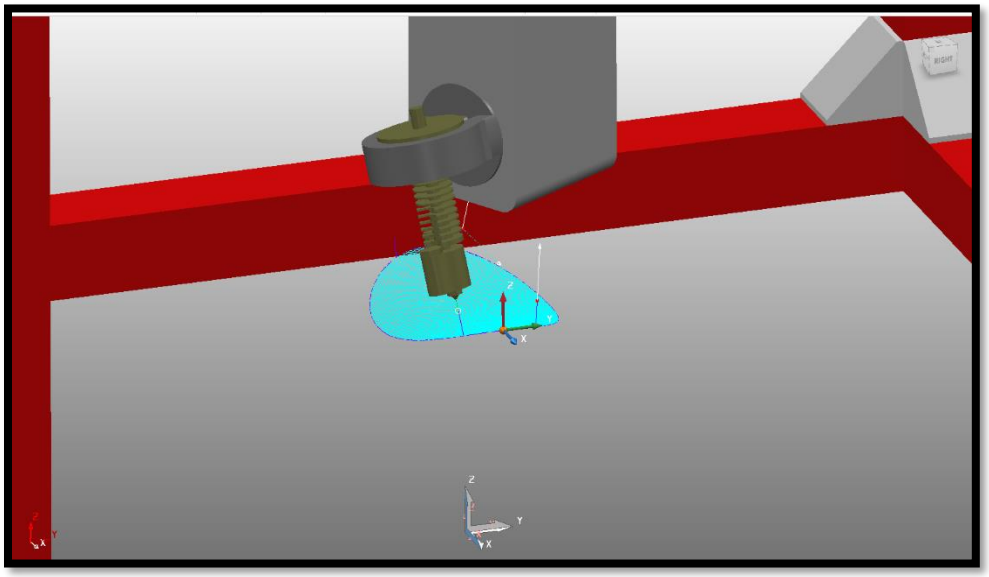

Figure 78 Non Planar Part Created In the Simulation

Hardware

As a skin will be printed on top of an existing non-planar surface, it will be necessary to make changes in the machine setup part of the process. These changes are described below. As the machine used for the preliminary proof-of-concept demonstrations did not have the ability to

probe the surface of a part, datums (i.e. zero points) for all the axes were manually set. The zero point for all axes must be the same as the corresponding Workplanes created in Powermill while generating the toolpath.

In this research, the machined aluminum hyperbolic paraboloid part was held firmly in place. Using Mach4's jog feature, all the X, Y and Z axes are jogged to the datum and zeroed. At this point, the g-code can be imported into Mach4, and printing can be started. The B and C axes are calibrated as described in the previous section.

After printing is complete, the non-planar part is removed from the base and will have a non-planar shell part. This process can be repeated multiple times on the same base to get multiple parts.

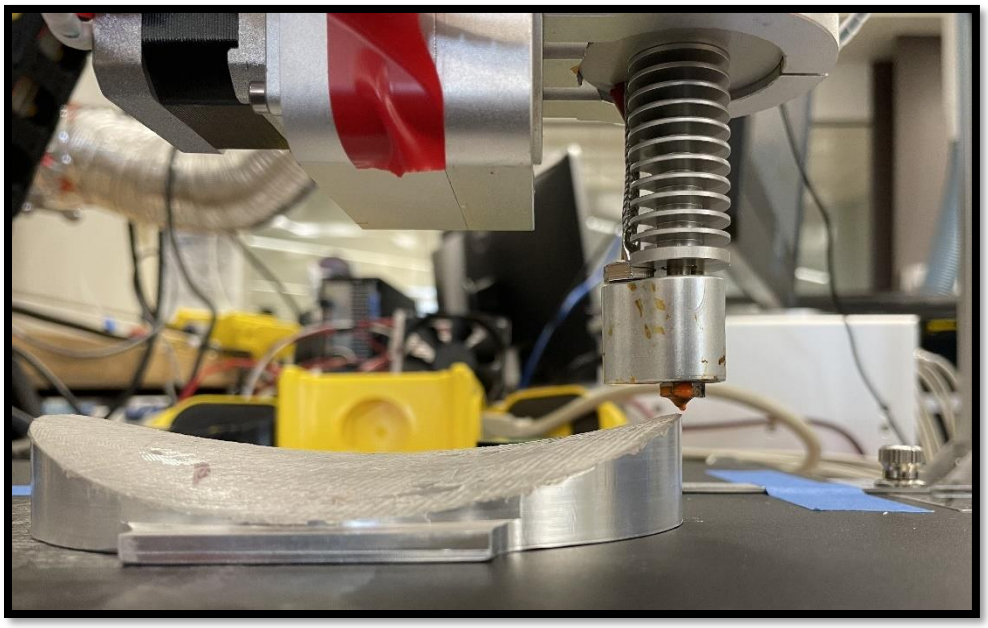

Figure 79 Zeroing the X axis

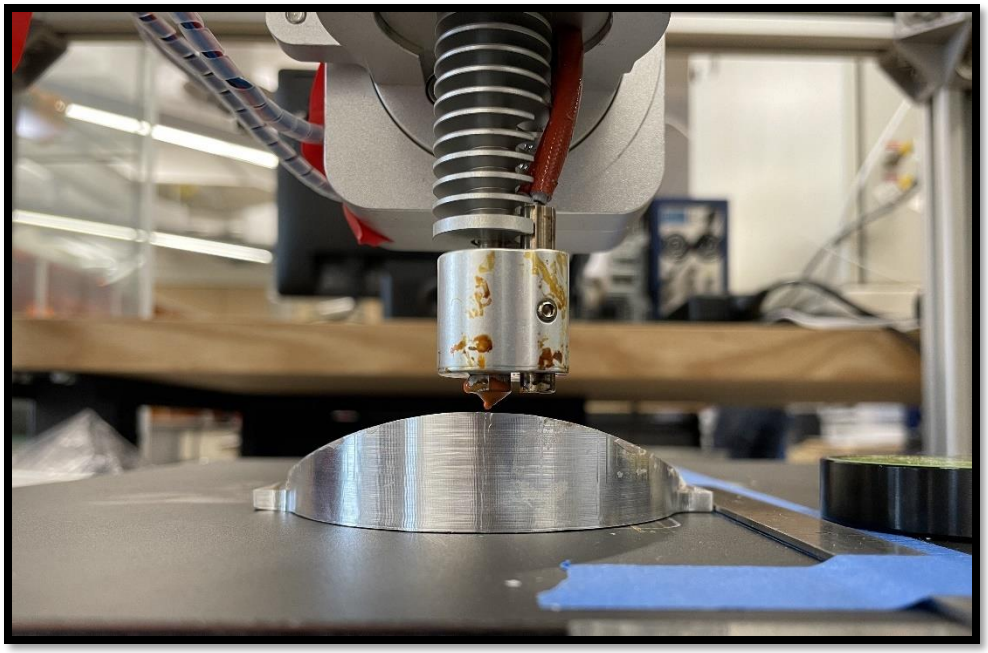

Figure 80 Zeroing the Y and Z Axes

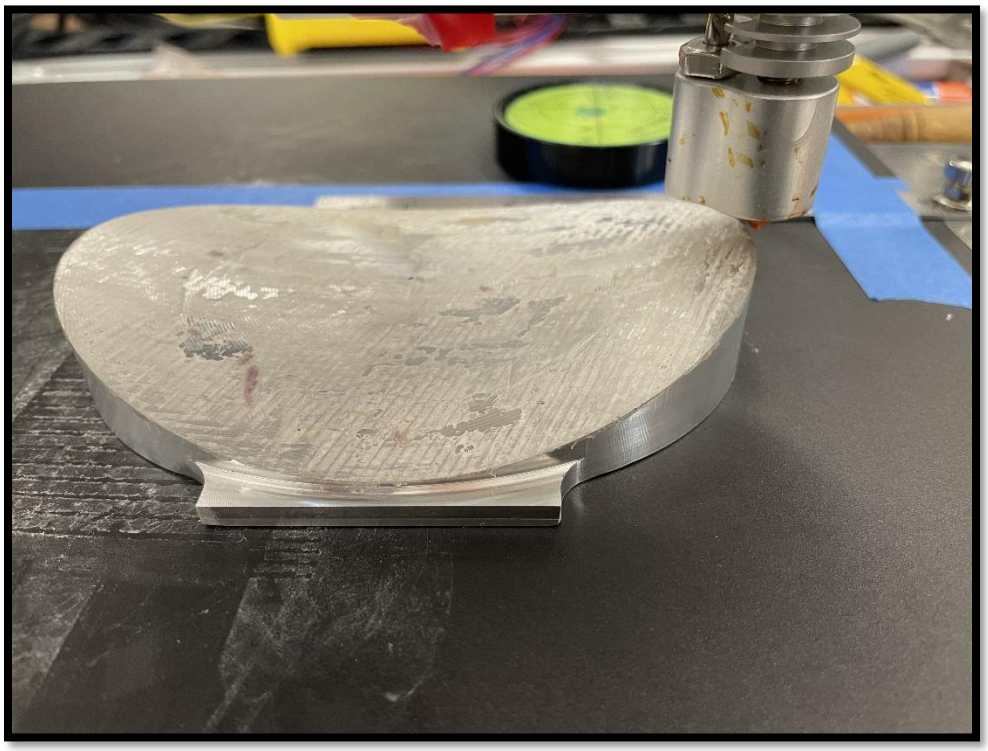

Figure 81 All Axes Calibrated and Machine Ready To Print.

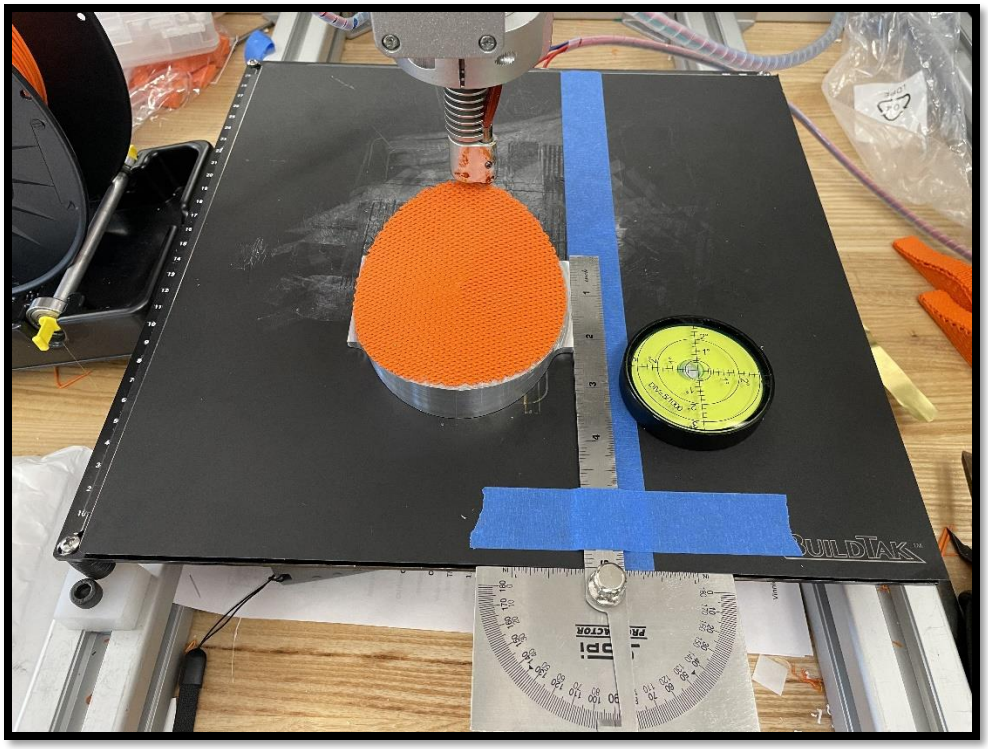

Figure 82 Skin or Shell Part Printed On Top of An Existing Structure

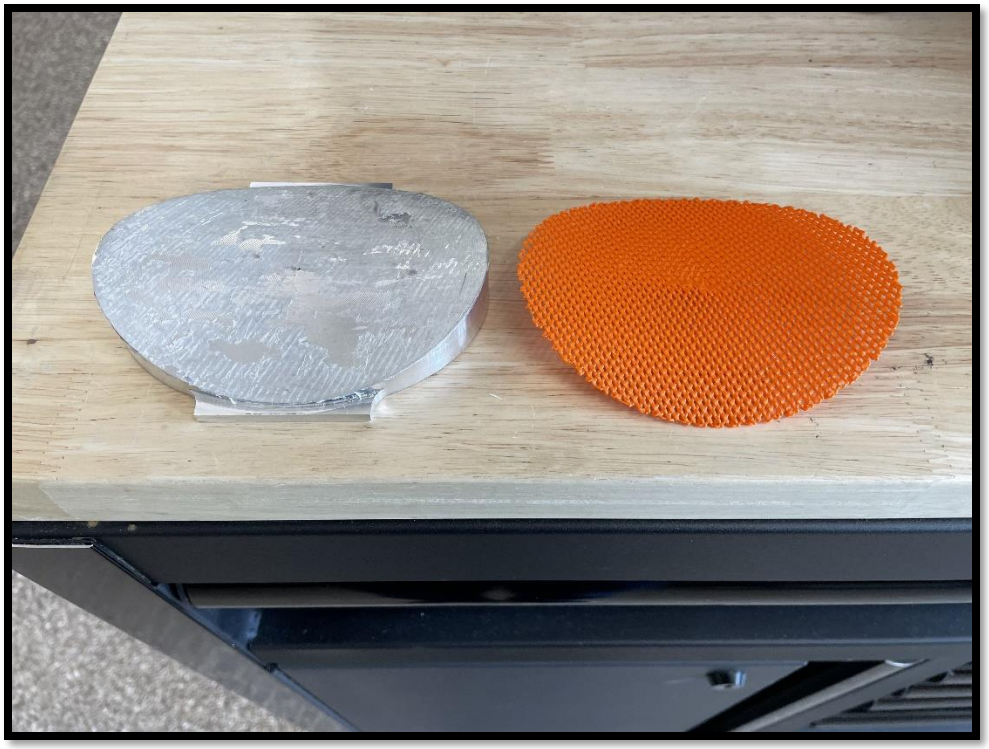

Figure 83 Shell Separated from Non-Planar Base

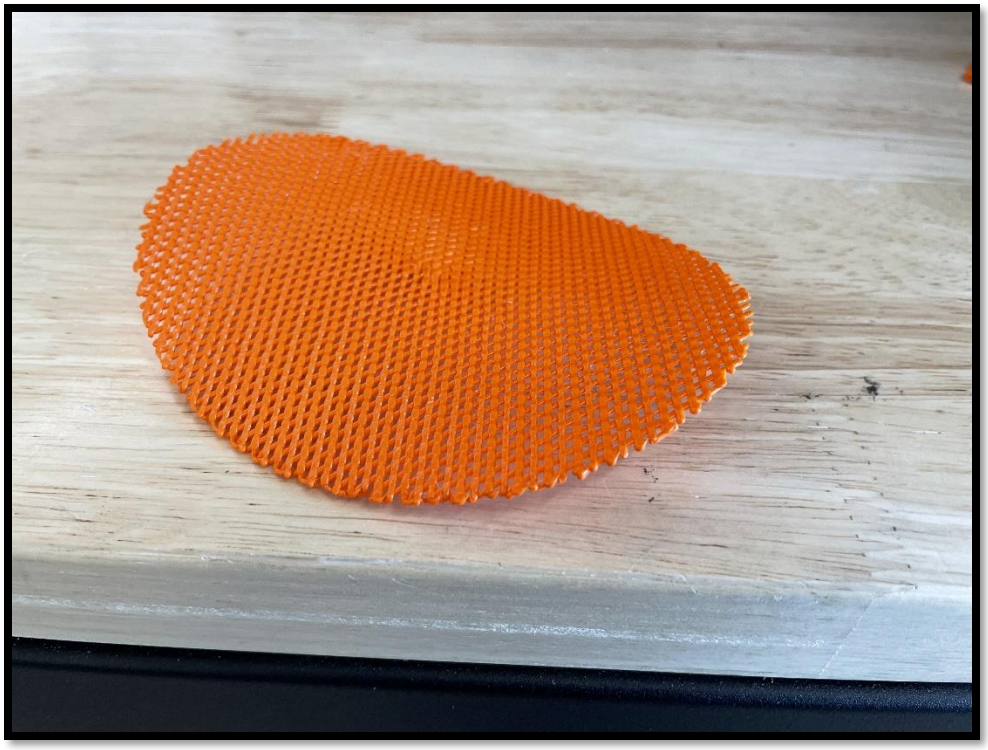

Figure 84 Hyperbolic Paraboloid Part

3.5.4 Non-Planar Woven Surfaces

As seen in the literature review, there are significant potential benefits of using woven carbon fiber skins in 3D printed FFF parts. In the few published studies of toolpath generation for woven 3D printed skins, all examples involved planar printing. By using the tool-path edit feature in Powermill, this section presents what is believed to be the first example of a toolpath to produce a non-planar woven skin with interlocking behavior. The 5Axis Maker cannot print continuous carbon fiber at this time, however, the toolpath generation process demonstrated here can be used as a proof of concept in support of further research. Figure 85 shows the interlocking nature of the non-planar hyperbolic paraboloid woven skin.

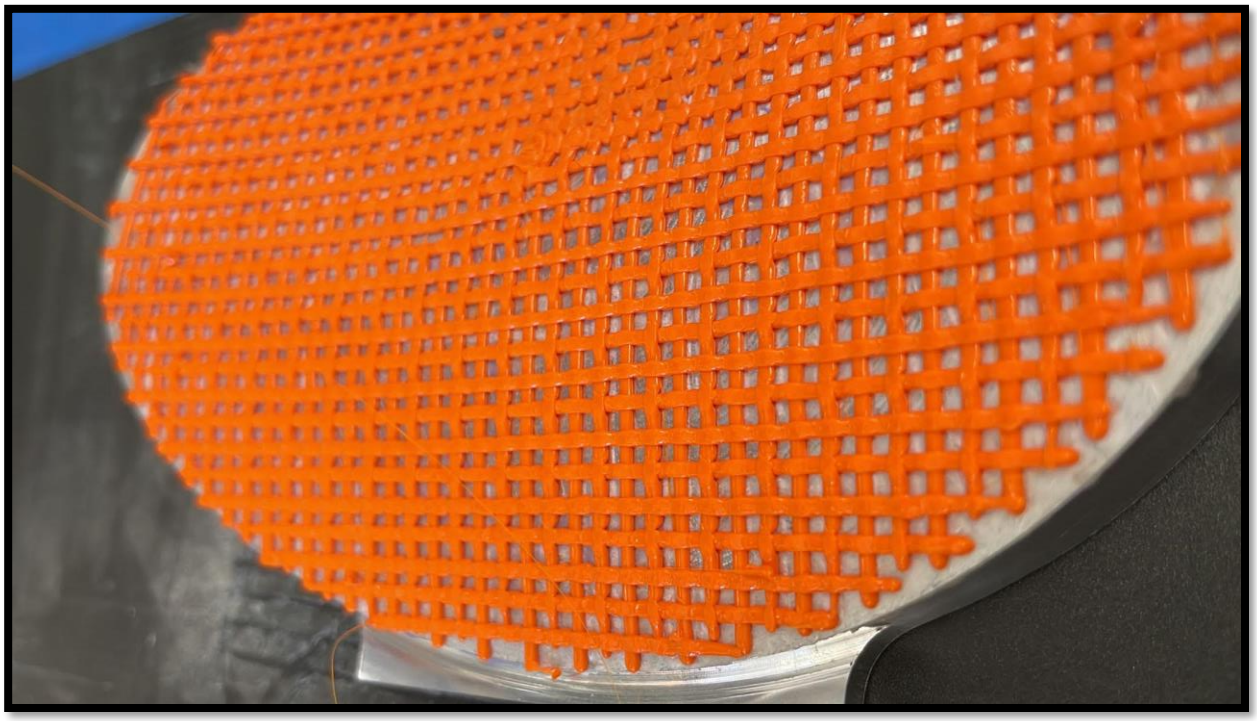

Figure 85 Non-Planar Woven Skin

4.0 MECHANICAL TESTING

As discussed in the literature review, the mechanical strength of FFF parts depends on many factors. For test results reported here, print parameters have been held constant between each experimental trial, and only the material deposition strategy (i.e. planar printing versus conformal printing) has been varied. The material used in all experiments was PLA, and the orientation of the parts during printing was the same. All parts were printed on a 5Axis Maker machine using the aforementioned Powermill Ultimate CAM software process for toolpath generation.

As there is no ASTM standard that exists today for testing non-planar AM parts, characterization methods were adapted in an attempt to study differences in properties between parts printed using both planar and non-planar deposition strategies.

4.1 3-Point Bend Test

This test was performed on two different sets of samples. The first set of parts were produced using traditional layerwise deposition. The second set of parts started with base features produced by layerwise printing. The base features were then topped off with two non-planar top surface skins produced via conformal printing.

4.1.1 3-Point Bend Test Part Preparation

A total of five specimens of each set of planar and nonplanar FFF parts were printed and tested. Each part was printed on the 5Axis Maker machine with the following standard printing parameters:

Table 1 Printing Parameters for all Test Specimens

Parameter Name	Planar Part		Non-Planar Part	
	Value	**Units**	**Value**	**Units**
Focal Length	83.3	mm	83.3	mm
Bead Width	1	mm	1	mm
Stepover	0.4	mm	0.4	mm
Angle of Rotation	90	Degree	90	Degree
Layer Height	0.55	mm	0.55	mm
Filament Diameter	0.75	mm	0.75	mm
Filament Material	PLA	___	PLA	___
Nozzle Diameter	0.4	mm	0.4	mm
Bed Temperature	Non	---	Non	---
Filament Temperature	230	Degree Celsius	230	Degree Celsius
Filament Feed rate	500	mm/min	500	mm/min
Print time	17min 15sec	min	17min 39sec	min
Filament Used	7268	mm	7310	mm

Planar Parts

All five planar parts were printed using the standard layerwise FFF method with the printing parameters shown in Table 1.

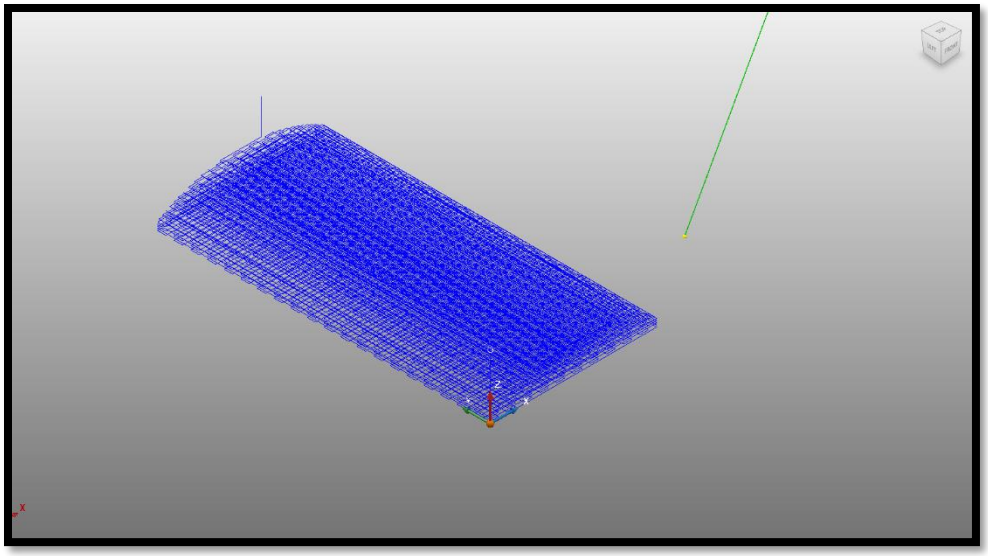

Figure 86 Planar 3DP Part

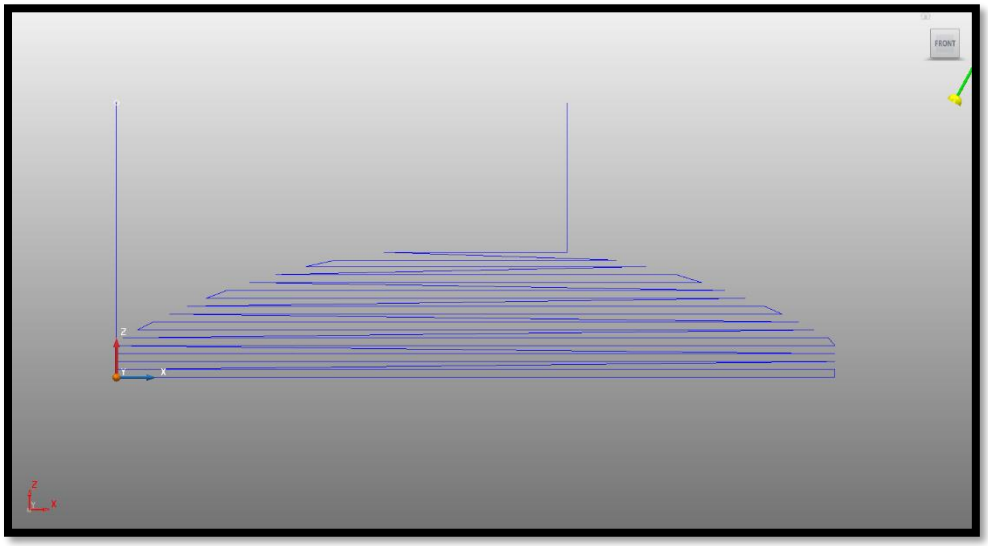

Figure 87 Planar Part Side View

Non-Planar Parts

All 5 non-planar parts started with a base that was printed using the standard layerwise FFF method, however, the top two surfaces (orange in Figure 88 and 89) were printed using the 5 axis capabilities of the machine and are non-planer. To get all the axes working together at the same

time these layers were printed at a 60-degree angle to the X axis of the machine. The top layers are called Surface coating layers in Powermill, and they are printed using the same parameters as those of the planar layers. Figure 90 and Figure 91 show the original printed parts.

The only difference between the parts is that the planar parts have all the layers printed one on top of the other, while the nonplanar parts have the top two surfaces printed in a non-planar fashion as surface coatings on top of the planar base.

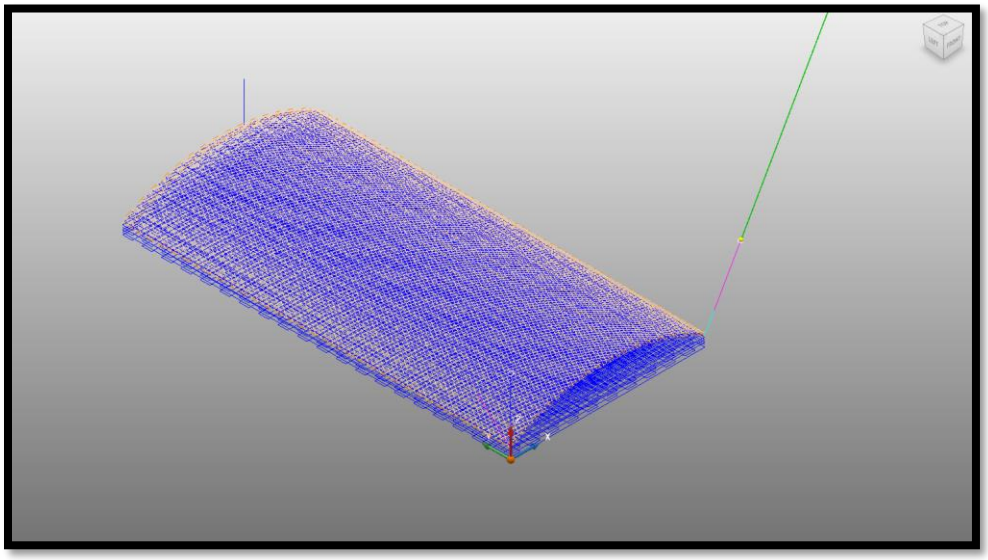

Figure 88 Planar Part with Non-Planar Surface Coating

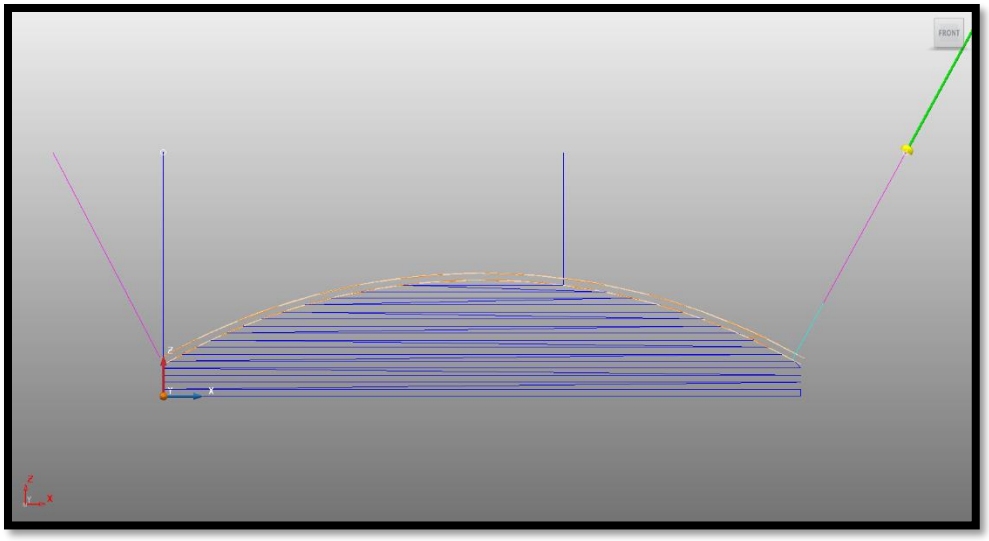

Figure 89 Planar Part with Non-Planar Top Layers (Orange)

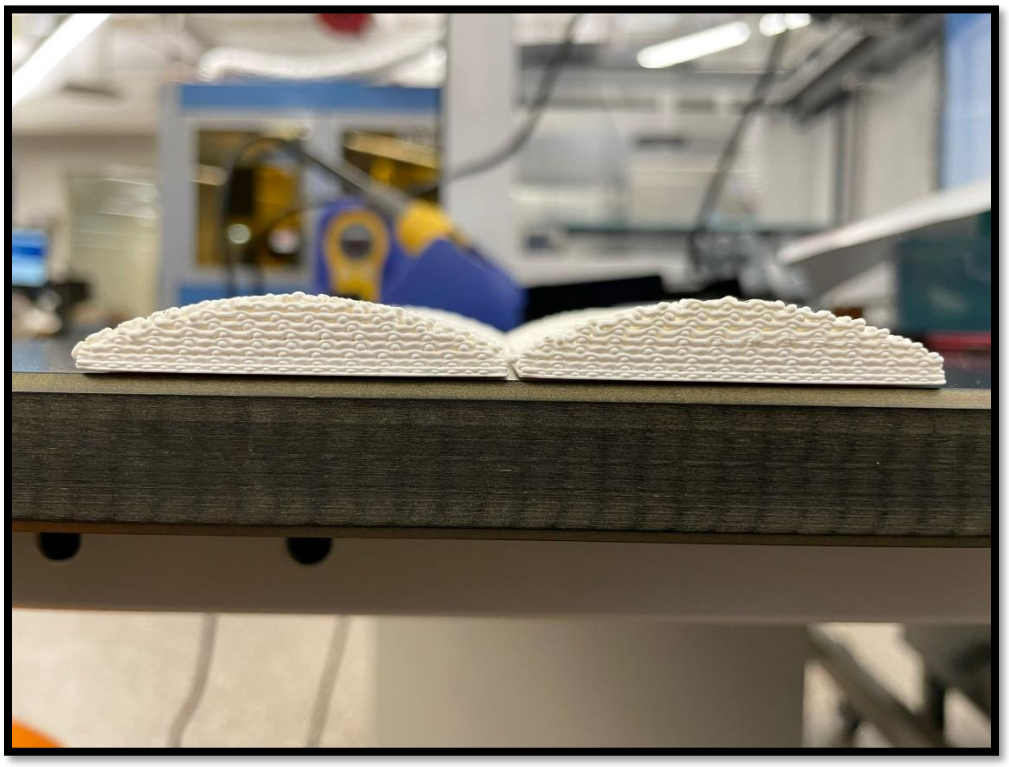

Figure 90 Side View of 3-Point Bend Test Specimen

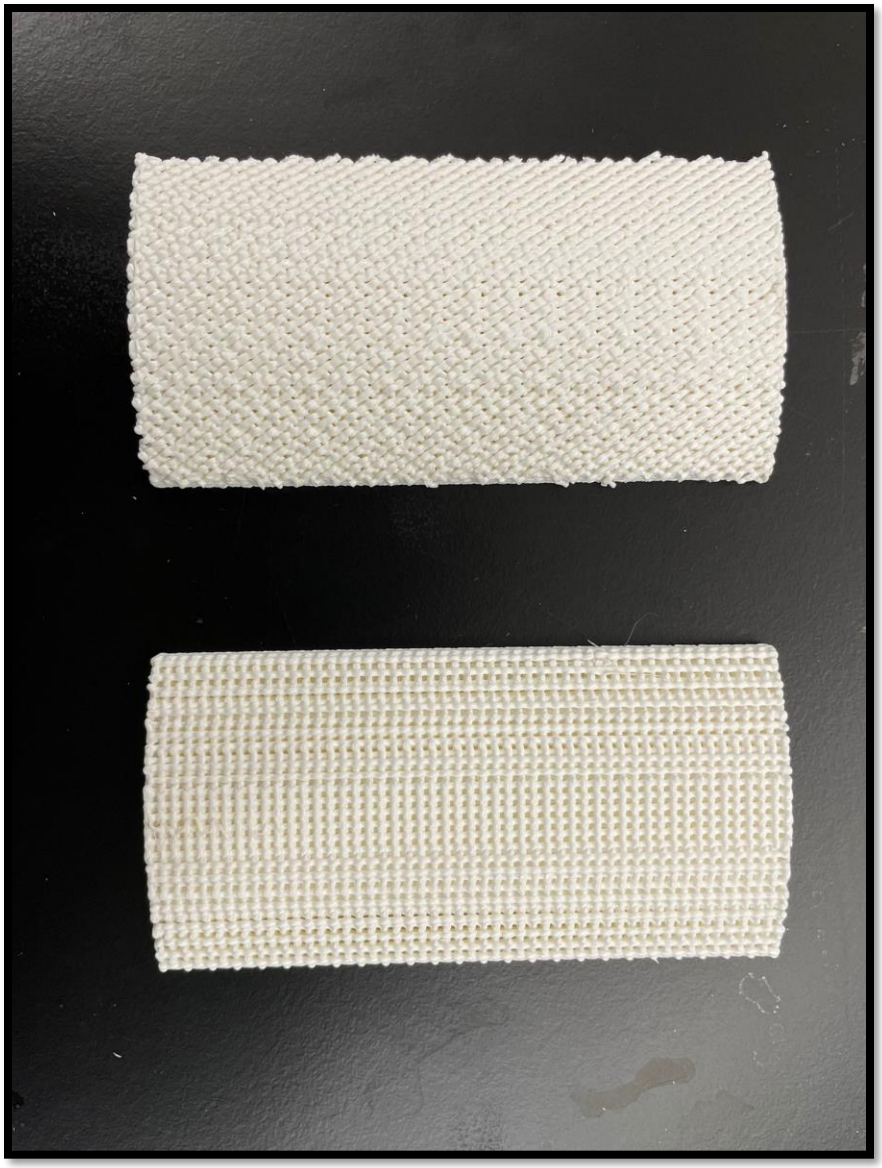

Figure 91 Top View of 3-Point Bend Test Specimen

4.1.2 3-Point Bend Test Setup

Three-point bend tests were performed on an Instron Universal Testing Machine (UTM), and the data was collected using Test Works 4 software. A 2500 kgf bi-directional load cell was used to record the compressive load. The tests were conducted using a data acquisition rate of 20 Hz. The stationary support span was 80 mm long. The test speed (load application speed) was 2.54 mm/sec.

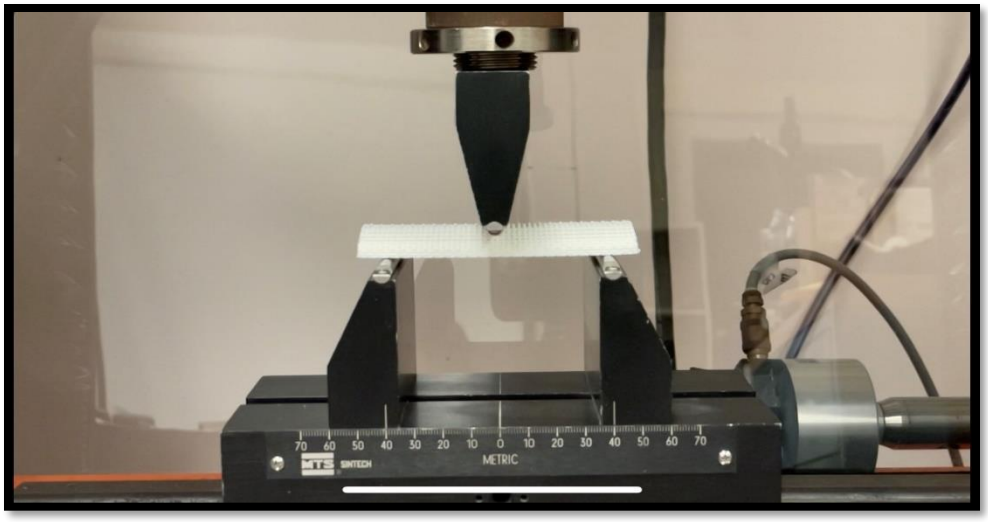

Figure 92 3-Point Bend Test Setup

4.1.3 3-Point Bend Test Results

Table 2 and Table 3 show that the average, maximum and minimum load at which the planar specimen and non-planar specimen failed. It is seen that all the results of maximum load are in the range of 2 standard deviation of the average load value.

Figure 93 and Figure 94 show us the graph of load (kgf) vs Extension (mm). It is observed that the average extension of planar specimens is 3.65 mm and the average extension of the non-planar specimens is 3.60 mm.

Table 2 3-Point Bend Test Results for Planar Parts

Planar Specimen Results				
	Width (mm)	Max Thickness (mm)	Weight(gms)	Max Load (kgf)
Specimen 1	49.98	9.98	36.23	82.41
Specimen 2	49.98	9.98	36.55	78.60
Specimen 3	49.98	9.98	36.15	83.91
Specimen 4	49.98	9.98	36.68	79.28
Specimen 5	49.98	9.98	36.78	86.81
			Average:	82.23
			Max:	86.81
			Min:	78.60
			Plus:	4.58
			Minus:	3.62
			Standard Deviation:	3.38

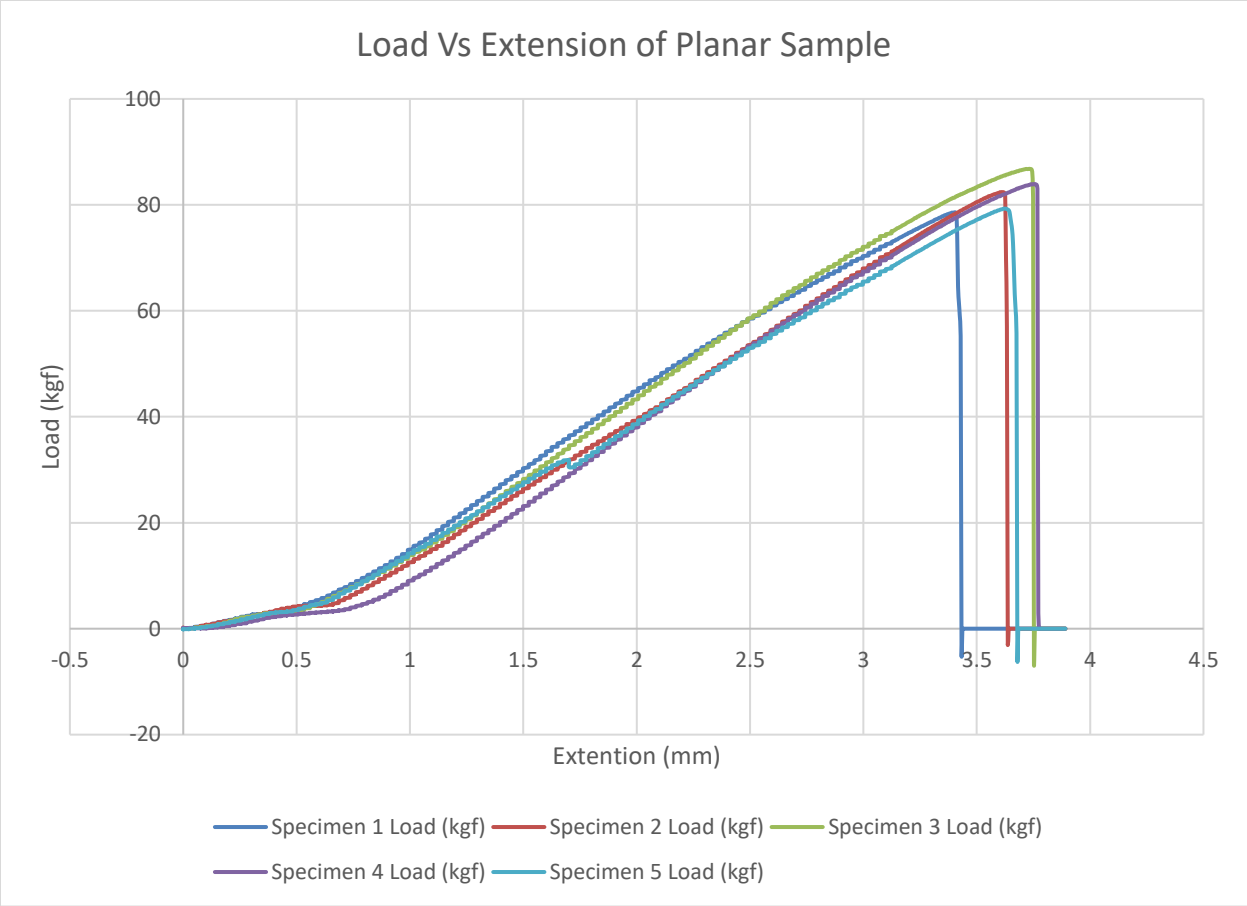

Figure 93 Graph of Load vs Extension for Planar Samples

Table 3 3-Point Bend test Results for Non-Planar Parts

Non-Planar Specimen Results				
	Width (mm)	Max Thickness (mm)	Weight (gms)	Max Load (kgf)
Specimen 1	49.98	9.98	36.59	94.21
Specimen 2	49.98	9.98	36.91	100.24
Specimen 3	49.98	9.98	36.63	98.79
Specimen 4	49.98	9.98	36.89	96.97
Specimen 5	49.98	9.98	36.87	90.4
			Average:	96.11
			Max:	100.24
			Min:	90.4
			Plus:	4.08
			Minus:	5.71
			Standard Deviation:	3.91

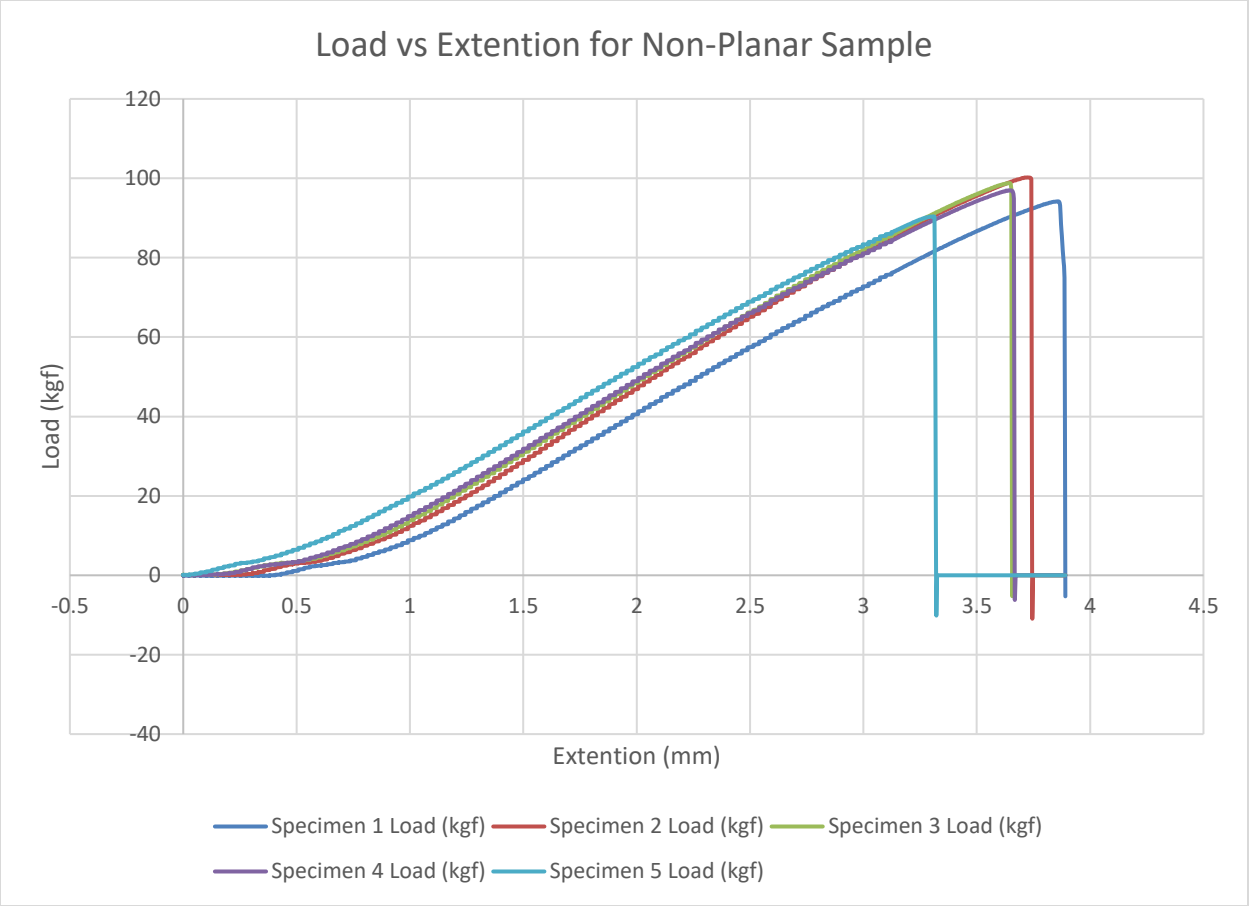

Figure 94 Graph of Load vs Extension for Non-Planar Samples

Percent Differences in Load

Table 4 Percent Differences in load at fracture between Planar and Non-Planar parts

	Planar Part Max Load (kgf)	Non-Planar Part Max Load (kgf)	Percent Increase (%)
Specimen 1	82.41	94.21	
Specimen 2	78.60	100.24	
Specimen 3	83.91	98.79	
Specimen 4	79.28	96.97	
Specimen 5	86.81	90.4	
Standard Deviation	3.38	3.91	
Average	82.23	96.11	16.88
Max	86.81	100.24	15.47
Min	78.60	90.4	15.01

3 Point Bend Test Result Analysis

- The time increased for printing non-planar surfaces by 24 seconds as compared to planar samples. This is due to the fact after printing the feature construction the machine calibrates itself by moving to a safe point and then starts printing the non-planar surfaces.
- 100% of both planar and non-planar parts are in the range of 2 standard deviation.
- The average percent increase in load-bearing capacity for all 5 non-planar specimens is 16.88 %.

- There is no substantial difference in the mass of samples printed with the two different strategies as the average weight of planar samples is 36.47 gms and the average weight for non-planar samples is 36.77 gms.

4.2 Impact Toughness Test

To measure the impact toughness, Charpy Impact toughness tests were performed on sets of parts printed with each of the two strategies. In this test, there were two set of parts with 10 parts in each set. The first set was printed using the traditional layerwise (planar) method. The second set was printed with a layerwise base upon which two non-planar surface coating layers were printed.

4.2.1 Charpy Impact Toughness Part Preparation

All Charpy impact test specimens were printed on the 5Axis Maker machine with the following standard printing parameters:

Table 5 Printing Parameters for Charpy Impact test Specimen

Parameter Name	Planar Part		Non-Planar Part	
	Value	Units	Value	Units
Focal Length	83.3	mm	83.3	mm
Bead Width	1	mm	1	mm
Step over	1.5	mm	1.5	mm
Angle of Rotation	90	Degree	90	Degree
Layer Height	0.55	mm	0.55	mm
Filament Diameter	0.75	mm	0.75	mm
Filament Material	PLA	---	PLA	---
Nozzle Diameter	0.4	mm	0.4	mm
Bed Temperature	Non	---	Non	---
Filament Temperature	230	Degree Celsius	230	Degree Celsius
Filament Feed rate	500	mm/min	500	mm/min
Print time	6	min	6	min
Filament Used	11350.86	mm	11350.86	mm
Non-Planar Layers	non	---	2	---
Surface finish angle with X-axis	non	---	60	Degree

Non-Planar Charpy Test Specimens

There were 10 specimens printed on the 5Axis Maker machine with the above mentioned printing parameters. For the non-planar printing specimens, the surface coating layers were printed at a 60 degree angle relative to the X-axis so as to use the full potential of the 5-axis printing.

As shown in the Figure 95 and Figure 96, the orange part volume is printed using the feature construction method, and the non-planar surface coating to be printed is represented by the blue mesh on top.

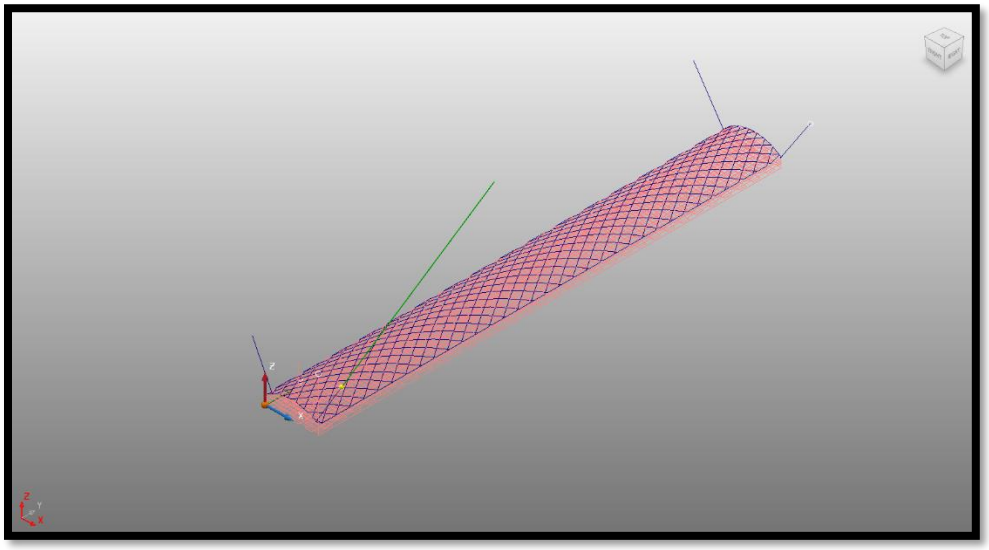

Figure 95 Non-Planar Charpy Specimen

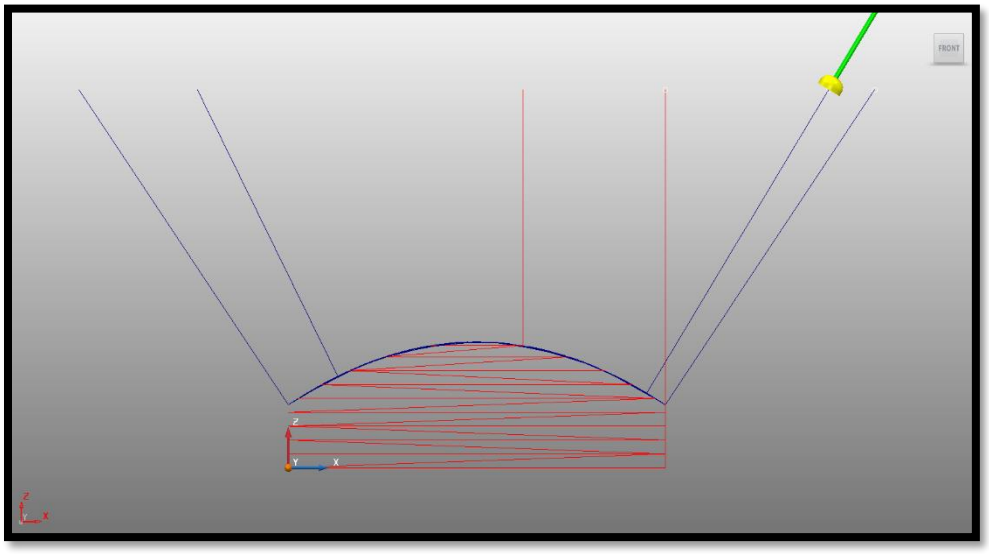

Figure 96 Non-Planar Charpy Specimen Side View (Blue Layers are Non-Planar)

Planar Charpy Specimens

A total of 10 planar parts were printed on the 5Axis Maker machine. Each entire part was constructed using the feature construction option using the printing parameters from Table 5. No surface finishing option was used.

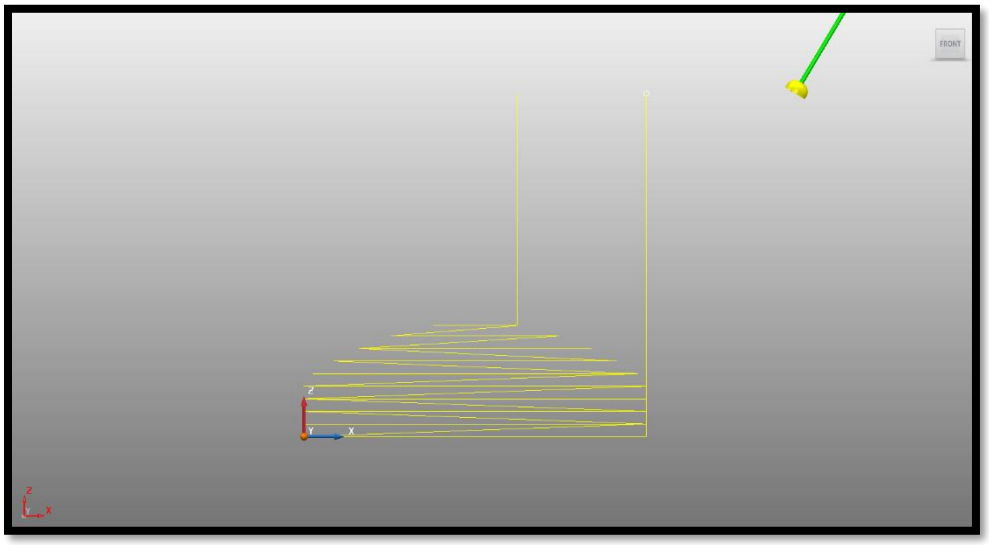

Figure 97 Planar Charpy Specimen Side View

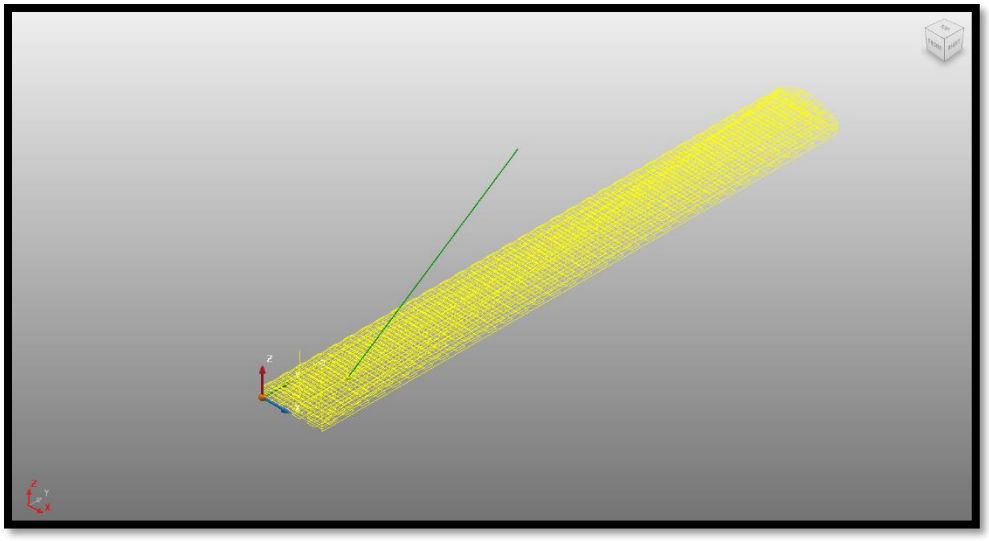

Figure 98 Planar Charpy Specimen

Figure 99 shows the final Charpy specimens printed alongside the standard calibration specimen.

Figure 99 Printed Charpy Specimens

4.2.2 Charpy Impact Test Setup

The above mentioned specimens were tested using a Galdabini Charpy Impact Testing Machine. An impact blow is delivered to a test specimen by means of a pendulum-type hammer. The impact value of the material is determined from the energy required to break the specimen. The pendulum hammer had a mass of 113.98 gms, and the maximum impact energy produced by this setup was 2.70 J.

Figure 100 Galdabini Charpy Impact Tester

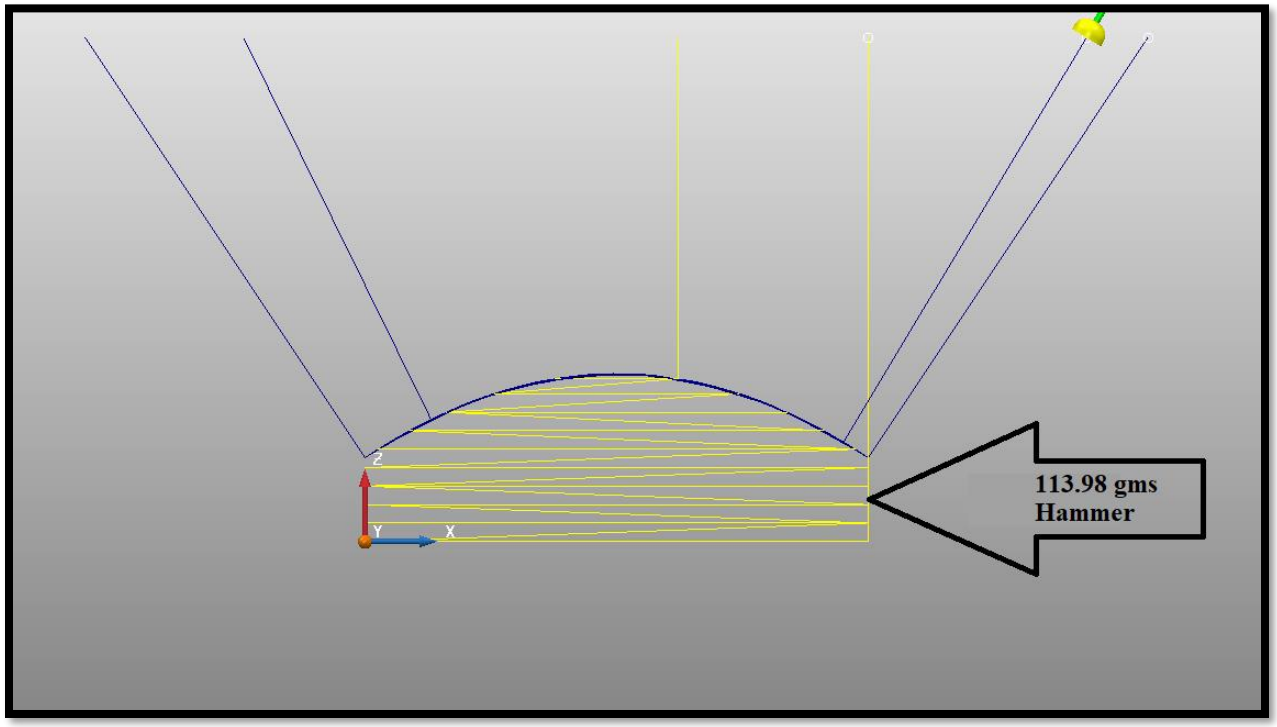

Figure 101 Side View of Hammer Impact Location On Charpy Specimen

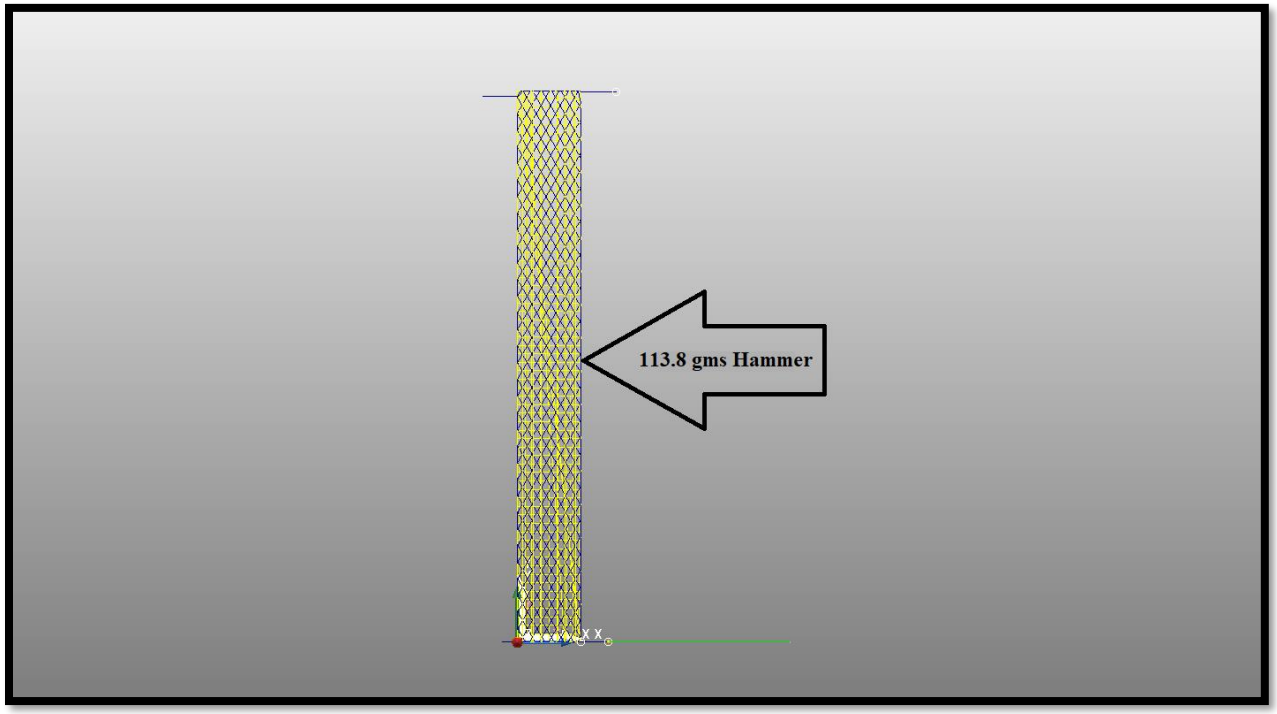

Figure 102 Top View of Hammer Impact Location On Charpy Specimen

4.2.3 Charpy Impact Test Results

The 10 planar test samples were subjected to the impact toughness test with results as shown in Table 6.

Table 6 Impact energy absorbed in Joules (J) by Planar Charpy Specimens

Specimen number	Width (mm)	Thickness (mm)	Impact Energy Absorbed (J)
1	16.73	4.99	0.263
2	16.81	4.97	0.282
3	16.79	4.99	0.298
4	16.77	5.05	0.308
5	16.8	5.03	0.277
6	16.83	4.97	0.278
7	16.81	4.99	0.267
8	16.79	5.01	0.280
9	16.76	5.03	0.233
10	16.82	5.01	0.271
Standard Deviation			0.020
Maximum			0.308
Minimum			0.233
Average			0.276

The 10 non-planar specimens were subjected to the impact toughness test with results as shown in Table 7.

Table 7 Impact energy absorbed in Joules (J) by Non-Planar Charpy Specimens

Specimen number	Width (mm)	Thickness (mm)	Impact Energy Absorbed (J)
1	16.77	5.06	0.435
2	16.8	5.01	0.359
3	16.81	4.95	0.392
4	16.75	5.01	0.362
5	16.79	4.96	0.442
6	16.72	4.98	0.380
7	16.81	5.03	0.380
8	16.83	5.02	0.416
9	16.82	4.99	0.350
10	16.78	4.97	0.373
Standard Deviation			0.032
Maximum			0.442
Minimum			0.350
Average			0.389

Comparison of results

Specimen No-	Impact energy Absorbed by Non-Planar Specimen (J)	Impact energy Absorbed by Non-Planar Specimen (J)	Percent Increase in impact energy (%)
1	0.263	0.435	
2	0.282	0.359	
3	0.298	0.392	
4	0.308	0.362	
5	0.277	0.442	
6	0.278	0.380	
7	0.267	0.380	
8	0.280	0.416	
9	0.233	0.350	
10	0.271	0.373	
Maximum	0.308	0.442	43.51
Minimum	0.233	0.350	50.21
Average	0.276	0.389	40.94

Table 8 Percent Differences Between Impact energy absorbed by planar and Non-Planar Specimen

A summary of the key observations from the Charpy impact test results is as follows:

- On an average all planar parts had a mass of 9.33 gms and the average mass of non-planar parts was 9.61 gms.
- 100% of the planar and non-planar specimen are in the 2 standard deviation range from the mean.
- On average, the planar samples absorbed 0.276 J of energy.
- On average, the non-planar samples absorbed 0.389 J of energy.
- Samples printed with the non-planar surface printing strategy absorbed an average of 40.94% more energy than the planar samples.

5.0 SURFACE ROUGHNESS TESTS

5.1 Surface Roughness Part Preparation

One of the objectives of this research were to improve the surface finish of the printed parts by adding a conformal surface coating layer to eliminate printed stair stepping artifacts. There were 18 different parts printed for this test. These 18 parts were split into 2 sets of 9 parts. Both the sets were printed on the 5Axis Maker machine.

These 2 sets of parts were printed with up-facing surface slopes from 5 degrees to 45 degrees. One of these sets was printed using a conventional 3DP approach and the other was printed using the conformal surface printing approach for the up-facing surface. These 9 parts in each set were printed with different slope angles from 5 to 45 degrees in increments of 5 degrees.

5.1.1 Planar Parts

First 9 parts were printed with full density and were planar in nature with no conformal surface printing.

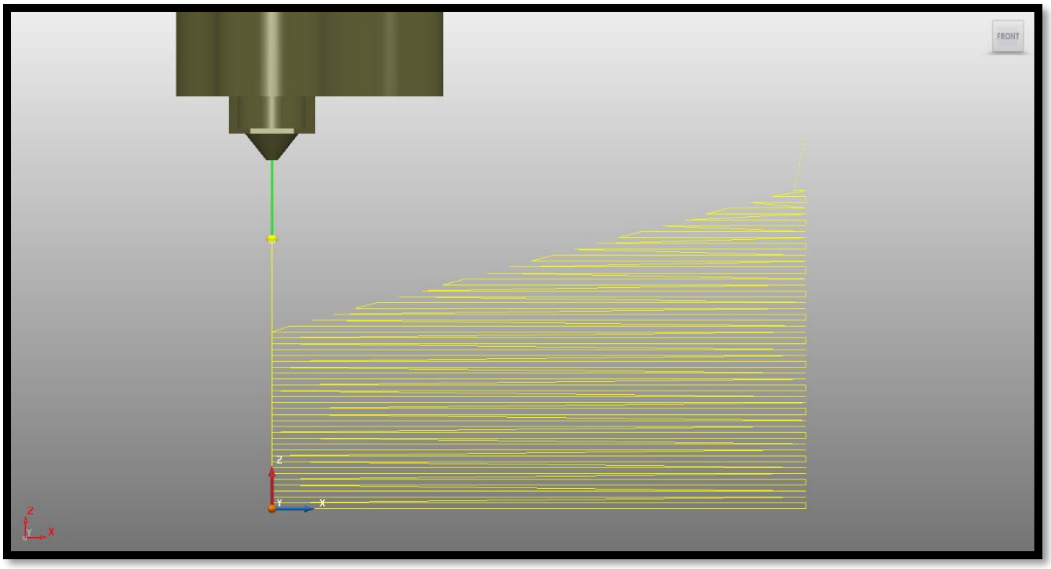

Figure 103 Planar Surface Roughness Specimen

5.1.2 Non-Planar Parts

The second set of parts were printed using the 5-axis conformal printing approach with a planar base and 2 conformal top layers.

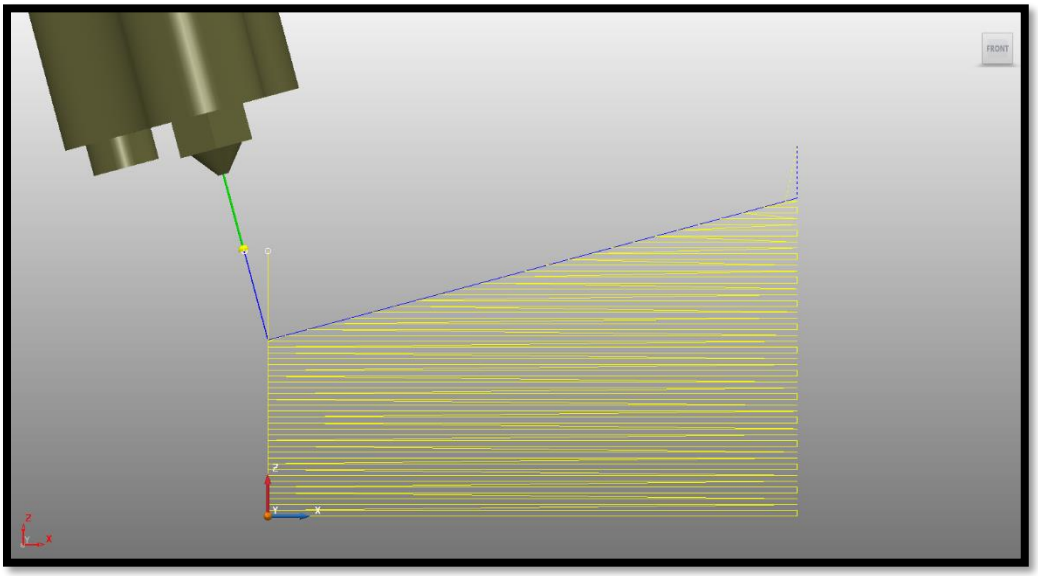

Figure 104 Non-Planar Surface Roughness Specimen

5.2 Surface Roughness Testing Procedure.

On every specimen, a 5 mm X 5 mm square area was scanned using a Nanovia Optical Profiler. The scan was a single direction scan. The step size in both the X and Y axis directions was 30 µm. The Topography surface scan method was used with a 1.1 mm pen tip.

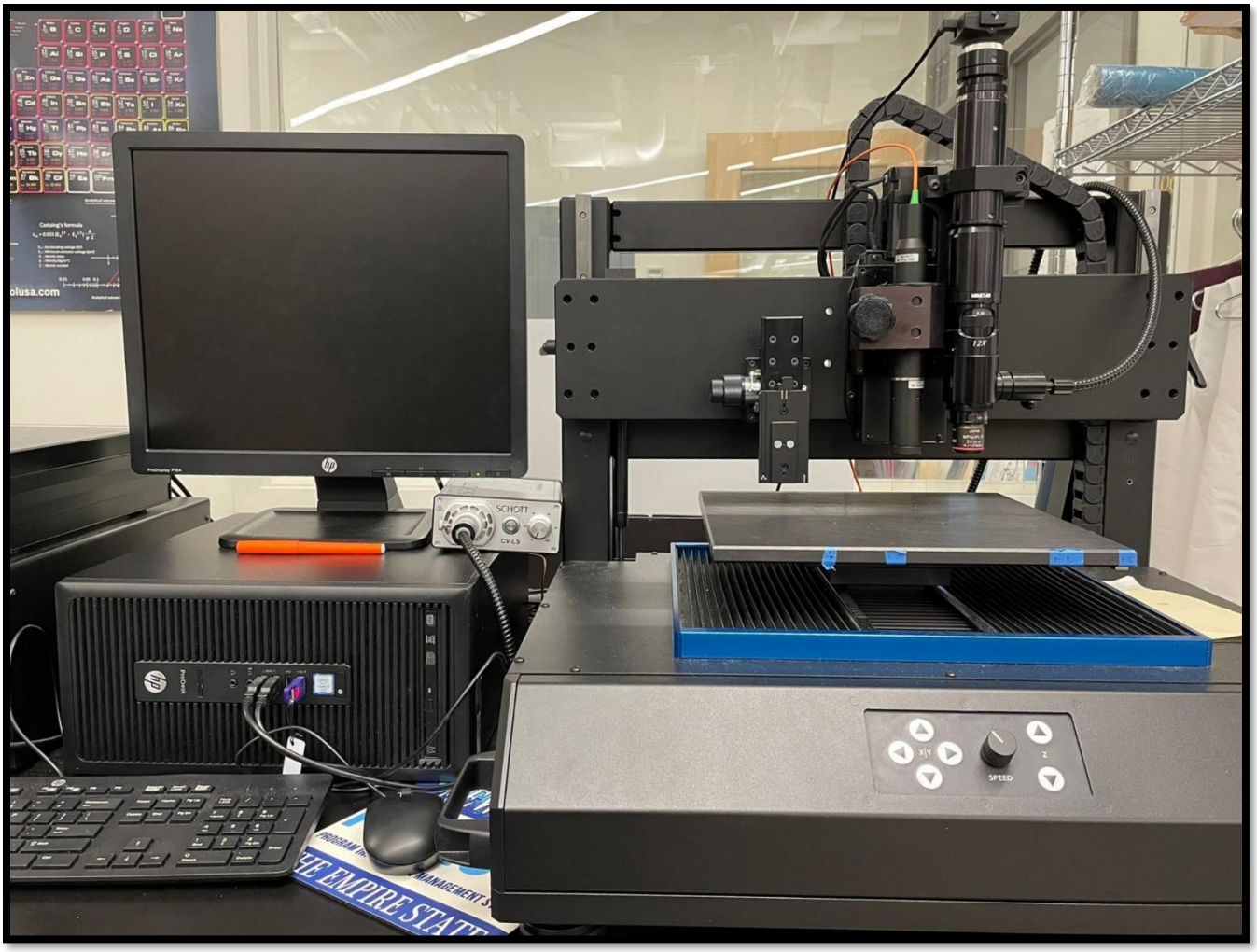

Figure 105 NANOVIA Optical Profiler 3D setup

S_a surface roughness measurements were taken which indicate the difference in height of each point compared to the arithmetical mean of the surface. This parameter is used generally to evaluate surface roughness.

5.3 Results of Surface Roughness Values

As seen in our literature review, the lower the angle between the sloped surface and the horizontal build plane, the higher the stair stepping effect becomes. The same is seen in our results. The planar parts with lower angles show higher surface roughness, and as the angle of slope with the horizontal build plane increases, the surface roughness decreases.

The non-planar parts on the other hand have consistently lower surface roughness. At higher slope angles, the surface roughnesses of planar and non-planar parts are comparable.

Table 9 S_a values of planar and non-planar parts printed at different slope angles.

Slope Angle in degrees	Planar Parts	Non-Planar Parts
	Sa value	Sa value
5	105.77	33.14
10	101.69	26.18
15	99.72	16.43
20	92.86	24.40
25	86.81	37.29
30	74.46	21.92
35	77.13	38.69
40	66.03	21.56
45	54.73	36.07

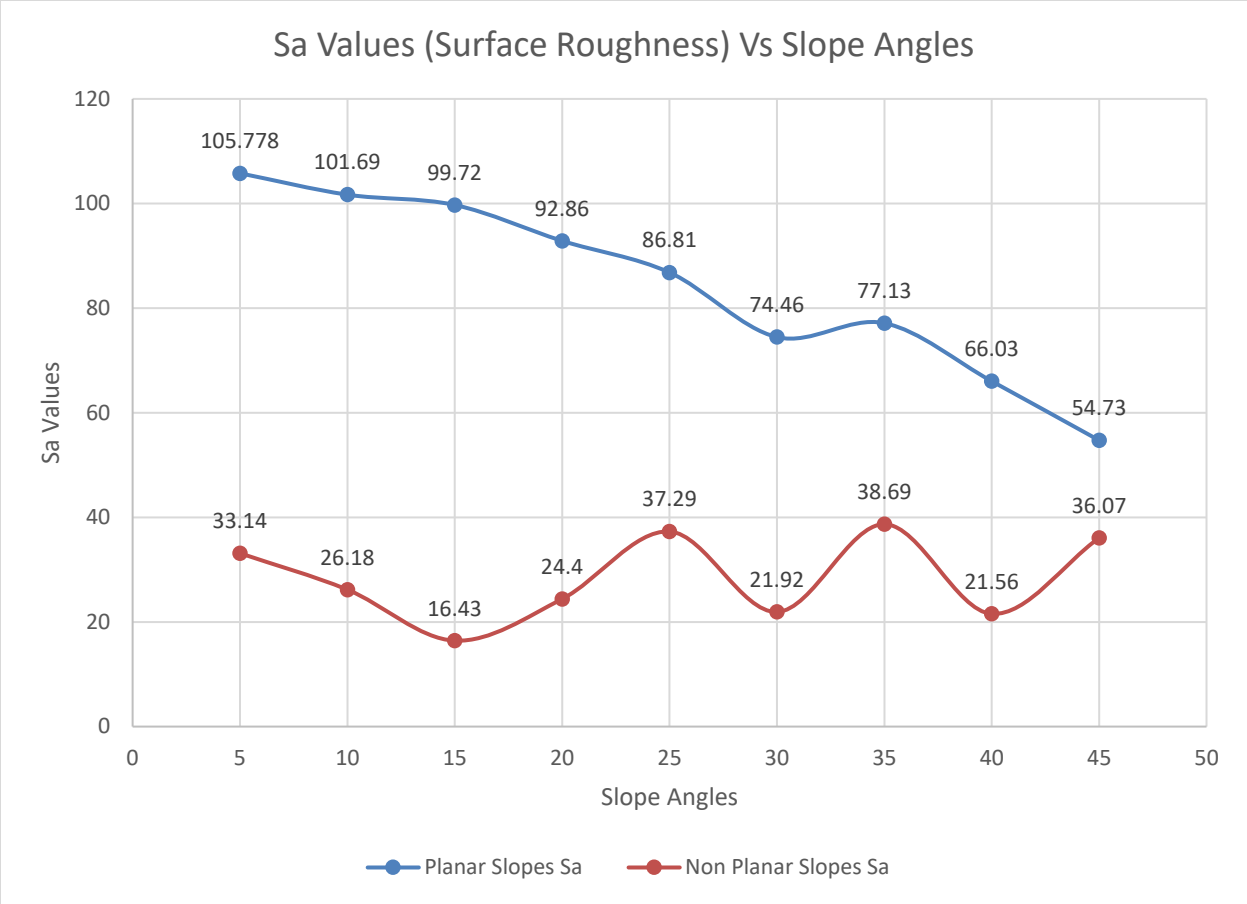

Figure 106 Graph of Slope Angle vs Sa Value for Planar and Non-Planar parts

Figure 107 shows scanned images of both planar and non-planar parts. As the angle of slope increases, the stair stepping effect starts reducing and the S_a values of non-planar parts become much closer to the S_a values of non-planar parts.

Scanned surface of Planar Sloped Parts	Scanned Surface of Non-Planar Sloped parts.
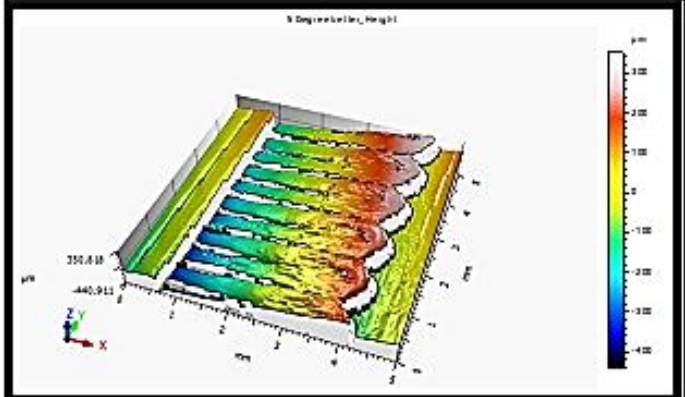	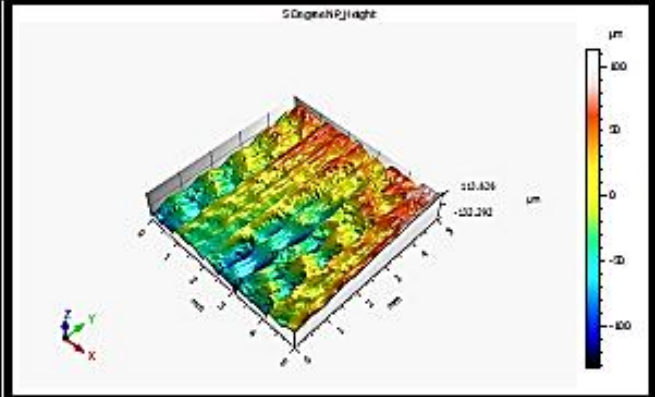
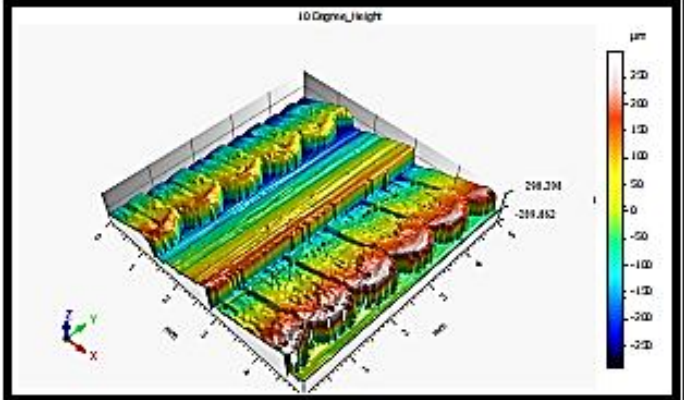	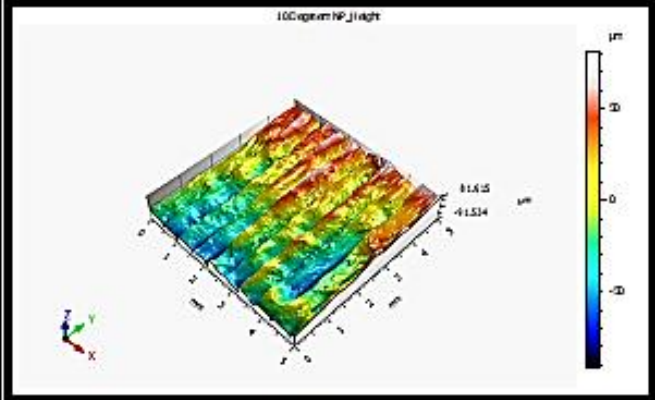
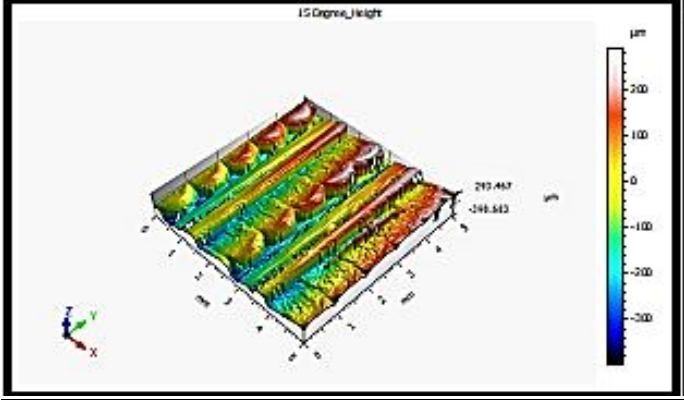	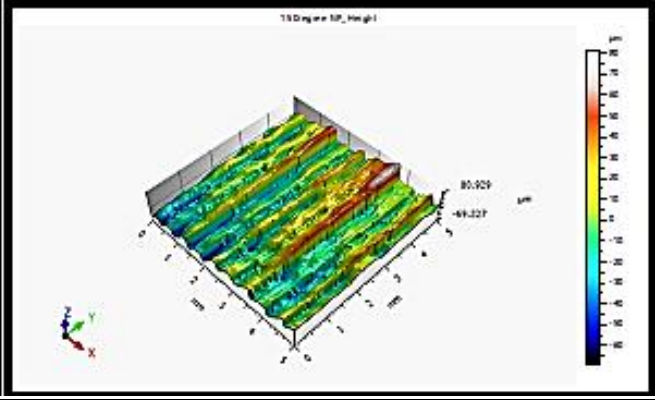

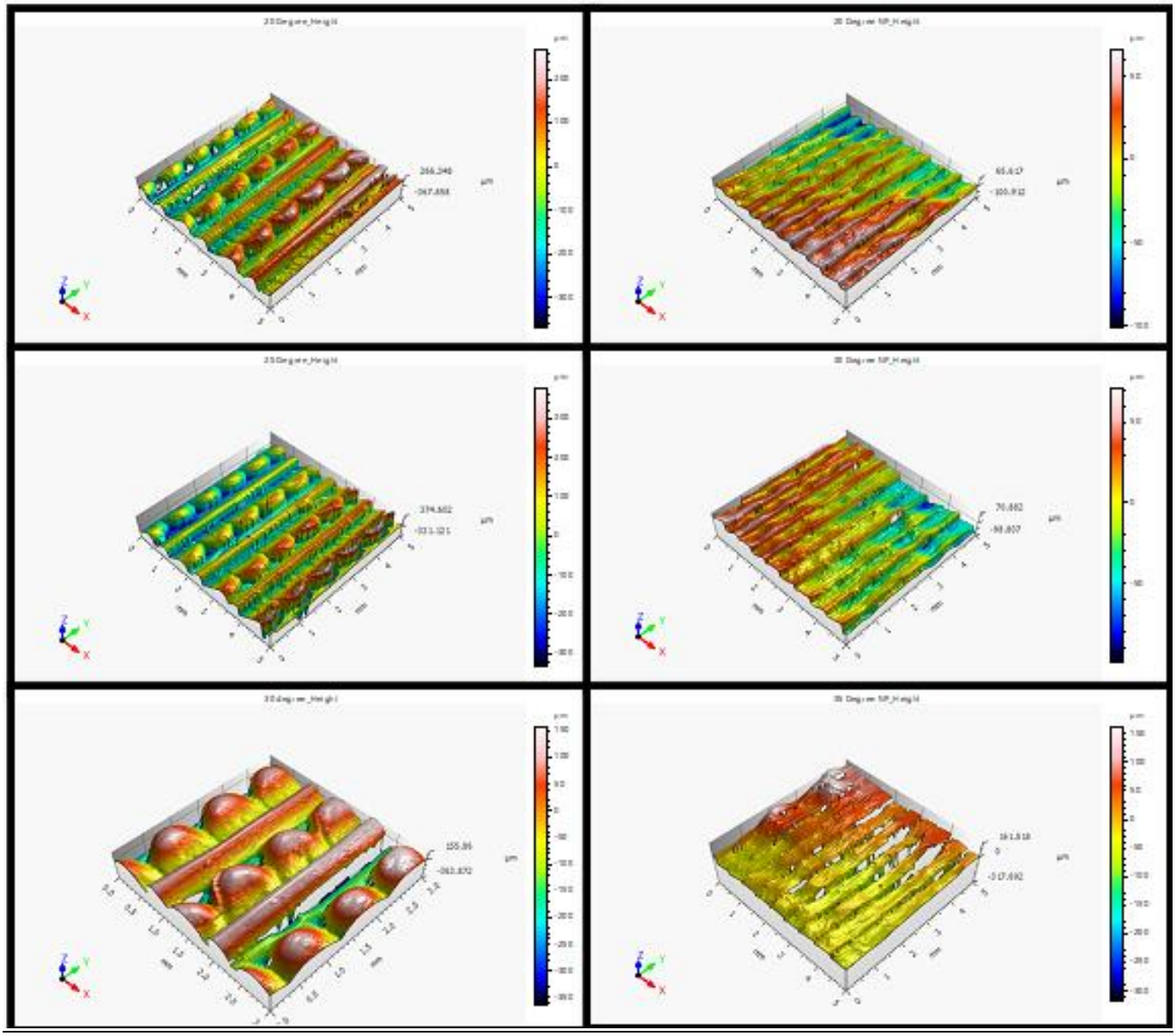

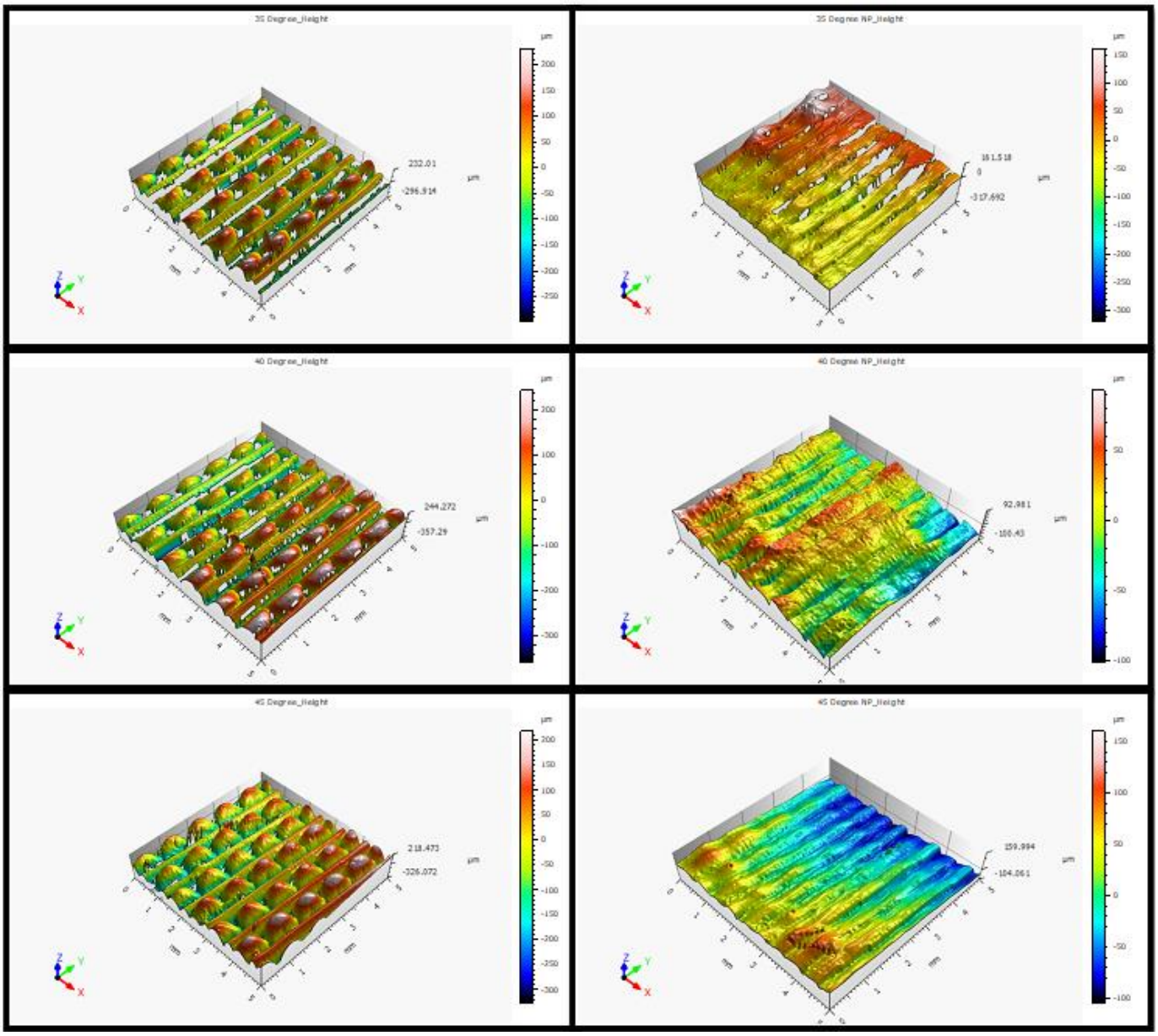

Figure 107 Surface Scans Of Planar (left) and Non-Planar (right) Parts With Slopes From 5 Degrees to 45 Degrees

A summary of the key points pertaining to the surface roughness analysis is as follows:

- All measured Sa values in planar parts were higher than the Sa values in non-planar (conformal printing) parts.
- The images in Figure 107 are the 3D scanned images of all the tested samples.
- We can see the effect of stair stepping in planar parts in the scanned images.

6.0 CONCLUSIONS AND RECOMMENDATIONS FOR FUTURE RESEARCH

This thesis has presented a detailed literature review of approaches to non-planar surface printing. A proposed workflow for using commercially available CAM software and a 5 axis FFF printer is introduced. This method can produce non-planar FFF parts and surfaces for further research. Three different types of parts were printed using this process planning workflow.

Mechanical tests were performed on one type of FFF parts with nonplanar surfaces, and the results were compared to conventional 3DP parts. The results of 3-point bend tests and Charpy impact toughness tests clearly showed the enhanced mechanical properties of the parts printed with non-planar surfaces. Likewise, the surface roughness test results showed the improved finish of sloped surfaces produced with nonplanar printing.

For the first time, a nonplanar woven toolpath pattern was produced using a 5-axis FFF machine. This proof of concept justifies further efforts to perform printing with continuous carbon fiber. Future researchers can also work on producing parts with different weave geometries using this technique.

6.1 Future Improvements

While this thesis has demonstrated benefits of 5-axis non-planar printing in both increased mechanical strength and improved surface roughness, there is a great deal of additional research that can be done. As mentioned above, extending the method to embed continuous carbon fiber filament into non-planar layers would be a high priority for future research.

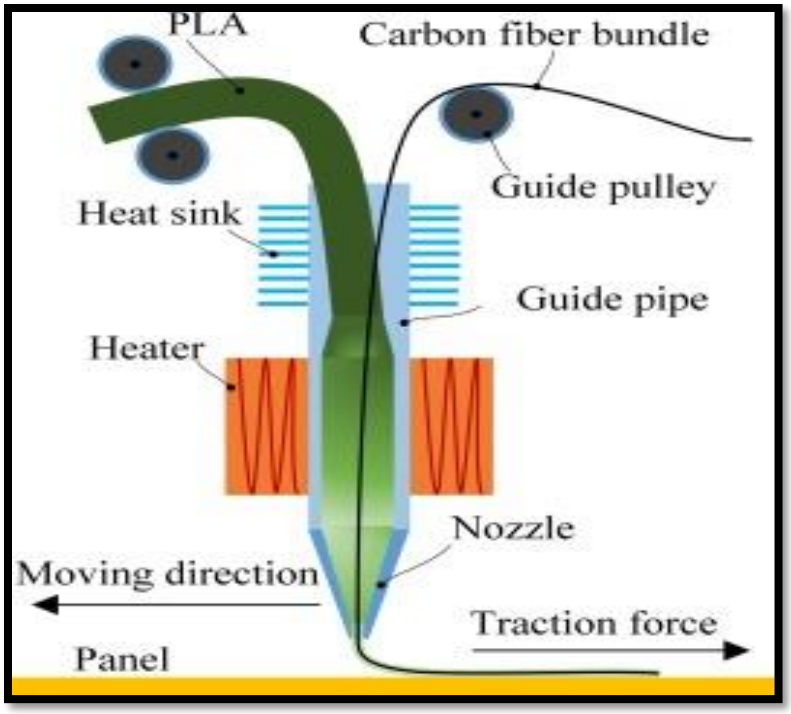

Figure 108 Continuous Carbon Fiber Nozzle [35]

These continuous carbon, glass, or Kevlar fiber strands can absorb and distribute loads across the entire body of the part, thus allowing the part to handle higher loads and impacts. These continuous carbon fiber filaments can be conformally printed in the stress concentration areas on non-planar surfaces. This strategic laying of carbon fiber filament only where it is needed, as opposed to printing an entire part with carbon-filled resin, can reduce the amount of carbon and hence the cost of the part. To print continuous carbon fiber, a mechanical upgrade to the 5 Axis Maker machine would be needed which would allow a dual material extrusion head with single nozzle. This mechanism can be seen in Figure 108 [35].

In normal FDM 3D printing, there is no flow of fibers across the layers in the Z direction. Each discrete planar layer is printed within an X-Y plane at some Z-height. As we have seen, interlayer boundaries are weak links when tensile or shear stress is applied across the layerwise direction [35]. Thus non-planar surfaces containing continuous fibers that can flow along the part in all three dimensions will likely result in increased mechanical properties as compared to conventionally printed parts.

A major problem with gantry type 5 axis printers is wire management. While printing complex geometries, the wires for the heating coil and thermocouple get tangled. To avoid the above issues, a trunnion style of 3-D printer is recommended to generate conformal surface prints.

7.0 REFERENCES

[1] M. Jiménez, L. Romero, I. A. Domínguez, M. D. M. Espinosa, and M. Domínguez, "Additive Manufacturing Technologies: An Overview about 3D Printing Methods and Future Prospects," *Complexity*, vol. 2019, 2019, doi: 10.1155/2019/9656938.

[2] S. Vyavahare, S. Teraiya, D. Panghal, and S. Kumar, "Fused deposition modelling: a review," *Rapid Prototyping Journal*, no. June, 2019, doi: 10.1108/RPJ-04-2019-0106.

[3] E. Yasa, O. Poyraz, E. U. Solakoglu, G. Akbulut, and S. Oren, "A Study on the Stair Stepping Effect in Direct Metal Laser Sintering of a Nickel-based Superalloy," *Procedia CIRP*, vol. 45, pp. 175–178, 2016, doi: 10.1016/j.procir.2016.02.068.

[4] E. J. Ekoi, A. N. Dickson, and D. P. Dowling, "Investigating the fatigue and mechanical behaviour of 3D printed woven and nonwoven continuous carbon fibre reinforced polymer (CFRP) composites," *Composites Part B: Engineering*, vol. 212, p. 108704, May 2021, doi: 10.1016/J.COMPOSITESB.2021.108704.

[5] B. N. Turner, R. Strong, and S. A. Gold, "A review of melt extrusion additive manufacturing processes: I. Process design and modeling," *Rapid Prototyping Journal*, vol. 20, no. 3, pp. 192–204, 2014, doi: 10.1108/RPJ-01-2013-0012.

[6] J. Kietzmann, L. Pitt, and P. Berthon, "Disruptions, decisions, and destinations: Enter the age of 3-D printing and additive manufacturing," *Business Horizons*, vol. 58, no. 2, pp. 209–215, Mar. 2015, doi: 10.1016/J.BUSHOR.2014.11.005.

[7] A. Khan, P. Mcmenamin, W. Rozen, M. Chae, A. Saxena, and M. Kamran, "A Comprehensive Study on 3D Printing Technology Investigation of Heat Storage Performance of a Solar Pond with P... aiman nud Emerging Applicat ions of Bedside 3D Print ing in Plast ic Surgery A Comprehensive Study on 3D Printing Technology Investigation of Heat Storage Performance of a Solar Pond with Potassium Chloride View project 1. Efficiency Enhancement of a PV module View project A Comprehensive Study on 3D Printing Technology," *MIT International Journal of Mechanical Engineering*, vol. 6, no. 2, pp. 63–69, 2016, Accessed: May 01, 2022. [Online]. Available: https://www.researchgate.net/publication/310961474

[8] D. L. Glasco, A. Sheelam, N. H. B. Ho, A. M. Mamaril, M. King, and J. G. Bell, "Editors' Choice—Review—3D Printing: An Innovative Trend in Analytical Sensing," *ECS Sensors Plus*, vol. 1, no. 1, p. 010602, Apr. 2022, doi: 10.1149/2754-2726/AC5C7A.

[9] N. Shahrubudin, T. C. Lee, and R. Ramlan, “An Overview on 3D Printing Technology: Technological, Materials, and Applications,” *Procedia Manufacturing*, vol. 35, pp. 1286–1296, Jan. 2019, doi: 10.1016/J.PROMFG.2019.06.089.

[10] Jing Hu, “Study On STL-Based Slicing Process For 3D Printing,” *Solid Freeform Fabrication*, pp. 885–895, 2017, [Online]. Available: http://sffsymposium.engr.utexas.edu/sites/default/files/2017/Manuscripts/StudyonSTLBasedSlicingProcessfor3DPrinting.pdf

[11] J. Horvath, “Driving Your Printer: G-code,” *Mastering 3D Printing*, pp. 65–76, 2014, doi: 10.1007/978-1-4842-0025-4_6.

[12] B. Brenken, E. Barocio, A. Favaloro, V. Kunc, and R. B. Pipes, “Fused filament fabrication of fiber-reinforced polymers: A review,” *Additive Manufacturing*, vol. 21, no. October 2017, pp. 1–16, 2018, doi: 10.1016/j.addma.2018.01.002.

[13] “Customized extruder. (a) Printing thermoplastic material, the pinch... | Download Scientific Diagram.” https://www.researchgate.net/figure/Customized-extruder-a-Printing-thermoplastic-material-the-pinch-roller-engages-with_fig1_351834882 (accessed May 23, 2022).

[14] A. Bellini and S. Güçeri, “Mechanical characterization of parts fabricated using fused deposition modeling,” *Rapid Prototyping Journal*, vol. 9, no. 4, pp. 252–264, 2003, doi: 10.1108/13552540310489631.

[15] A. Uiversitatis and C.-T. Series, “EFFECTS OF RASTER ORIENTATION, INFILL RATE AND INFILL PATTERN ON THE MECHANICAL PROPERTIES OF 3D PRINTED MATERIALS,” 2017, doi: 10.1515/aucts-2017-0004.

[16] “Choosing Infill Percentage For 3D Printed Parts — 3DPros.” https://www.3d-pros.com/choosing-infill-for-3d-printed-parts (accessed May 01, 2022).

[17] F. Decuir, K. Phelan, and B. C. Hollins, “Mechanical strength of 3-D printed filaments,” *Proceedings - 32nd Southern Biomedical Engineering Conference, SBEC 2016*, pp. 47–48, 2016, doi: 10.1109/SBEC.2016.101.

[18] D. Ahlers, F. Wasserfall, N. Hendrich, and J. Zhang, *3D Printing of Nonplanar Layers for Smooth Surface Generation; 3D Printing of Nonplanar Layers for Smooth Surface Generation*. 2019.

[19] S. Lim, R. A. Buswell, P. J. Valentine, D. Piker, S. A. Austin, and X. de Kestelier, “Modelling curved-layered printing paths for fabricating large-scale construction components,” *Additive Manufacturing*, vol. 12, pp. 216–230, Oct. 2016, doi: 10.1016/J.ADDMA.2016.06.004.

[20] D. Ahlers, F. Wasserfall, N. Hendrich, and J. Zhang, “3D Printing of Nonplanar Layers for Smooth Surface Generation,” pp. 1737–1743, 2019, doi: 10.1109/coase.2019.8843116.

[21] J. B. Khurana, S. Dinda, and T. W. Simpson, “ACTIVE - Z PRINTING: A NEW APPROACH TO INCREASING3D PRINTED PART STRENGTH”.

[22] B. Huang and S. Singamneni, “A mixed-layer approach combining both flat and curved layer slicing for fused deposition modelling,” *Proceedings of the Institution of Mechanical Engineers, Part B: Journal of Engineering Manufacture*, vol. 229, no. 12, pp. 2238–2249, 2015, doi: 10.1177/0954405414551076.

[23] J. B. Khurana, S. Dinda, and T. W. Simpson, “Active - Z Printing: a New Approach To Increasing3D Printed Part Strength,” *Solid Freeform Fabrication Symposium*, pp. 1627–1644, 2017.

[24] D. Chakraborty, B. Aneesh Reddy, and A. Roy Choudhury, “Extruder path generation for Curved Layer Fused Deposition Modeling,” *CAD Computer Aided Design*, vol. 40, no. 2, pp. 235–243, 2008, doi: 10.1016/j.cad.2007.10.014.

[25] S. Singamneni, A. Roychoudhury, O. Diegel, and B. Huang, “Modeling and evaluation of curved layer fused deposition,” *Journal of Materials Processing Technology*, vol. 212, no. 1, pp. 27–35, Jan. 2012, doi: 10.1016/J.JMATPROTEC.2011.08.001.

[26] “(PDF) A Comparative Study Between 3-Axis and 5-Axis Additively Manufactured Samples and their Ability to Resist Compressive Loading.” https://www.researchgate.net/publication/360111656_A_Comparative_Study_Between_3-Axis_and_5-Axis_Additively_Manufactured_Samples_and_their_Ability_to_Resist_Compressive_Loading (accessed May 01, 2022).

[27] M. Asif *et al.*, “A new photopolymer extrusion 5-axis 3D printer,” *Additive Manufacturing*, vol. 23, pp. 355–361, Oct. 2018, doi: 10.1016/J.ADDMA.2018.08.026.

[28] R. C. Luo, L. C. Hsu, T. J. Hsiao, and Y. W. Perng, “3D Digital Manufacturing via Synchronous 5-Axes Printing for Strengthening Printing Parts,” *IEEE Access*, vol. 8, pp. 126083–126091, 2020, doi: 10.1109/ACCESS.2020.3007772.

[29] F. Hong, S. Hodges, C. Myant, and D. Boyle, “Open5x: Accessible 5-axis 3D printing and conformal slicing; Open5x: Accessible 5-axis 3D printing and conformal slicing”.

[30] C. Dai, C. C. L. Wang, C. Wu, S. Lefebvre, G. Fang, and Y.-J. Liu, “Support-Free Volume Printing by Multi-Axis Motion,” *ACM Trans. Graph*, vol. 37, no. 1, p. 14, 2018, doi: 10.1145/3197517.3201342.

[31] A. Teibrich, S. Mueller, F. Guimbretière, R. Kovacs, S. Neubert, and P. Baudisch, "Patching Physical Objects," *UIST 2015 - Proceedings of the 28th Annual ACM Symposium on User Interface Software and Technology*, pp. 83–91, Nov. 2015, doi: 10.1145/2807442.2807467/FORMAT/PDF.

[32] A. Diourté, F. Bugarin, C. Bordreuil, and S. Segonds, "Continuous three-dimensional path planning (CTPP) for complex thin parts with wire arc additive manufacturing," *Additive Manufacturing*, vol. 37, p. 101622, Jan. 2021, doi: 10.1016/J.ADDMA.2020.101622.

[33] A. N. Dickson, K. A. Ross, and D. P. Dowling, "Additive manufacturing of woven carbon fibre polymer composites," *Composite Structures*, vol. 206, pp. 637–643, Dec. 2018, doi: 10.1016/J.COMPSTRUCT.2018.08.091.

[34] "3.2. How to Run the Machine – 5AXISMAKER SUPPORT." https://support.5axismaker.com/hc/en-gb/articles/360012022680-3-2-How-to-Run-the-Machine (accessed May 23, 2022).

[35] N. Li, Y. Li, and S. Liu, "Rapid prototyping of continuous carbon fiber reinforced polylactic acid composites by 3D printing," *Journal of Materials Processing Technology*, vol. 238, pp. 218–225, Dec. 2016, doi: 10.1016/J.JMATPROTEC.2016.07.025.